# ORGANIC AND ELEMENTAL CARBON SIZE DISTRIBUTIONS OF LOS ANGELES AEROSOLS MEASURED DURING SCAQS

Final Report to

The Coordinating Research Council
219 Perimeter Center Parkway
Atlanta, GA 30346

CRC Project No. SCAQS–6–1

and

The California Air Resources Board
1102 Q Street
P.O. Box 2815
Sacramento, CA 95812

CARB Contract No. A732–075

Submitted by

Peter H. McMurry
Department of Mechanical Engineering
University of Minnesota
111 Church St. SE
Minneapolis, MN 55455

August, 1989

Revised December, 1989

Particle Technology Laboratory No. 713

TABLE OF CONTENTS

ABSTRACT 2

INTRODUCTION 3

EXPERIMENTAL

SAMPLE HANDLING AND ANALYSIS PROCEDURES 3

Substrates and Substrate Preparation 3
Sample Storage 3
Sample Analysis 4

DATA REDUCTION 4

Blank Correction and Uncertainty Estimates 4
Tabulated Data 5
MOUDI Size–Dependent Efficiencies and Data Inversion 5

RESULTS AND DISCUSSION 6

Uninverted Data 6
Inverted Data 13
Comparisons with Other Samplers 31

ACKNOWLEDGMENTS 36

REFERENCES 36

APPENDICES

I. Summary of MOUDI Samples Acquired During SCAQS 37
II. Size–dependent Collection Efficiencies 42
III. Loadings on MOUDI Stages for SCAQS Measurements 47
IV. Lognormal Fits to SCAQS Data 65

## ABSTRACT

This report summarizes measurements of size–resolved residual organic carbon (ROC) and elemental carbon (EC) made by researchers from the University of Minnesota during the Southern California Air Quality Study (SCAQS). Measurements were made with MOUDI impactors. Impactors were located at Claremont and Rubidoux during summer SCAQS sampling, and at Long Beach and Los Angeles during the fall.

It was found that the average mass mean diameter of ROC ranged from 0.43 μm at Los Angeles to 0.62 μm at Rubidoux. Mass mean diameters of EC were systematically smaller than for ROC, ranging from 0.39 μm at Los Angeles to 0.45 μm at Rubidoux. The Rubidoux ROC mean sizes were systematically and substantially larger than sizes at the other three sites.

The ROC/EC ratio varied with site, season, and particle size. Average ROC/EC ratios were 2.66 (Claremont), 2.12 (Rubidoux), 1.51 (Long Beach) and 1.26 (Los Angeles). Although there was no systematic dependence of ROC/EC ratios with particle size, there was a tendency for values to be higher for particles at the large ($\simeq$ 1 μm) and small ($\simeq$0.05–0.1 μm) extremes of the measured size spectrum.

The data were 'inverted' to account for the effect of size–dependent collection efficiencies on measured size distributions. All data were inverted with two inversion schemes: the modified Twomey routine developed by Walter John and coworkers at the Air and Industrial Hygiene Laboratory (Berkeley, CA), and the MICRON code developed by Wolfenbarger and Seinfeld (Caltech). Integral moments of inverted size distributions obtained with these two inversion schemes were compared. It was found that for the integral moment corresponding to particle mass (the 3rd moment) the two inversion methods were in good agreement. This is not surprising since the techniques are constrained to return the measured mass. However, for smaller or larger moments the integral moments can be up to several orders of magnitude different. Although resolving differences between inversion schemes is beyond the scope of the present research, the discrepancies in integral moments is a serious concern. Because size distributions are usually measured with the objective of calculating some integral moment (light scattering or absorption, dry deposition, lung deposition, etc.), it is essential to have some means of estimating most likely values and uncertainties of such integrals. This result suggests that uncertainties for integrals other than total mass can be large.

A limited number of comparisons between EC concentrations obtained with the MOUDI with other samplers was done for the Claremont site. As with previous studies it is found that correlations are poor, with $R^2$ values ranging down to 0.35. MOUDI EC data were found to be somewhat better correlated with the Ford Spectrometer (an optical absorption device) data than with data from a quartz filter. A similar result was found during the 1986 Carbonaceous Species Methods Comparison Study where the MOUDI agreed best with the LBL aethalometer, another optical absorption device. McMurry and Zhang (Aerosol Sci. Technol. 10:430–437) discussed discrepancies for carbon measurements among different samplers and conclude that impactors may be superior to filters for sampling carbon–containing particulate matter.

## INTRODUCTION

Particle size plays a sensitive role in atmospheric aerosol phenomena including optical extinction, dry deposition, and cloud nucleation. In order to evaluate the contributions of various chemical species to these effects, it is important to have information on size–resolved chemical composition. the measurements of organic and elemental carbon size distributions discussed in this paper were made with the objective of improving our understanding of such phenomena. Measurements were made with two microorif(MOUDIs) (1) during the Southern California Air Quality Study (SCAQS). Samples were analyzed for elemental and organic carbon by Dr. Kochy Fung and coworkers at ERT, Inc (2). Objectives of these measurements are to elucidate the role of organic and elemental carbon in phenomena including dry deposition and optical extinction, and to investigate the evolution of secondary organic aerosols by gas to particle formation in the atmosphere.

The use of MOUDIs to measure organic and elemental carbon size distributions has been discussed previously (3). The interested reader is referred to that previous paper for a more detailed discussion of measurement procedures and sampling artifacts with MOUDI and filter samplers.

## EXPERIMENTAL

MOUDIs were located at Claremont and Rubidoux, CA during summer–SCAQS intensive sampling days and at Long Beach and Los Angeles during fall–SCAQS intensive sampling days. The nominal sampling period for daytime measurements was four hours (06:00–10:00, 10:00–14:00, 14:00–18:00), while a twelve hour period was used at night (18:00–6:00) except on the last day of sampling intensives when sampling was stopped at 1:00. Summer samples were collected on a total of eleven days (June 19, 24, 25, July 13, 14, 15, Aug. 27, 28, 29, Sept 2, 3, 1989) and fall samples were collected on a total of six days (Nov 11, 12, 13, Dec. 3, 10, 11). A summary of information on all samples collected with MOUDIs during SCAQS is included in Appendix I.

The MOUDIs were preceded by cyclones (4) to remove particles larger than about 2 μm. A total of eight impaction stages was used with nominal 50% cut points ranging from 0.04 to 3.2 μm. Detailed information on size–dependent collection efficiencies for each stage is given in Appendix II. Particles were collected by inertial impaction on ungreased aluminum foil substrates. The foils were precleaned by baking for 3 hours at 600 °C in air.

## SAMPLE HANDLING AND ANALYSIS PROCEDURES

### Substrates and Substrate Preparation

Aerosol samples were collected on aluminum foil (impactor stages) or on quartz filters (impactor afterfilter). The aluminum foil was punched from 0.001 inch foil sheets with a 1 7/16 inch punch, and was precleaned by baking for 3 hours at 600 °C in air. The 37 mm Pallflex QAO Quartz afterfilters were precleaned by baking for 2 hours at 700 °C in air.

### Sample Storage

After sample collection was completed, samples were transferred to 47 mm petrislides. A stack of 9 petrislides from each MOUDI sample (8 impactor stages and one afterfilter) was wrapped in aluminum foil, enclosed in plastic ziploc bags, and placed in temporary storage in

the freezer in the SCAQS headquarters trailer. The trailers were located at Claremont during the summer intensives and at Long Beach during the Fall. Samples were hand carried on ice to ERT, Inc. twice during the summer and twice during the fall where they were again stored in a freezer until they were analyzed.

Sample Analyses

Samples were analyzed at ERT, Inc. using the technique described by Mueller *et al.* (1982). An aliquot from each sample was loaded into a platinum boat and put into contact with $MnO_2$ catalyst. The sample was first heated to 525 C in He, and then (with air addition) to 850 C. Carbonaceous material that is released from the sample (mostly as $CO_2$) is converted to methane and detected with a flame ionization detector. The material that is released at 525 C is defined as residual organic carbon (ROC), while the high temperature carbon is defined as elemental carbon (EC). Only a portion of each substrate was required for analysis, so it was possible to perform replicate analyses on a subset of the samples. Samples were analyzed during the summer and fall of 1988, and results were sent to the University of Minnesota both on floppy disk and in hardcopy form. Our primary contact at ERT was Ms. Amy Taketomo.

## DATA REDUCTION

The data from ERT were reduced in our lab by Mr. Mark Anderson, a Carleton College undergraduate. Steps that were involved in data reduction included:

- blank correction
- convert substrate mass loadings to airborne concentrations
- prepare tables of concentration data
- 'invert' MOUDI data to obtain better estimates of true size distributions (two inversion schemes were used for comparison)
- fit inverted size distributions with bimodal lognormal distributions
- prepare tables of inverted size distribution data.

Additional details of this work are provided below.

Blank Correction and Uncertainty Estimates

Blanks were estimated from several different types of information. Field and dynamic blanks were analyzed for EC and ROC loadings. Also, the top impactor stage serves as an excellent dynamic blank. The cyclone located upstream of the MOUDI collects all particles larger than about 2 μm, and the cutpoint of the top impactor stage is 3.2 μm. Therefore, no particles should have been collected on this stage, and visible deposits were not observed. However, this substrate was handled identically to all other substrates, and was exposed to the same gases for the same time period. Therefore the ROC and EC loading on this stage should be representative of blank values for the other stages.

Blank values for ROC and EC during summer and fall SCAQS measurements are summarized in Table I. In estimating blank values for the quartz filters, information from previous field studies with similar filters was used to supplement SCAQS data. The foil blanks are based solely on SCAQS measurements. The blank values in Table I. were subtracted from all loadings reported by ERT, Inc.

Table I. Summary of Blanks (μg/substrate)

| | Summer SCAQS | Fall SCAQS |
|---|---|---|
| ROC, Aluminum Foil | 3.0 ± 3.0 | 1.5 ± 0.7 |
| ROC, Quartz Afterfilter | 7.0 ± 3.0 | 7.0 ± 3.0 |
| EC, Aluminum Foil | 0.0 ± 0.05 | 0.0 ± 0.1 |
| EC, Quartz Afterfilter | 0.1 ± 0.05 | 0.1 ± 0.05 |

The variability in the blanks provides a measure of noise in the data. In addition, uncertainties associated with the analytical technique can be determined from replicate analyses of the same substrate. Replicate analyses were performed on 77 foil samples. It was found that variabilities among replicate samples could be approximated by:

$$\text{Replicate Variability for ROC} \approx 0.5 + 0.03*\text{ROC}.$$

$$\text{Replicate Variability for EC} \approx 0.1*\text{EC}.$$

where ROC and EC are the total ROC or EC loadings on the substrates. Based on the variability in the blanks and on variabilities in replicate analyses the following uncertainties for elemental (EC) and organic (ROC) carbon measurements are estimated:

$$\Delta\text{EC } (\mu g/m^3) = (1.0 + 0.05*\text{EC per stage})/V_s$$

$$\Delta\text{ROC } (\mu g/m^3) = (1.0 + 0.05*\text{ROC per stage})/V_s$$

where $V_s$ is the total volume of air sampled. Flow rates (and therefore sample volumes) were accurate to within about 5%.

Tabulated Data

After correcting for blanks, stage loadings were converted to concentrations by dividing by the volume of air sampled. A summary of all data acquired during the study is tabulated in Appendix III. A separate page is included for each intensive sampling day. Data from the upwind sites (Claremont or Long Beach) is shown on the top of the page, and data from the downwind site is shown on the bottom. Two columns are shown for each sample. The first column is for ROC and the second is for EC.

The data in Appendix III were also submitted to the SCAQS data base on floppy disc.

MOUDI Size–Dependent Efficiencies and Data Inversion

For a given input aerosol size distribution, the loading per MOUDI stage depends on the size–dependent collection efficiency for that stage and upstream stages. A zeroth order approximation for determining size distributions from an impactor assumes that all mass collected on a stage is associated with particles having diameters between the 50% cut point ($D_{50}$) for that stage and the stage immediately upstream. This approach can be used to directly estimate size distributions from the data in Appendix III given the impactor cut points. $D_{50}$s

for the MOUDIs are included in Appendix II.

A more refined estimate of size distributions measured with impactors can be achieved by taking into account the size–dependent collection efficiencies of each stage. This procedure is commonly referred to as 'data inversion'. Data inversion requires a detailed knowledge of size–dependent collection efficiencies for each stage. The MOUDIs used during SCAQS were calibrated in our laboratory immediately before the program, and a spot check was done between the summer and fall measurements. The MOUDI calibration data that were used to invert the data are summarized in Appendix II.

Several research groups have recently developed schemes for inverting impactor data. We have inverted all of our data using two different inversion schemes: "Twomey" and "MICRON". The Twomey routine was developed Dr. Walter John and coworkers at the Air and Industrial Hygiene Laboratory in Berkeley, CA. The MICRON routine was developed by Mr. Kenneth Wolfenbarger, a Ph.D. candidate working under the supervision of Prof. John Seinfeld at Caltech. These algorithms are mathematically quite different. Our objective in using two schemes was to determine whether the inversion method substantially affects the results.

The Twomey code was used by John and Winklmayr to reduce all of the data for ion size distributions that were collected with the Berner Impactors during SCAQS. Dr. Winklmayr assisted us in adapting their algorithm to the MOUDI impactors. The data inversion program outputs values for the size distribution at 65 particle sizes. These size distributions were fitted with single mode or bimodal lognormal size distributions. Results of these lognormal fits are given in Appendix IV. Again, the lognormal fitting program that was used was developed by Winklmayr in Walter John's group at AIHL, and is the same routine that was used with the ion size–distribution data.

The lognormal results for the Twomey inversions are summarized by site. Two pages are included for each site: one for ROC and one for EC. Again, ASCII files for the data in Appendix IV were submitted to the SCAQS data base. The data in Appendix IV indicate that in some cases the mass in mode 2 is zero. This indicates that a single mode lognormal size was sufficient to account for at least 90% of the mass in the measured distribution.

Mr. Kenneth Wolfenbarger (Caltech) was most helpful in implementing MICRON for inverting our MOUDI data. In the following sections results of the MICRON and Twomey inversions are compared. Tabulated results for the MICRON inversions are not presented.

## RESULTS AND DISCUSSION

### Uninverted Data

The discussion in this section applies to the 'raw' uninverted data. Size distributions and mean and median sizes are estimated from the impactor $d_{50}$s.

Average values of EC and ROC mass concentrations are tabulated as a function of time of day in Table II. Note that fall values (Long Beach and Los Angeles) are higher than summer values for this data set.

Mass mean diameters for ROC and EC size distributions are given as a function of time of day in Table III. Note that ROC sizes are systematically greater than EC sizes. Note also that ROC sizes measured at Rubidoux are substantially larger than sizes at other locations.

Table II. Average Mass Concentrations (sum of all stages) Versus Time of Day ($\mu g/m^3$)

Organic Carbon

| | 6:00–10:00 | 10:00–14:00 | 14:00–18:00 | 18:00–6:00 |
|---|---|---|---|---|
| Summer | | | | |
| Claremont | 7.24±1.25 | 8.63±3.99 | 8.33±3.79 | 4.50±2.21 |
| Rubidoux | 5.70±2.24 | 5.02±3.01 | 5.08±2.81 | 3.37±1.25 |
| Fall | | | | |
| Long Beach | 14.62±12.24 | 7.59±7.44 | 6.11±5.16 | 7.29±4.94 |
| Los Angeles | 12.32±7.15 | 7.40±4.61 | 7.91±4.43 | 9.53±4.84 |

Elemental Carbon

| | 6:00–10:00 | 10:00–14:00 | 14:00–18:00 | 18:00–6:00 |
|---|---|---|---|---|
| Summer | | | | |
| Claremont | 3.44±1.45 | 3.16±0.95 | 2.60±0.75 | 1.61±0.83 |
| Rubidoux | 2.93±1.09 | 2.32±1.80 | 2.11±2.17 | 1.71±0.76 |
| Fall | | | | |
| Long Beach | 10.2±6.84 | 6.11±4.29 | 4.97±3.44 | 3.72±1.93 |
| Los Angeles | 11.4±6.29 | 6.12±3.79 | 5.88±3.36 | 6.93±3.52 |

Table III. Average Mass Mean Diameters Versus Time of Day ($\mu m$)

Organic Carbon

| | 6:00–10:00 | 10:00–14:00 | 14:00–18:00 | 18:00–6:00 |
|---|---|---|---|---|
| Summer | | | | |
| Claremont | 0.47±0.09 | 0.48±0.13 | 0.46±0.11 | 0.48±0.12 |
| Rubidoux | 0.66±0.21 | 0.66±0.21 | 0.59±0.14 | 0.56±0.15 |
| Fall | | | | |
| Long Beach | 0.49±0.17 | 0.46±0.13 | 0.43±0.10 | 0.46±0.07 |
| Los Angeles | 0.36±0.14 | 0.43±0.16 | 0.45±0.14 | 0.47±0.04 |

Elemental Carbon

| | | | | |
|---|---|---|---|---|
| Summer | | | | |
| Claremont | 0.36±0.08 | 0.39±0.09 | 0.37±0.08 | 0.38±0.11 |
| Rubidoux | 0.44±0.16 | 0.49±0.19 | 0.49±0.10 | 0.38±0.10 |
| Fall | | | | |
| Long Beach | 0.43±0.11 | 0.40±0.08 | 0.36±0.07 | 0.45±0.10 |
| Los Angeles | 0.35±0.09 | 0.40±0.08 | 0.38±0.10 | 0.42±0.05 |

An attempt was made to determine whether average ROC or EC sizes are correlated with ROC or EC concentrations. It was concluded that if there is a dependence of size on concentration it is a very weak dependence.

Average ROC and EC size distributions are shown for the four sampling sites as functions of time of day in Figures 1 to 4. The data suggest that on some occasions (e.g., 6:00–10:00 at Long Beach) a significant amount of ROC and EC may have been associated with particles larger than the 2 μm cut for this sampling system.

# CLAREMONT

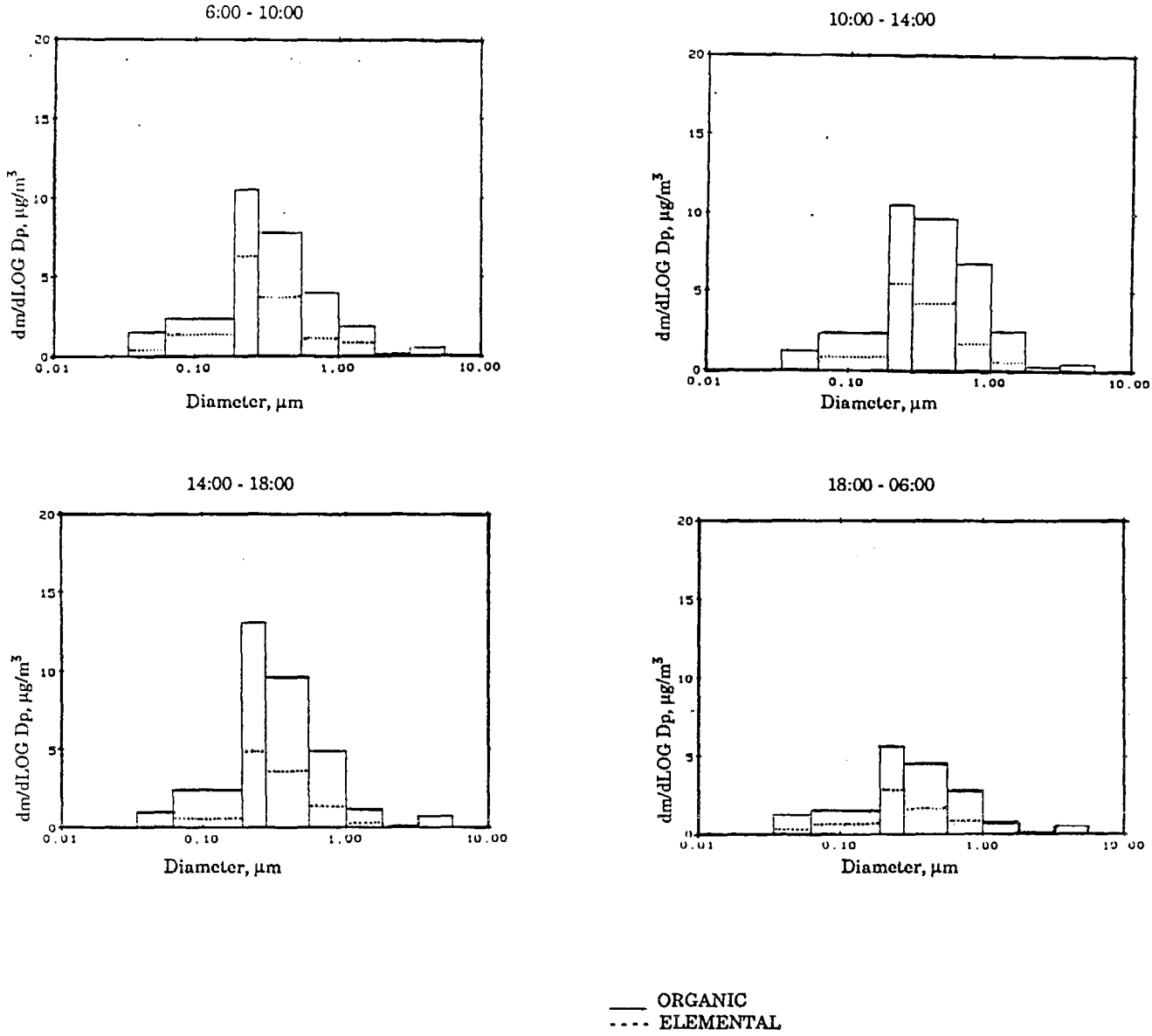


Figure 1. Average organic and elemental carbon size distributions measured at Claremont.

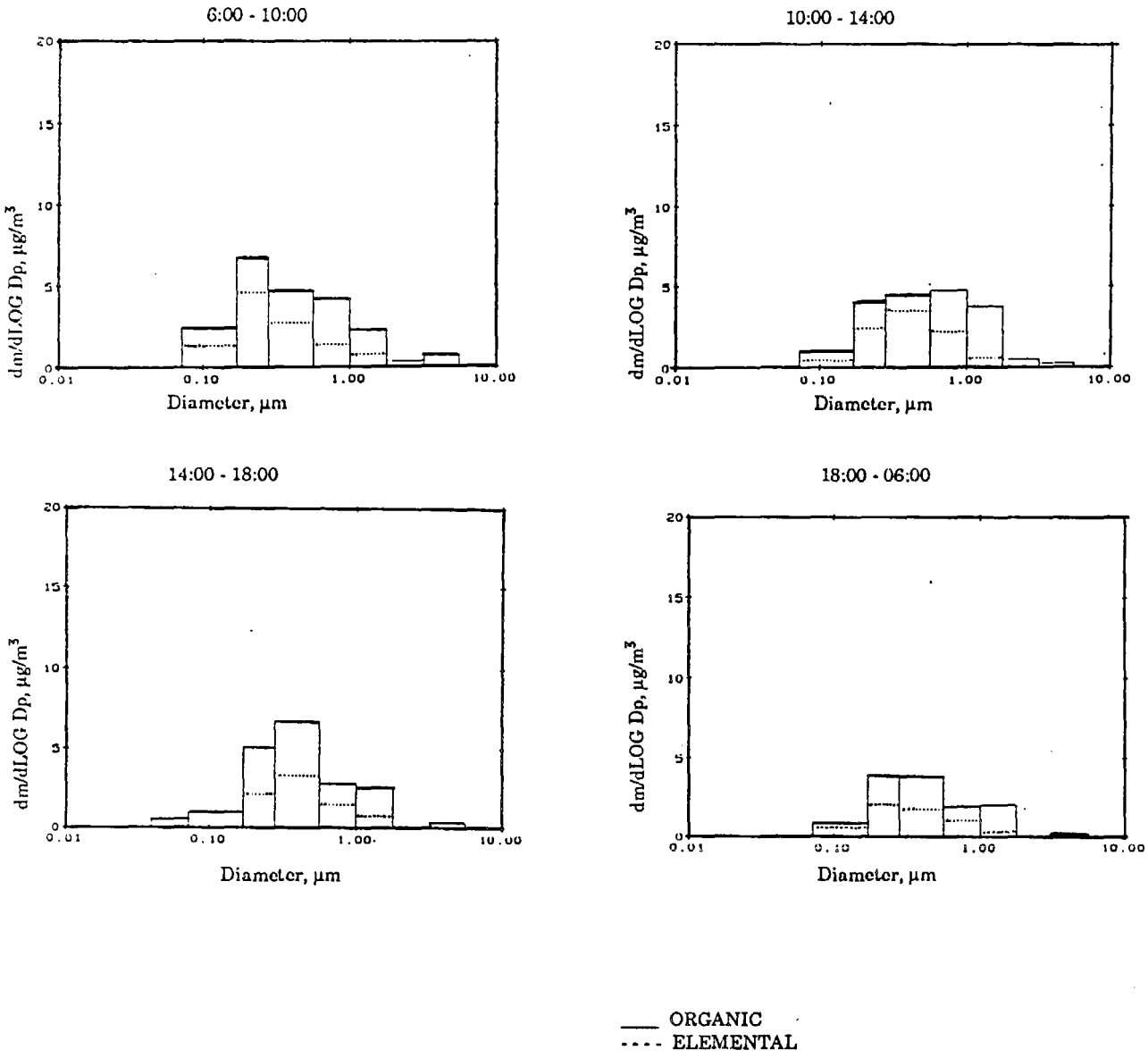


Figure 2. Average organic and elemental carbon size distributions measured at Rubidoux.

# LONG BEACH

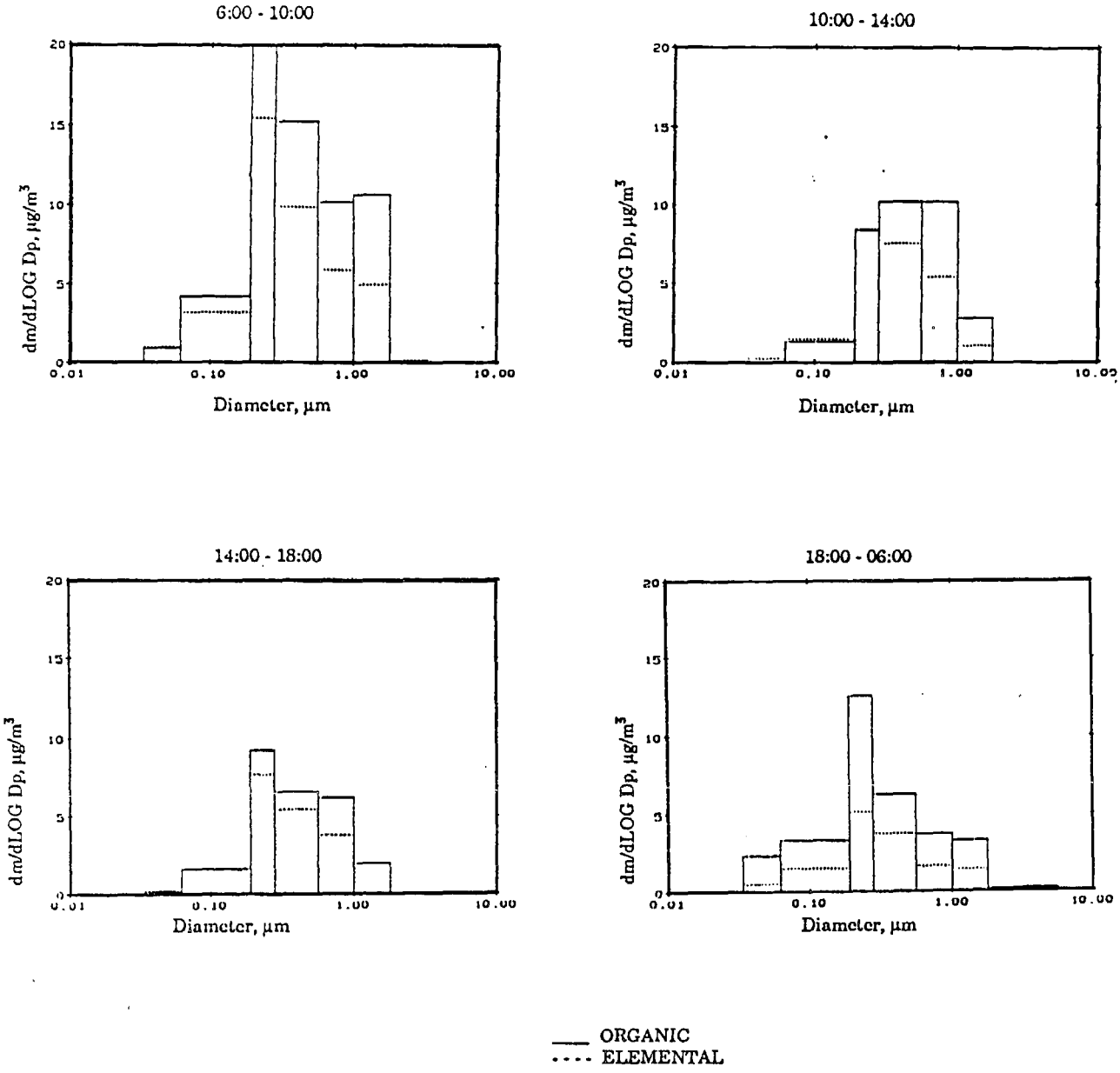


Figure 3. Average organic and elemental carbon size distributions measured at Long Beach.

# LOS ANGELES

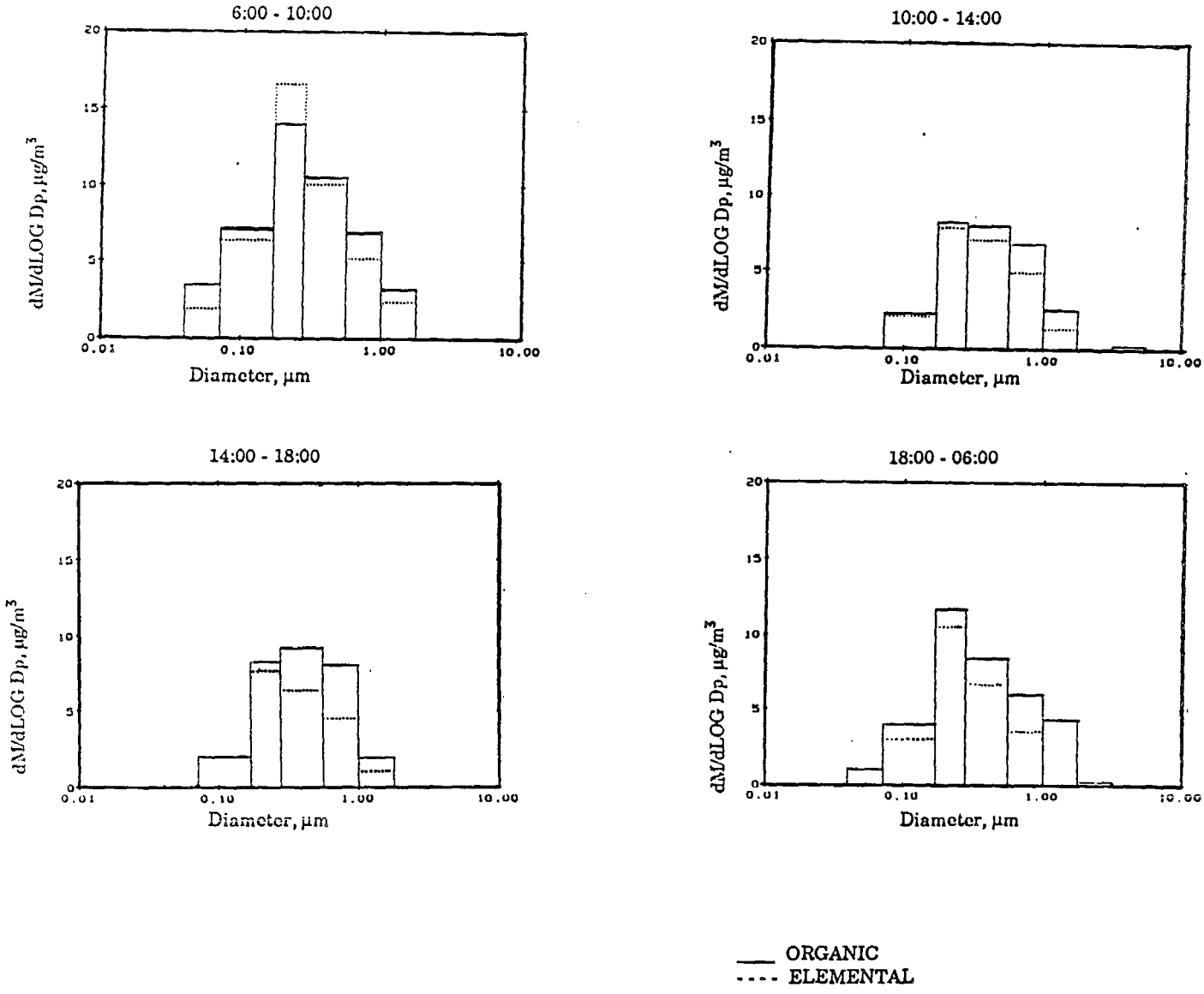


Figure 4. Average organic and elemental carbon size distributions measured at Los Angeles.

Average size–dependent ROC/EC ratios are shown as a function of particle size for each of the four sampling sites in Figures 5 to 8. The data do not show any systematic size dependence of ROC/EC ratios. For samples collected during daytime (10:00–14:00), however, there appears to be a tendency for ROC/EC to increase with increasing particle size.

Inverted Data

Examples of size distributions obtained with the Twomey and MICRON inversion algorithms are compared in Figures 9 and 10. Histograms obtained by assuming that the impactor cuts are perfectly sharp with cut points at the impactor $D_{50}$s are also shown. Note that there are distinct qualitative differences between results from the two inversion schemes. In particular, the MICRON results tend to be broader and less sharply peaked than the Twomey results. It should be noted that the size distribution that is returned by MICRON was found to be highly sensitive to estimated data uncertainties. The uncertainties that were used for these inversions are those discussed above in the section on blank correction and uncertainty estimates.

Size distributions are often measured with the objective of calculating some integral property. Examples of such integral properties include total mass concentration, total number concentration, optical properties (scattering, absorption or extinction coefficients), dry deposition rates, lung deposition rates, gas–particle chemical reaction rates, etc. In some cases these integral properties are proportional to integral moments of the size distribution. The $m^{th}$ integral moment is defined by:

$$I_m = \int_0^\infty D_p^{\,m}\, n(D_p) dD_p$$

where

$I_m$ = $m^{th}$ integral moment ($0 \le m \le 6$)
$D_p$ = particle diameter
$n(D_p) = dN/dD_p$ = size distribution function

Note, for example, that the total mass concentration is proportional to $I_3$ while the total number concentration is proportional to $I_0$. More complex integral properties such as optical properties require integration over a more complicated function of diameter. However, it is often found that over a sufficiently narrow range of particle sizes such functions are reasonably approximated by an integral moment over that size range. With this in mind, integral moments ranging from the 0th to the 6th have been calculated for all of the Twomey and MICRON inverted MOUDI size distributions measured during SCAQS. The objective of this analysis was to determine the sensitivity of the integral moments to the data inversion method.

Comparisons of integral moments obtained with Twomey and MICRON for ROC and EC are shown in Figures 11 and 12 respectively. Note that for $I_3$ the agreement is quite good. This is because $I_3$ corresponds to total mass which was measured directly. As values of m become either larger or smaller than 3, however, the correlations between Twomey and MICRON results deteriorate. As a general rule, MICRON results are systematically greater than Twomey results for both small and large m values. Discrepancies as large as two orders of magnitude are common for $I_0$ or $I_6$.

CLAREMONT OC/EC vs Dp

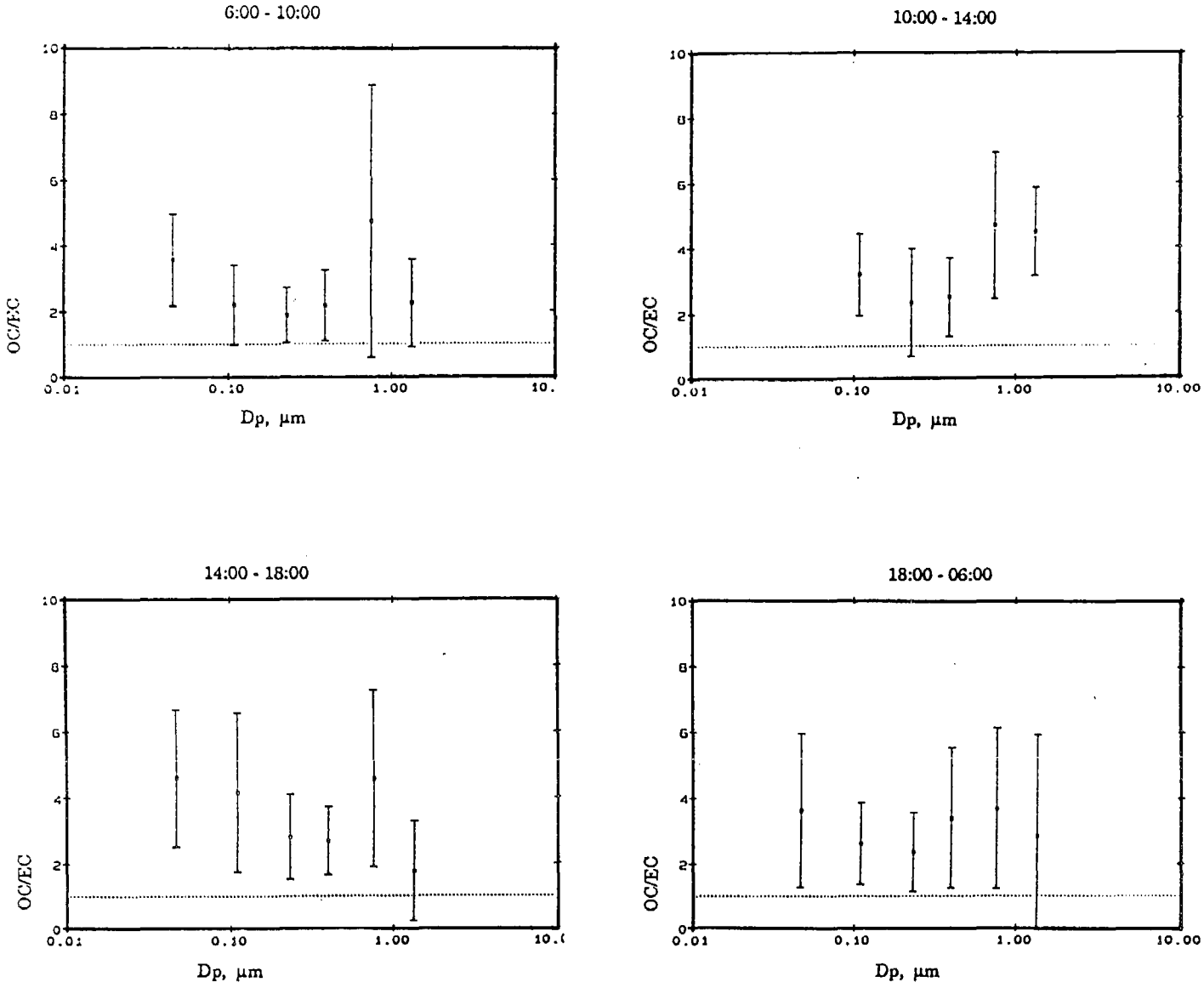


Figure 5. Average ROC/EC ratios for MOUDI data collected at Claremont as a function of particle size. Results are shown for four sampling times. The bars represent standard deviations of the means.

RUBIDOUX OC/EC vs Dp

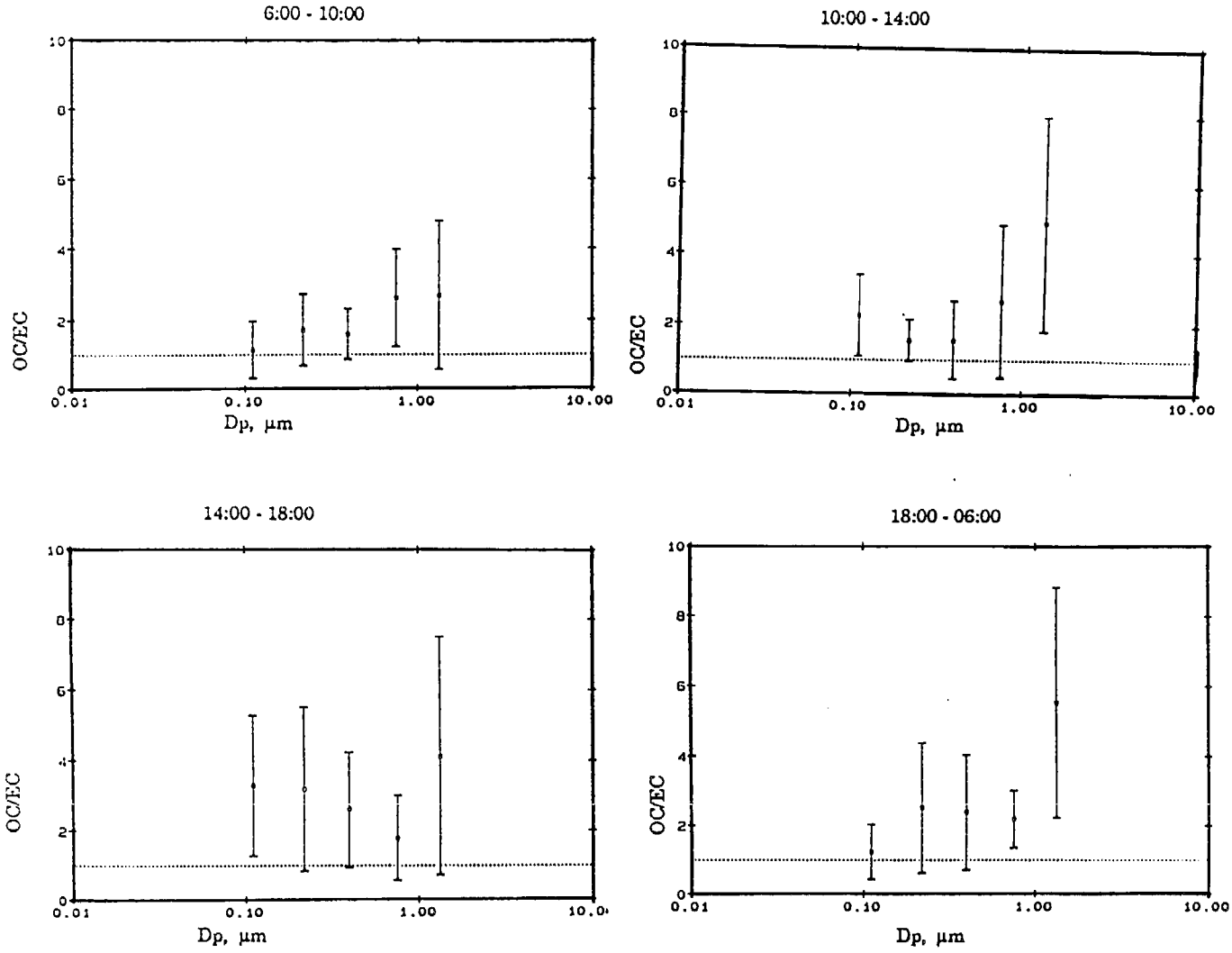


Figure 6. Average ROC/EC ratios for MOUDI data collected at Rubidoux as a function of particle size. Results are shown for four sampling times. The bars represent standard deviations of the means.

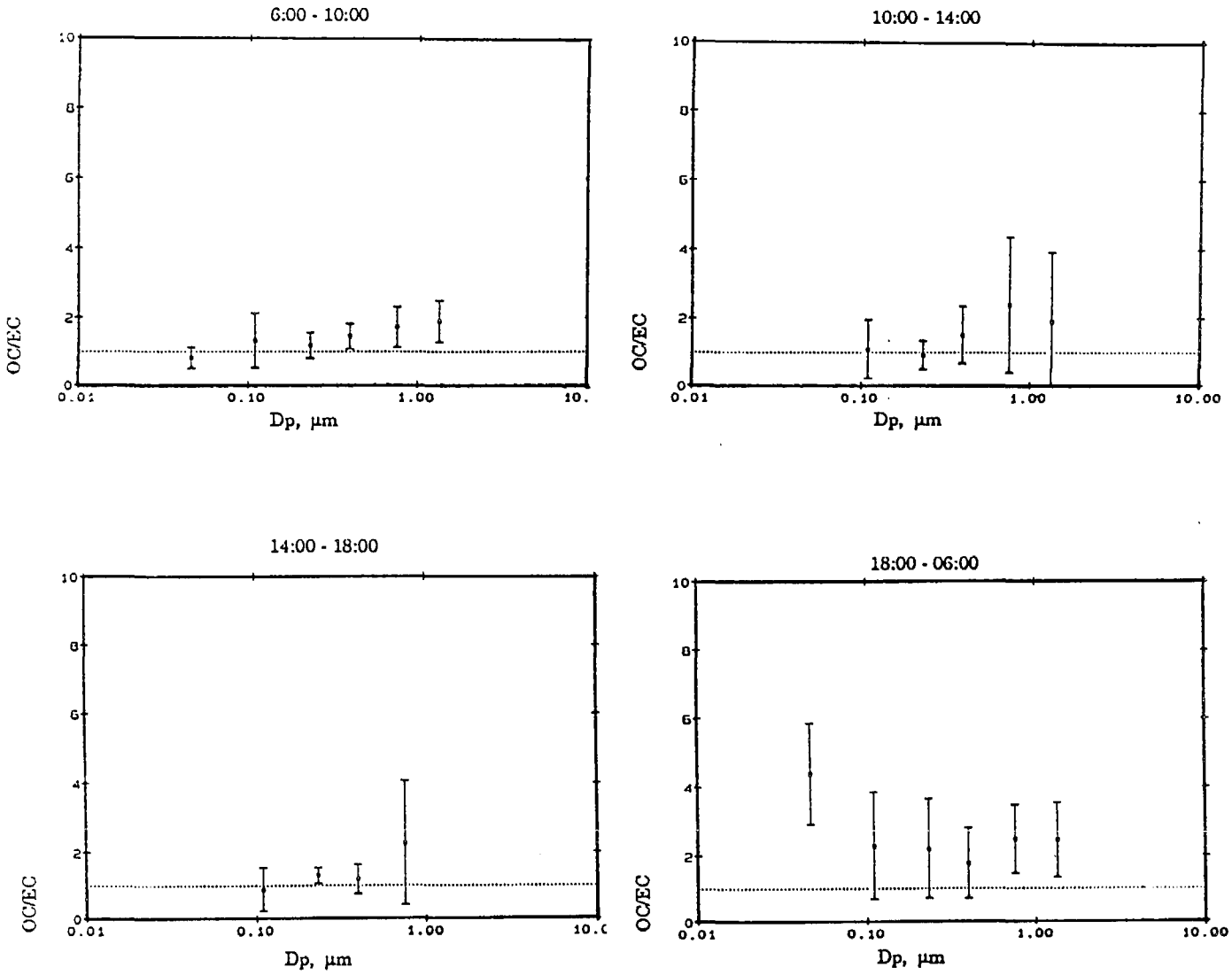


Figure 7. Average ROC/EC ratios for MOUDI data collected at Long Beach as a function of particle size. Results are shown for four sampling times. The bars represent standard deviations of the means.

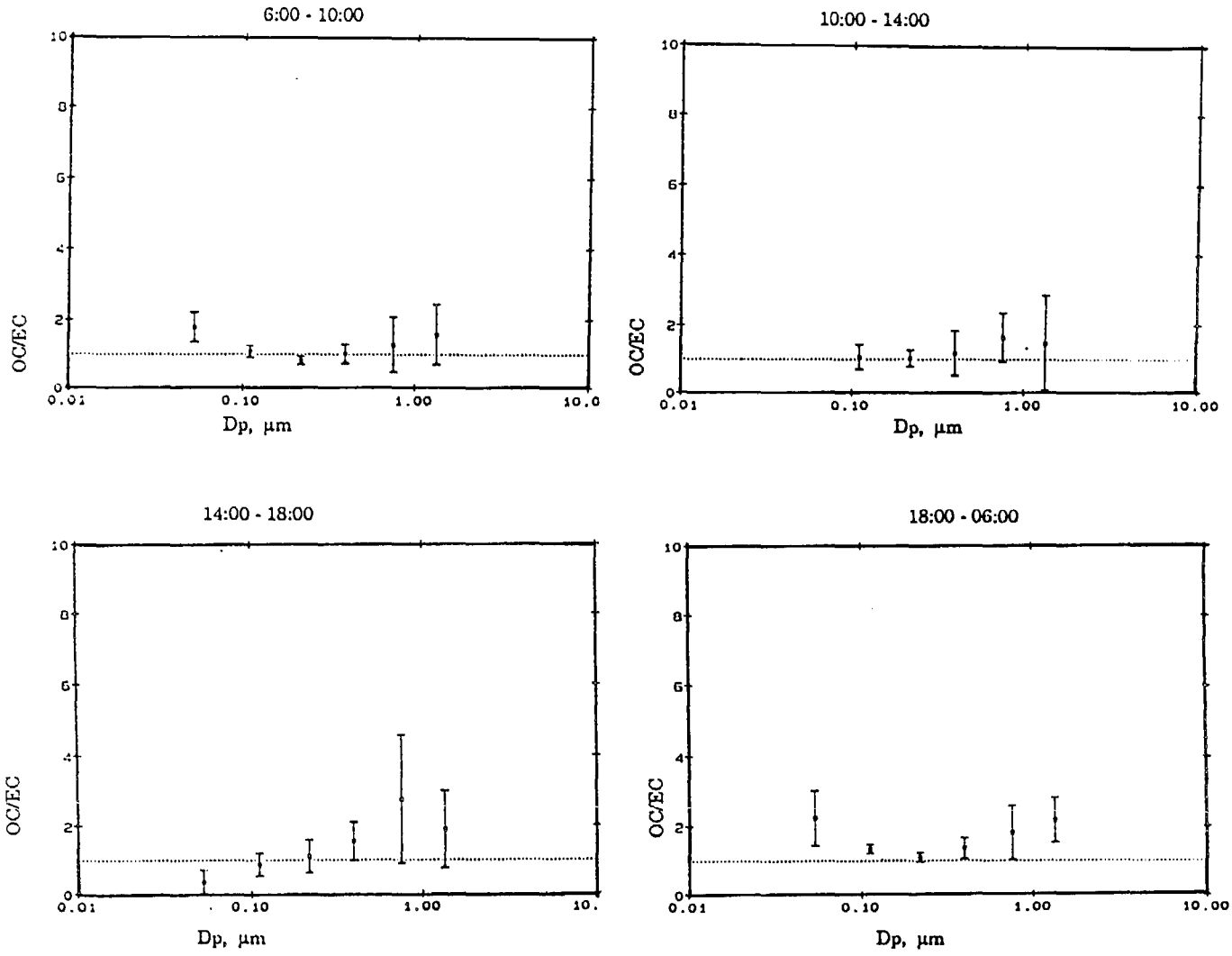


Figure 8. Average ROC/EC ratios for MOUDI data collected at Los Angeles as a function of particle size. Results are shown for four sampling times. The bars represent standard deviations of the means.

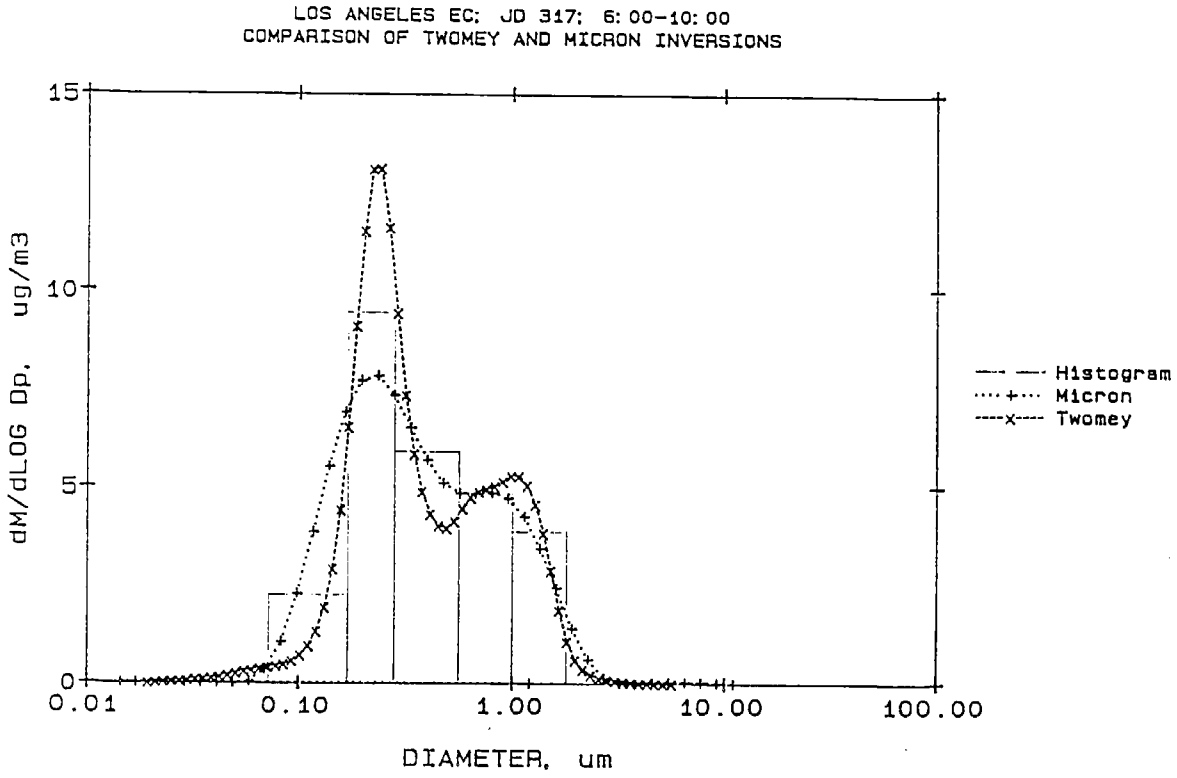


Figure 9. A comparison of raw data (histogram) with inverted size distributions obtained with the MICRON and Twomey methods.

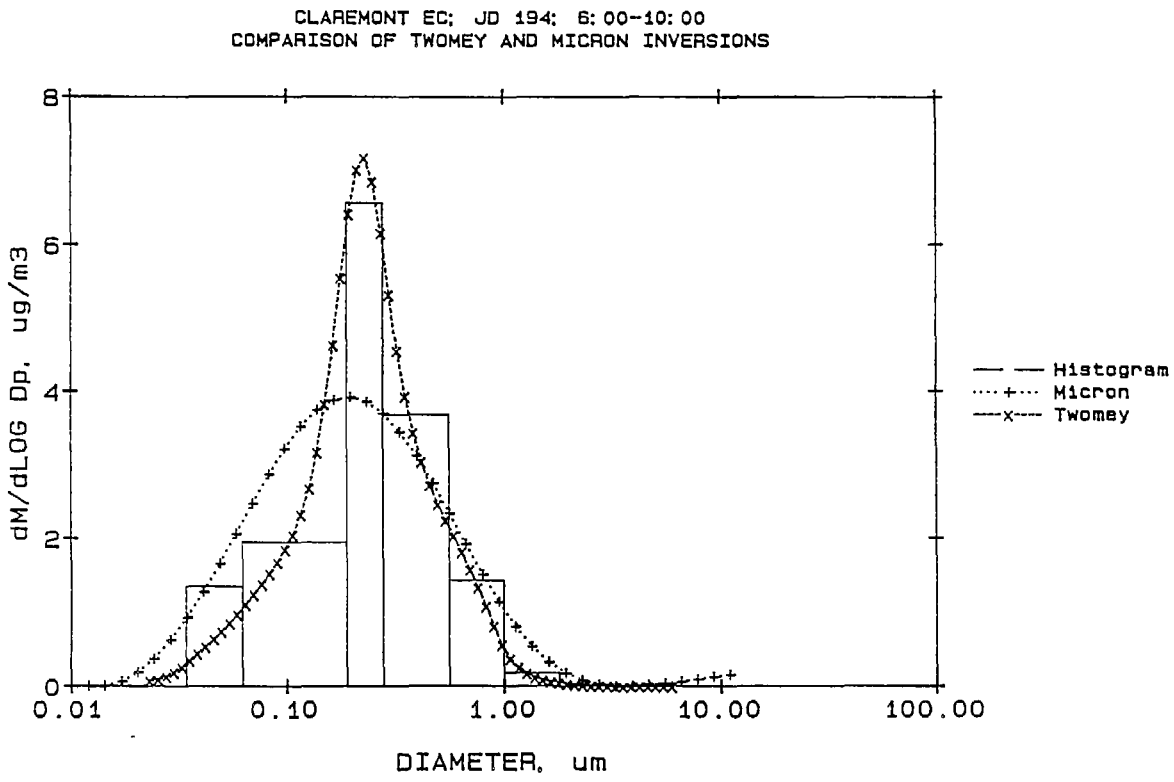


Figure 10. A comparison of raw data (histogram) with inverted size distributions obtained with the MICRON and Twomey methods.

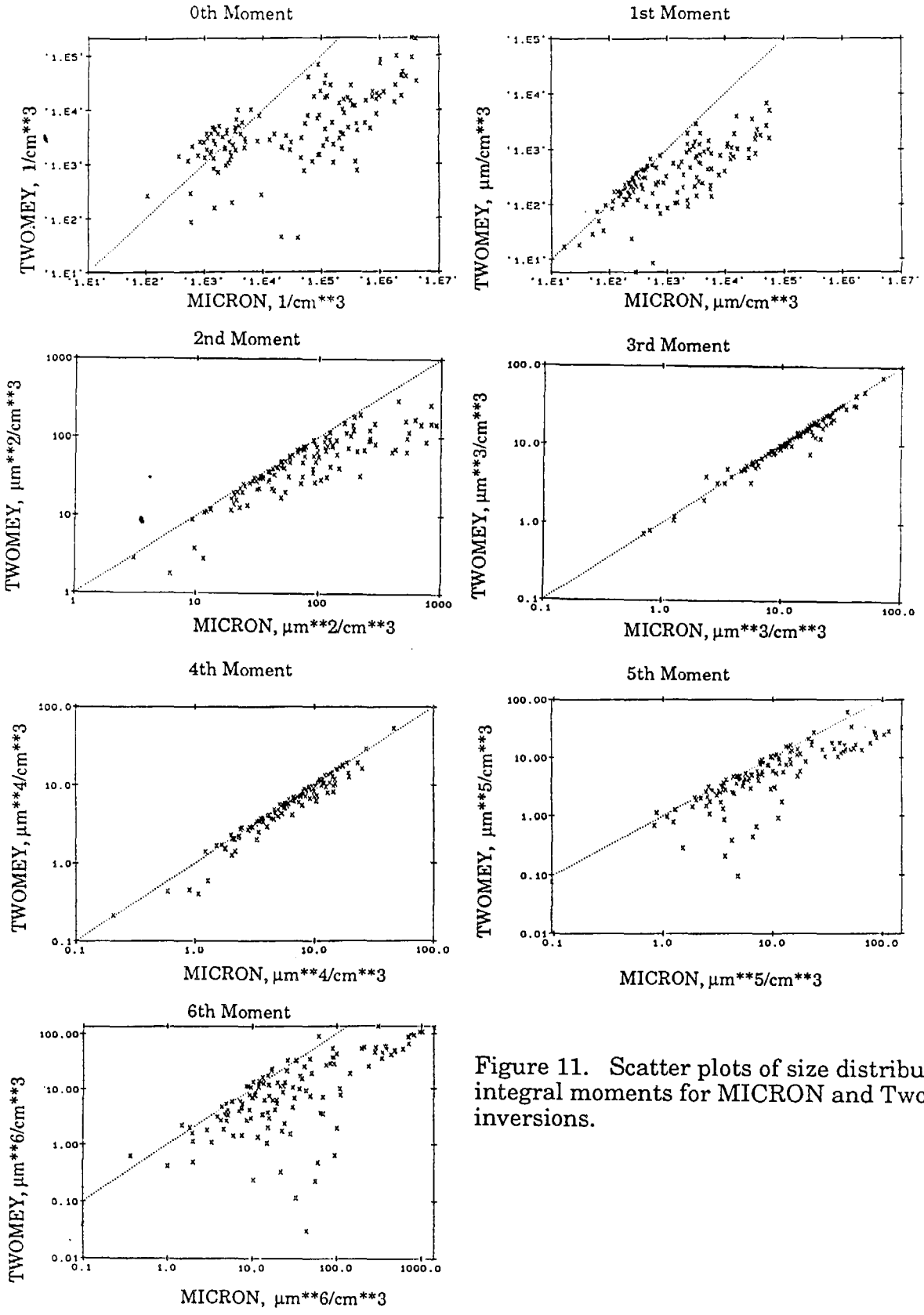


Figure 11. Scatter plots of size distribution integral moments for MICRON and Twomey inversions.

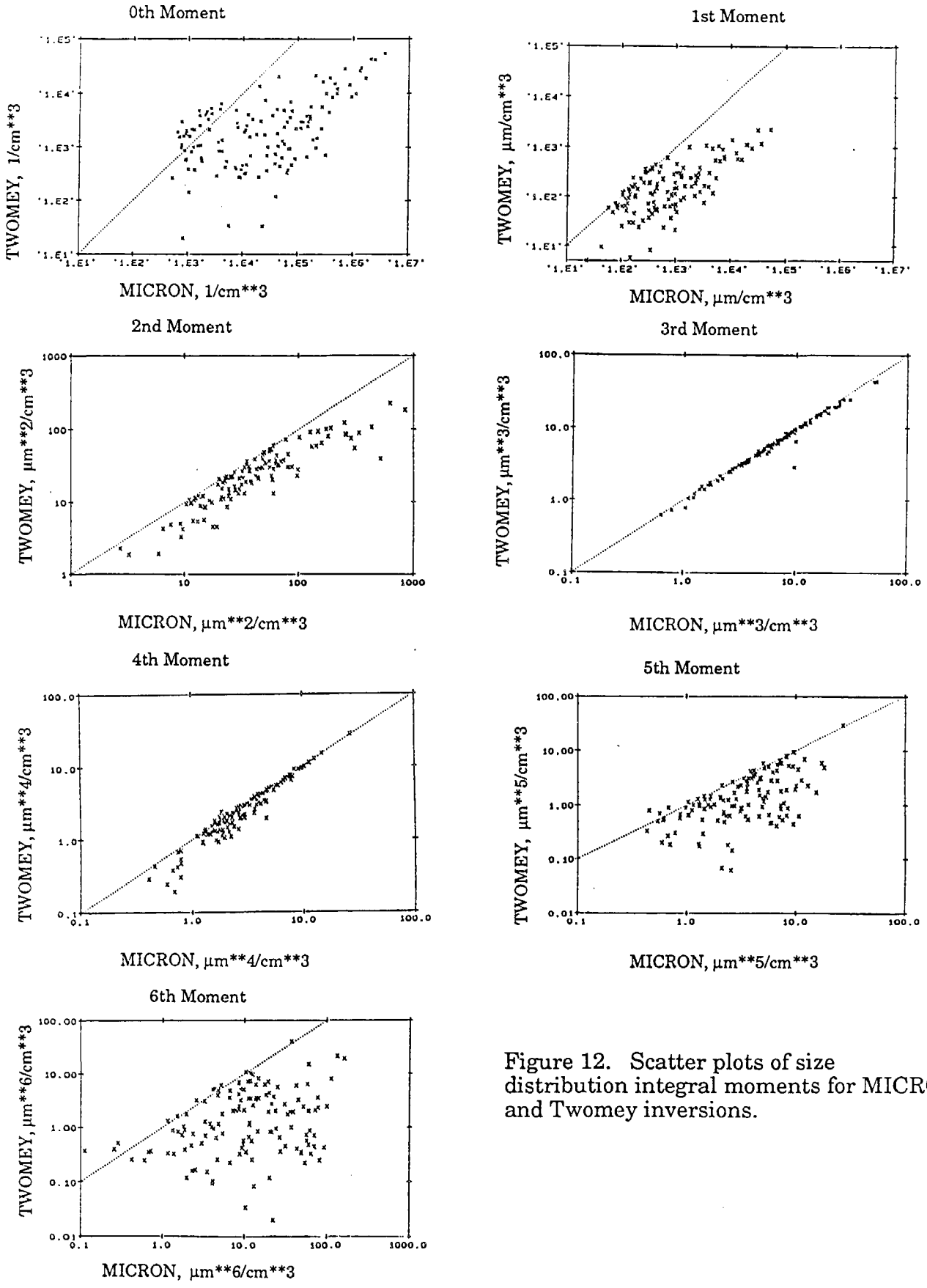


Figure 12. Scatter plots of size distribution integral moments for MICRON and Twomey inversions.

Based on the results shown in Figures 9 and 10 it is not surprising the MICRON integral moments tend to be greater than Twomey integral moments as m becomes larger or smaller than 3. Values of $I_m$ are dominated by the small end of the mass distribution for m<3, and are dominated by the large end of the distribution for m>3. MICRON size distributions are greater than Twomey size distributions at both the small and large end of the size spectrum, and the integral moments for small or large m accentuate these differences.

The discrepancies between the Twomey and MICRON integral moments are disturbing. It is beyond the scope of this report to reach any firm conclusions regarding the validity of one or the other technique. Both methods claim to produce size distributions that are consistent with the data to within experimental uncertainties. The large discrepancies for large and small moments probably occur because they are dominated by loadings on the top and bottom impactor stages, respectively. The reported loadings on these stages were often much smaller than estimated uncertainties. Therefore, the inverted size distribution for particles that might have been caught on these stages could, in principle, vary over a wide range and still fall within uncertainty estimates. We conclude that if integral moments calculated with two different inversion methods are greatly different, then it is probably not possible to determine an accurate value for that integral with the reported data. For consistency with other SCAQS impactor measurements we have chosen to report results based on the Twomey inversion algorithm.

Winklmayr and John routinely fit multimodal lognormal distributions to the inverted size distributions. The purpose of this is to determine simple distribution parameters that can be used to characterize essential features of the size distribution, and to simplify computations involving the use of size distributions. We have used the multimodal fitting program of Winklmayr and John to fit all of the inverted MOUDI ROC and EC data. Sample comparisons of inverted size distributions and bimodal lognormal fits to the inverted size distributions are shown in Figures 13 and 14. Note that the bimodal fits are in reasonable agreement with the inverted size distributions. It was found that on average the mass of the fitted size distribution was within 3% of the mass of the measured mass.

Scatter plots showing mode mass versus mode geometric mean diameter are shown in Figures 15 to 18 for the four sampling sites. Each figure shows results for a given site. The results on the top of the figures apply to the Twomey inversions while the results on the bottom apply to MICRON. The two figures on the left side of each page are for ROC and the two on the right are for EC. The most striking result is in these figures is in Figure 18. Note that Twomey shows both ROC and EC to be separated into two modal groups. Modal separations from MICRON are not so distinct.

Frequency distributions for mode geometric mean diameters are shown in Figures 19 and 20. Again, results are given for both the Twomey (top) and MICRON (bottom) inversions. Each distribution contains results for ROC and EC. Figure 19 applies to Claremont and Rubidoux data, and Figure 20 applies to Long Beach and Los Angeles data. Note that bimodal fits to Twomey inversions are more likely to produce a mode at the large particle end (near 1 μm) of the size spectrum. Note also that there is typically a rather close correlation between modal frequencies for ROC and EC.

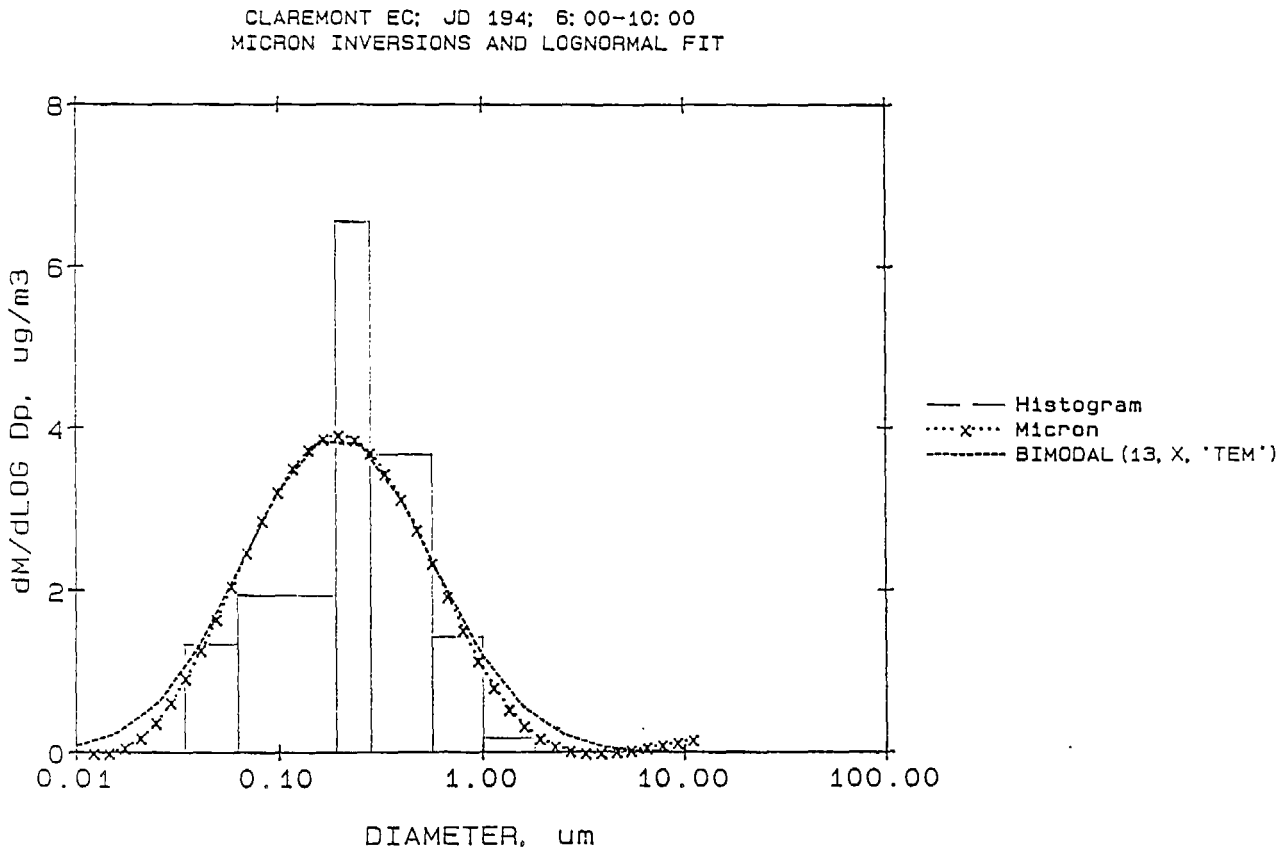


Figure 13. Comparison of raw data (histogram), MICRON inverted size distribution, and lognormal fit to the MICRON inverted size distribution.

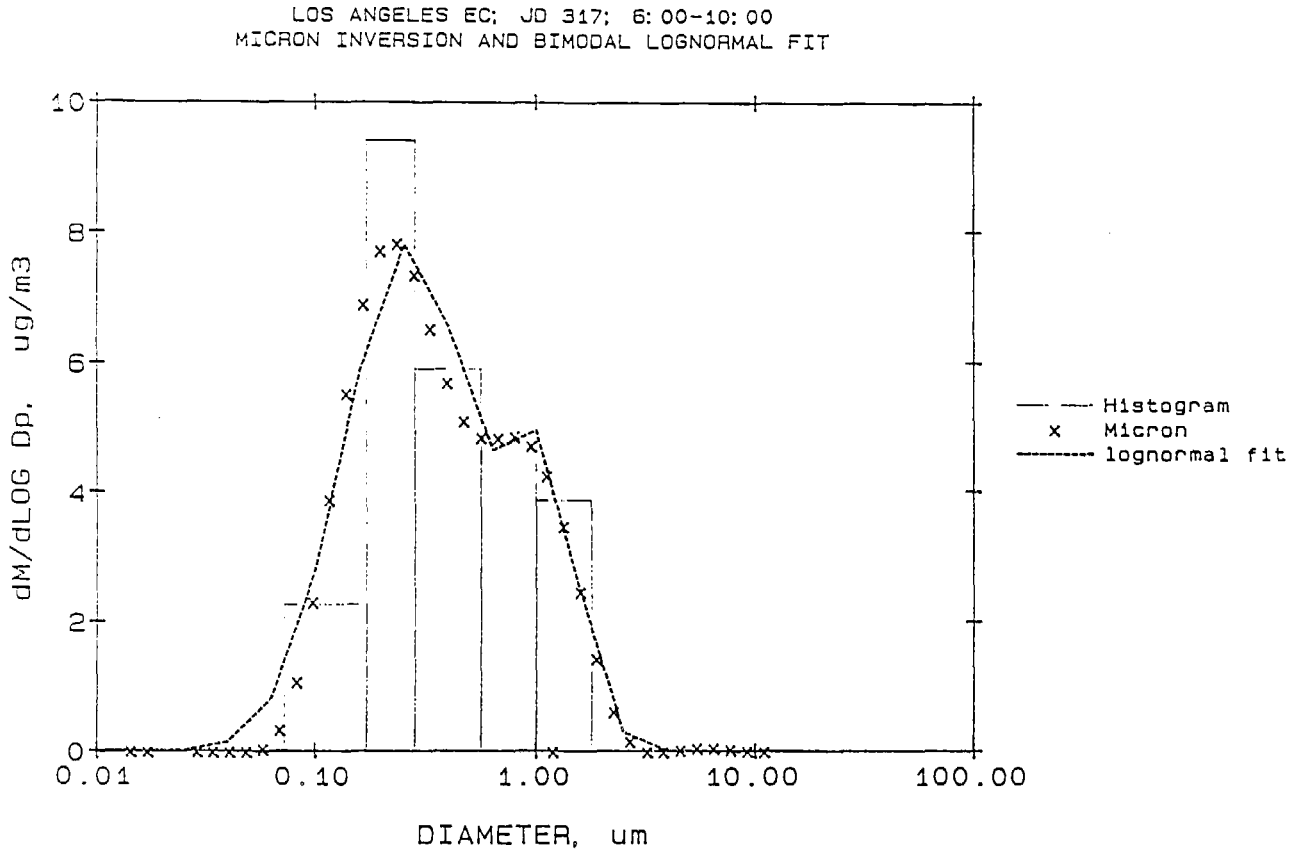


Figure 14. Comparison of raw data (histogram), MICRON inverted size distribution, and lognormal fit to the MICRON inverted size distribution.

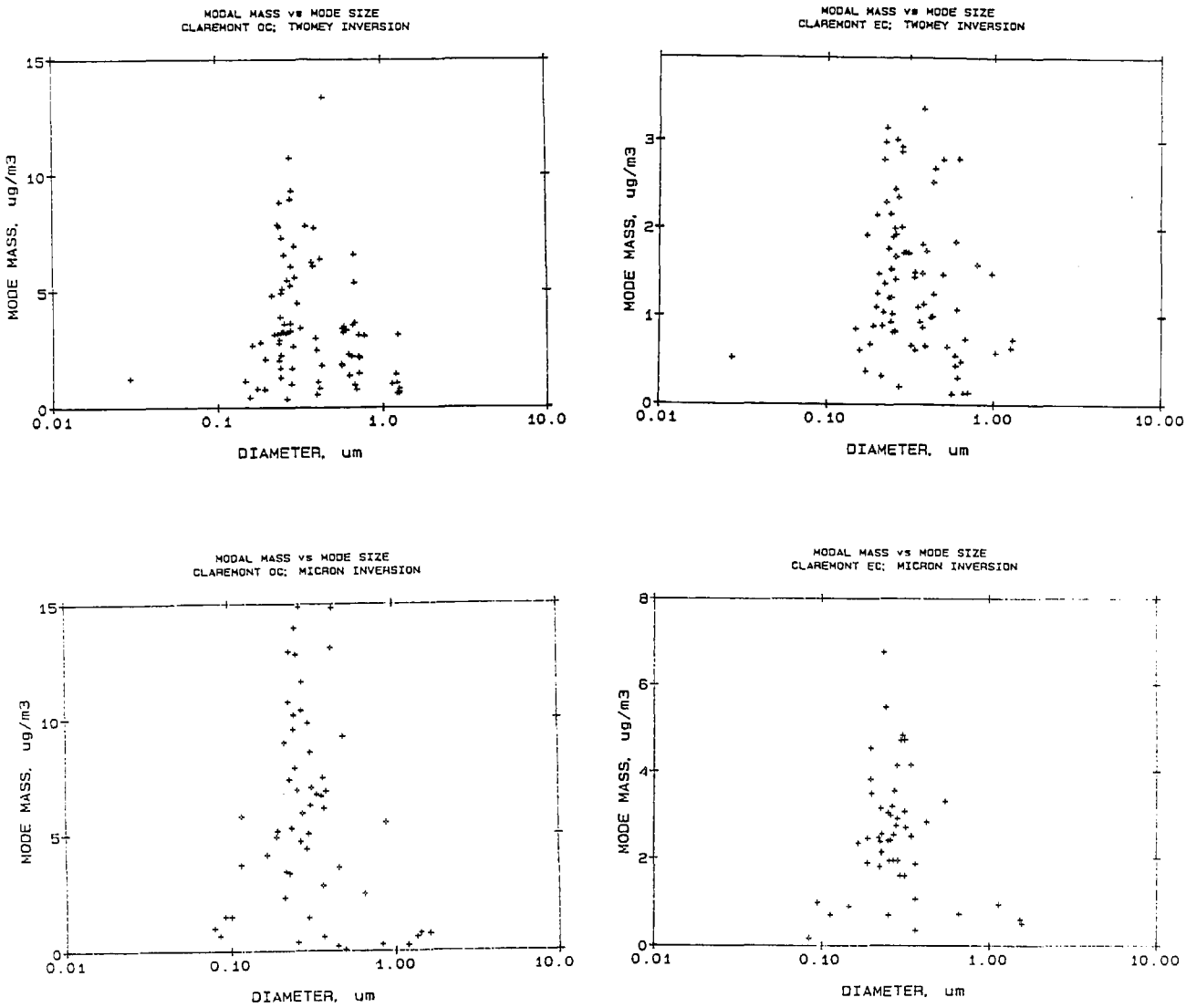


Figure 15. Modal mass versus geometric mean diameter for Claremont ROC and EC data. The results on the top of the page were obtained with the TWOMEY inversion while the results on the bottom were obtained with MICRON.

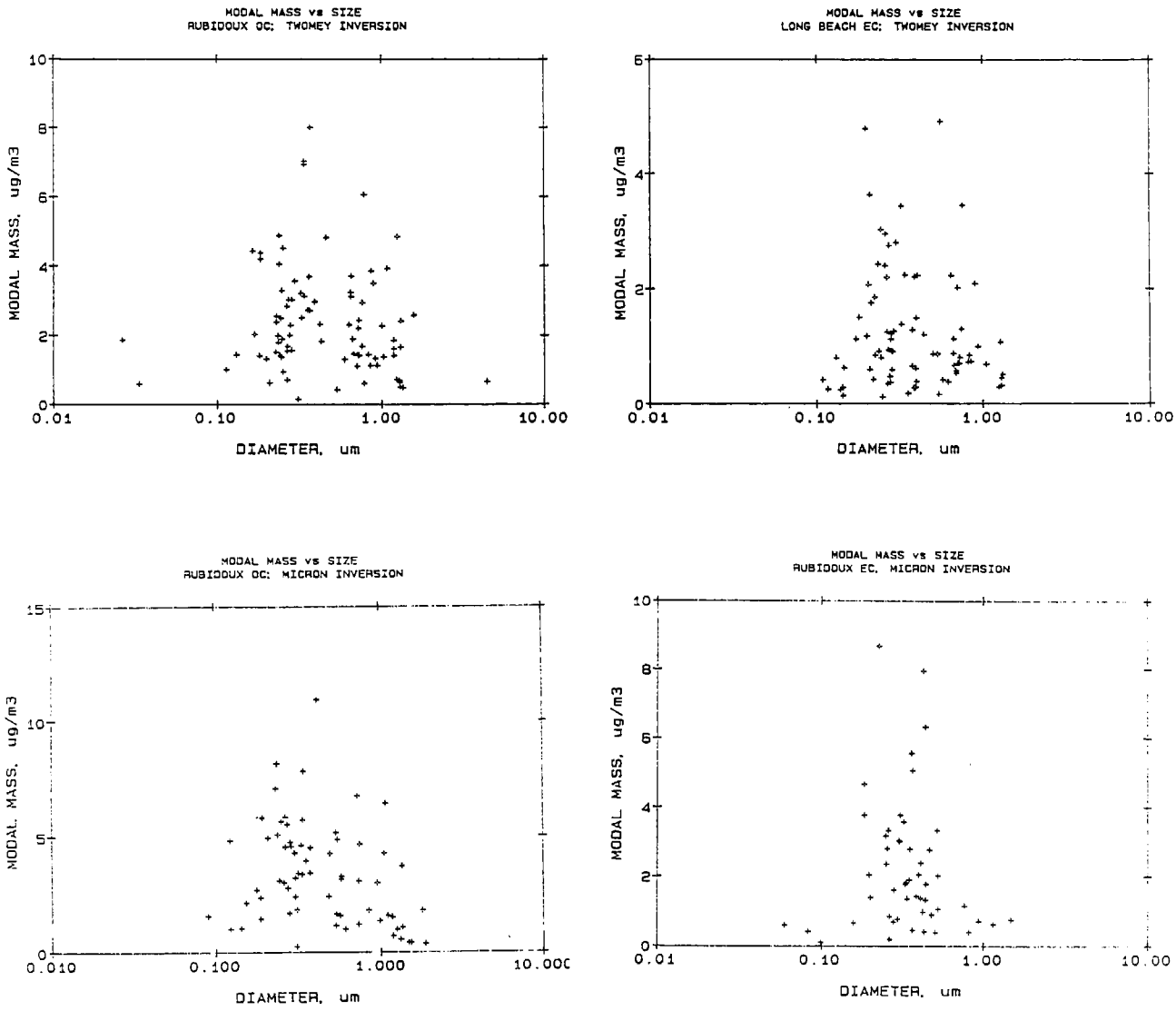


Figure 16. Modal mass versus geometric mean diameter for Rubidoux ROC and EC data. The results on the top of the page were obtained with the Twomey inversion while the results on the bottom were obtained with MICRON.

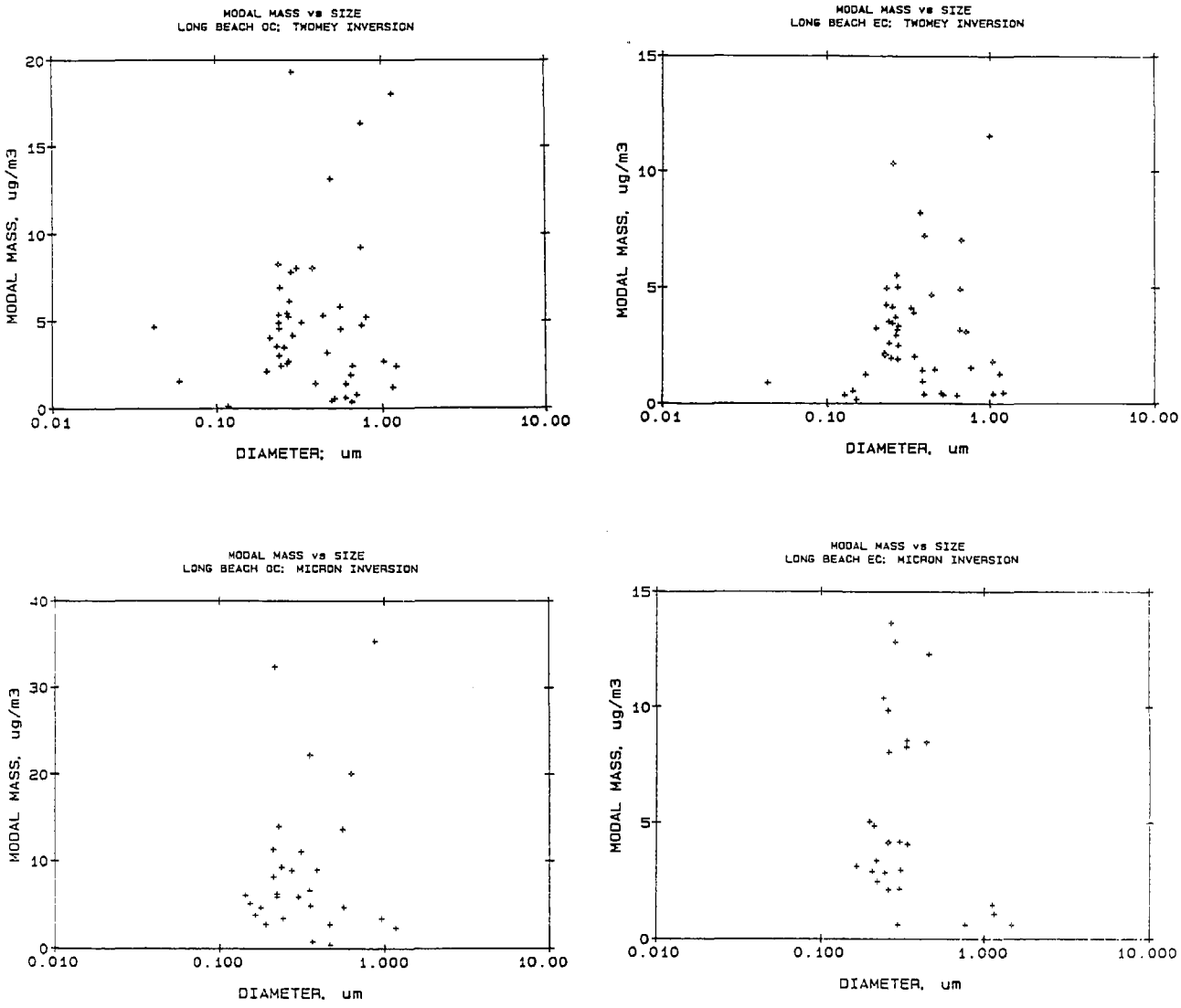


Figure 17. Modal mass versus geometric mean diameter for Long Beach ROC and EC data. The results on the top of the page were obtained with the Twomey inversion while the results on the bottom were obtained with MICRON.

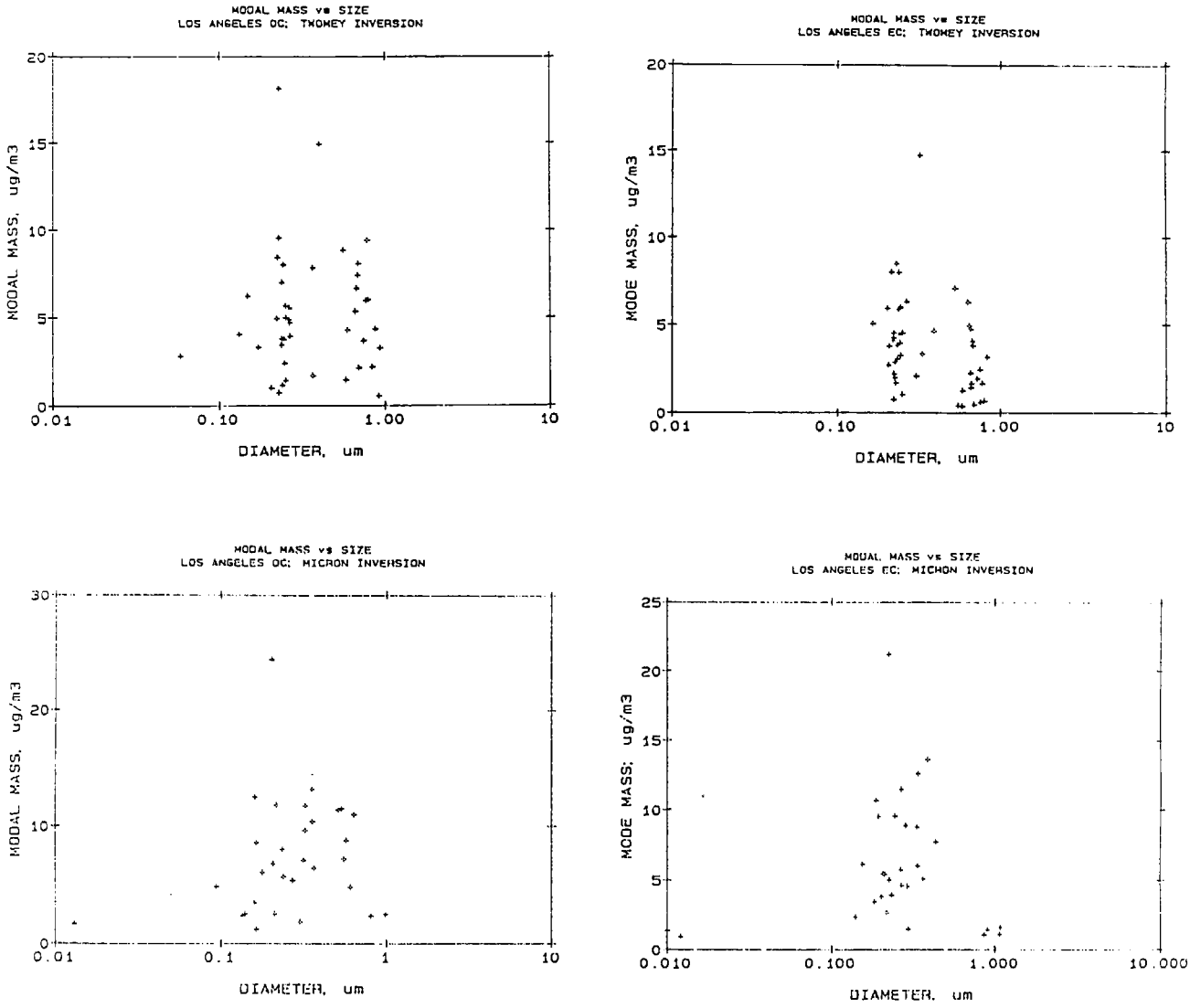


Figure 18. Modal mass versus geometric mean diameter for Los Angeles ROC and EC data. The results on the top of the page were obtained with the Twomey inversion while the results on the bottom were obtained with MICRON.

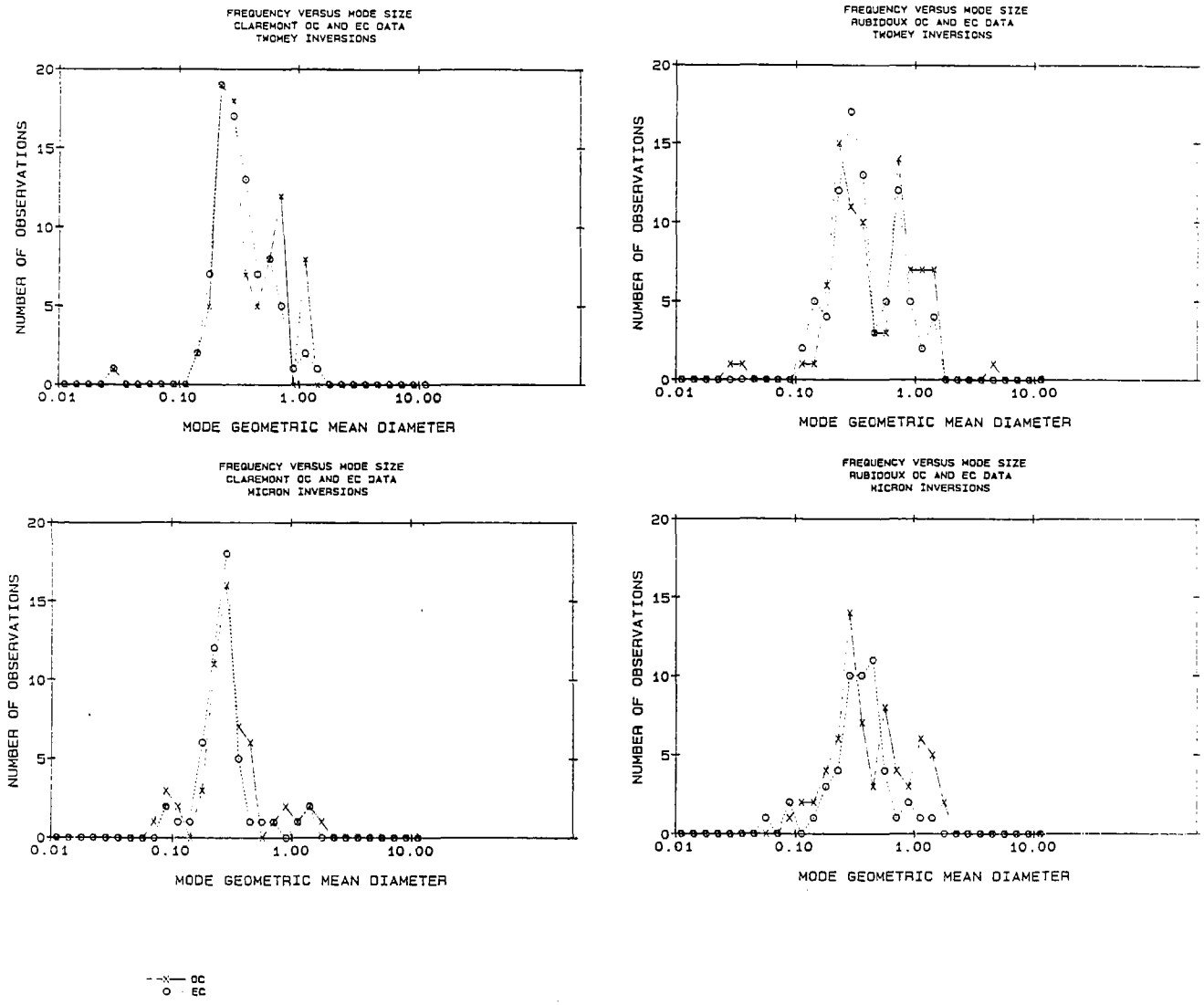


Figure 19. Frequency distributions for Claremont and Rubidoux modal geometric mean diameters for ROC and EC. Results are shown for both Twomey (top) and MICRON (bottom) inversions.

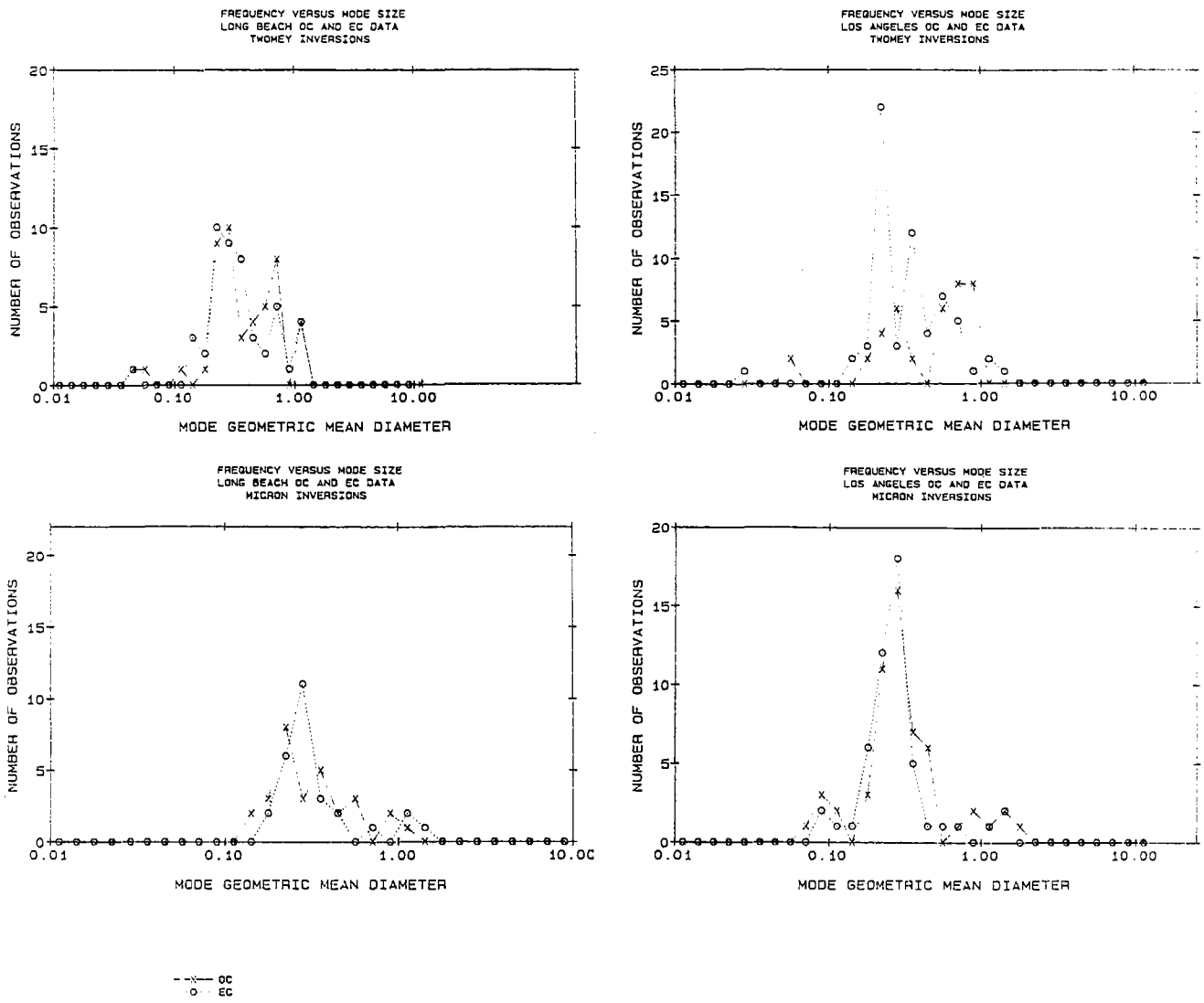


Figure 20. Frequency distributions for Long Beach and Los Angeles modal geometric mean diameters for ROC and EC. Results are shown for both Twomey (top) and MICRON (bottom) inversions.

Comparison With Data From Other Carbon Samplers

MOUDI ROC and EC data from Claremont have been compared with similar data from other samplers. Results of those comparisons are discussed in this section. The total ROC and EC concentrations from MOUDI samples were obtained by adding the loadings on all stages excluding the afterfilters. The afterfilters were excluded because of adsorption artifacts that have been encountered in previous work (McMurry and Zhang, 1989). Excluding the afterfilter data should have a minor effect on the total ROC or EC loadings since only a small fraction of the total fine particle loading is likely to be found in particles too small to be collected on the bottom impactor stage (≃0.05 μm cutoff diameter).

C with ROC collected with the SCAQS sampler are shown in Figures 21 to 23. Quartz filters were used to collect fine (sub–2.5 μm) samples for ROC and EC analyses. Samples were also collected on a quartz filter located downstream of a Teflon prefilter. The purpose of the quartz backup filter was to correct for artifacts due to gas adsorption. Analyses of filters collected with the SCAQS sampler were also done at ERT using the same technique that was used for the MOUDI samples.

In Figure 21 the SCAQS filter ROC loadings without adsorption correction are plotted against the MOUDI data (stages plus afterfilter). Note that the SCAQS filter data were systematically higher than the MOUDI data, but that the slope of the correlation (1.11) is reasonably good. McMurry and Zhang (3) present arguments to show that organic vapor adsorption can lead to substantially inflated ROC measurements on quartz filters such as those used in the SCAQS sampler. Based on these arguments it is believed that the SCAQS filter data in Figure 21 which are not corrected for adsorption probably overestimate the true ROC loadings.

In Figure 22 the adsorption–corrected SCAQS sampler fine particle ROC (filter minus afterfilter) are compared with MOUDI ROC (sum of stages excluding afterfilter). This plot provides our best estimate of the true ROC concentrations obtained with the SCAQS sampler and the MOUDI. Again, the SCAQS sampler is systematically higher than the MOUDI, and the correlation coefficient is poorer than for the data shown in Figure 21, where no adsorption correction was made.

Fine particle EC concentrations measured with the SCAQS sampler and the MOUDI are shown in Figure 23. Again, correlations are poor. MOUDI EC concentrations typically exceed Filter EC concentrations. This is in contrast to the ROC data where the filter concentrations are mostly higher.

MOUDI EC data are compared with data from the photoacoustic spectrometer operated by Ford (6) in Figure 24. Unlike the MOUDI method, the photoacoustic technique is based on insitu measurements of optical absorption. Although the MOUDI EC values are typically lower than the spectrometer, this correlation is better than the filter–MOUDI correlation. This is a surprising result given the different measurement principles. A similar result was found for data from the 1986 Carbonceous Species Methods Comparison Study (5) the where the best correlation for MOUDI EC data was with the LBL aethalometer (7), another optical absorption device.

The poor quality of the correlations between ROC and EC loadings for measurements with different samplers was expected based on previous experience (5). Reasons for these poor correlations are not understood. It is likely that both sampling and analytical methods play a significant role.

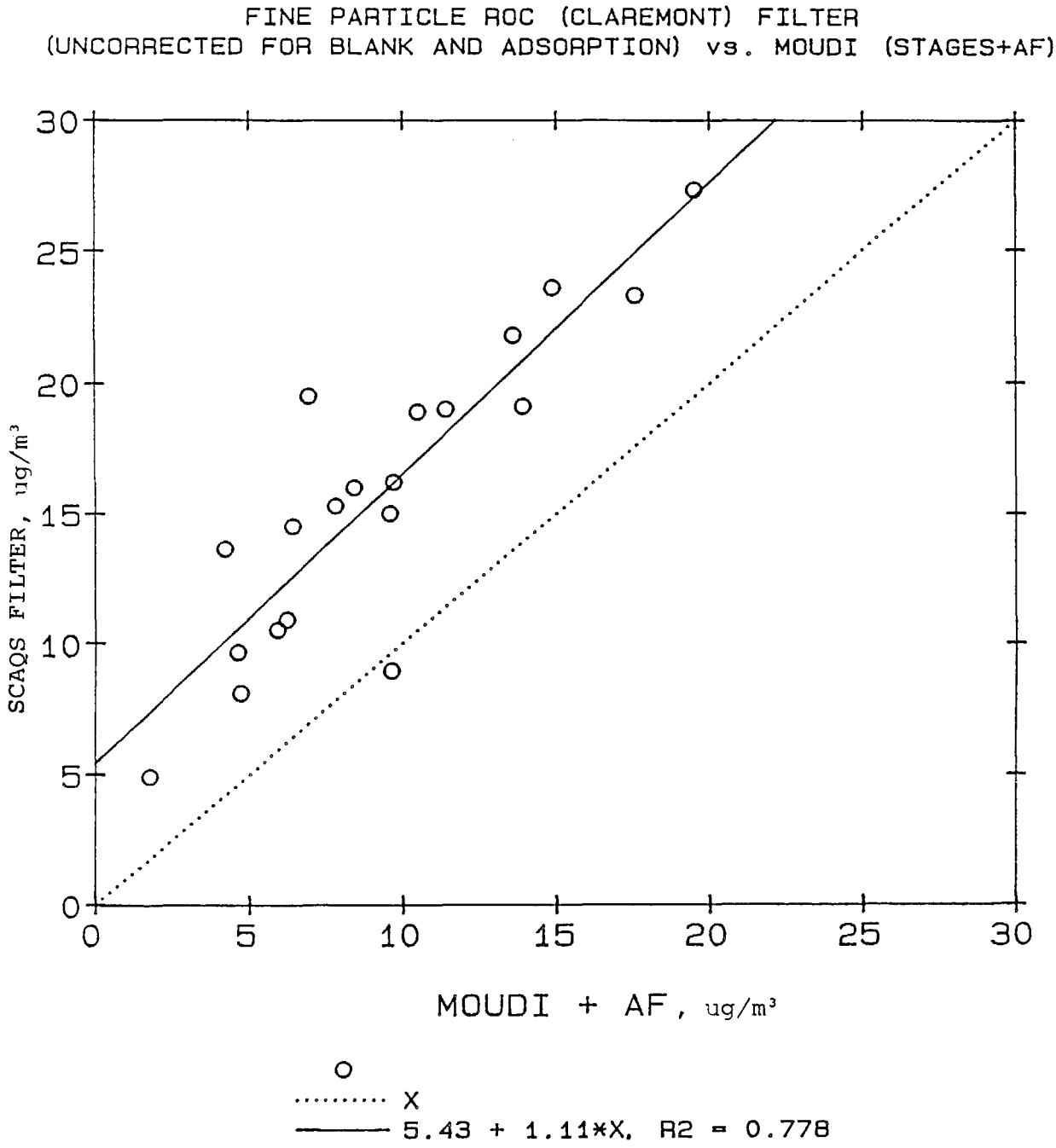


Figure 21. Fine particle ROC collected with the SCAQS sampler versus the MOUDI. No blank correction was done for the SCAQS sampler. The MOUDI data were obained by adding loadings from all stages plus the afterfilter.

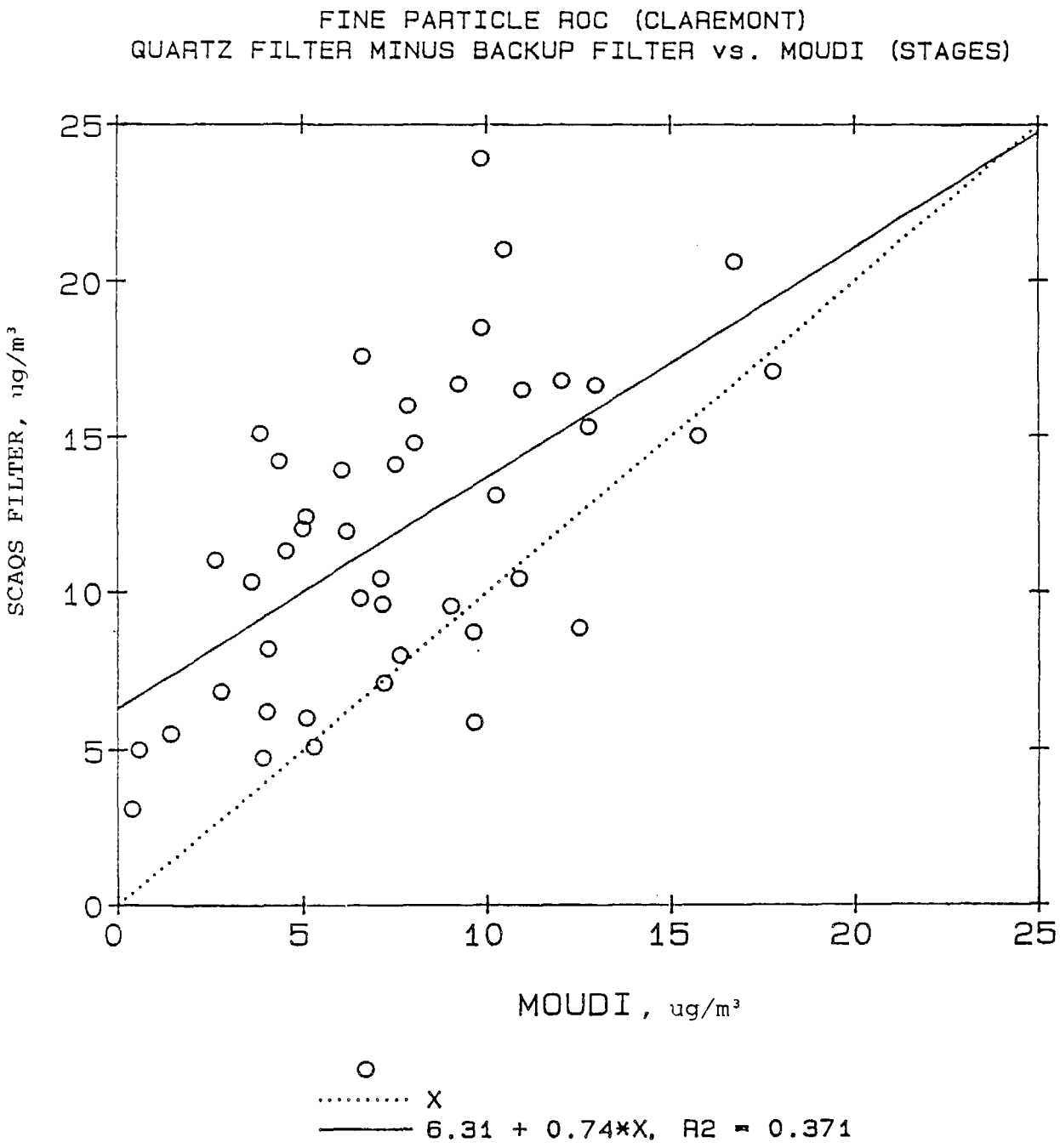


Figure 22. Fine particle ROC collected with the SCAQS sampler versus the MOUDI. The SCAQS sampler data have been corrected for blank and adsorption by subtracting the loading from a quartz filter located downstream of a Teflon filter. The MOUDI data were obtained by adding loadings from all stages (excluding the afterfilter). The amount of particulate ROC on the MOUDI afterfilter should be negligible since the lower size cuts of the bottom stages are about 0.05 um.

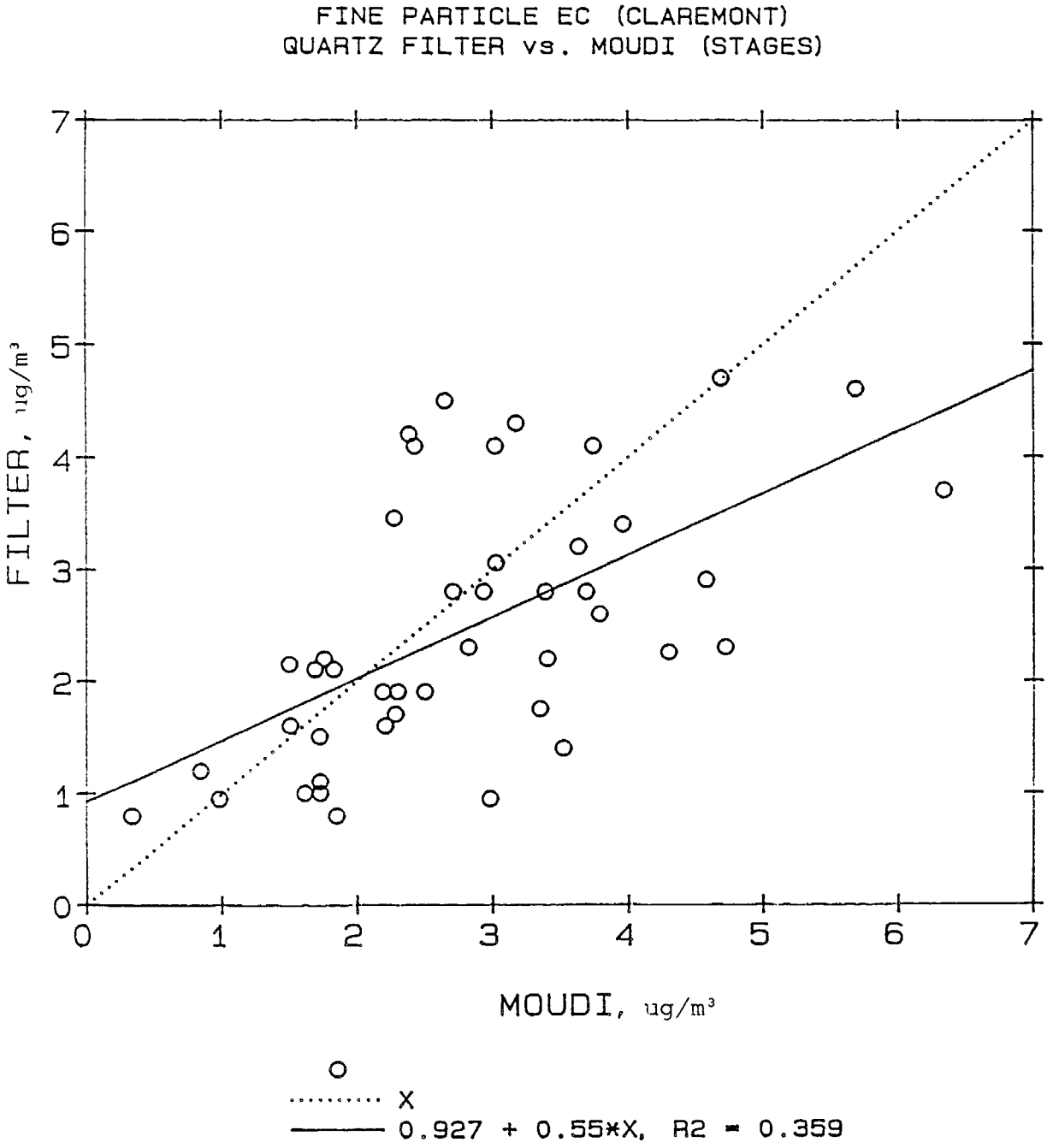


Figure 23. Fine particle EC collected with the SCAQS sampler versus the MOUDI.

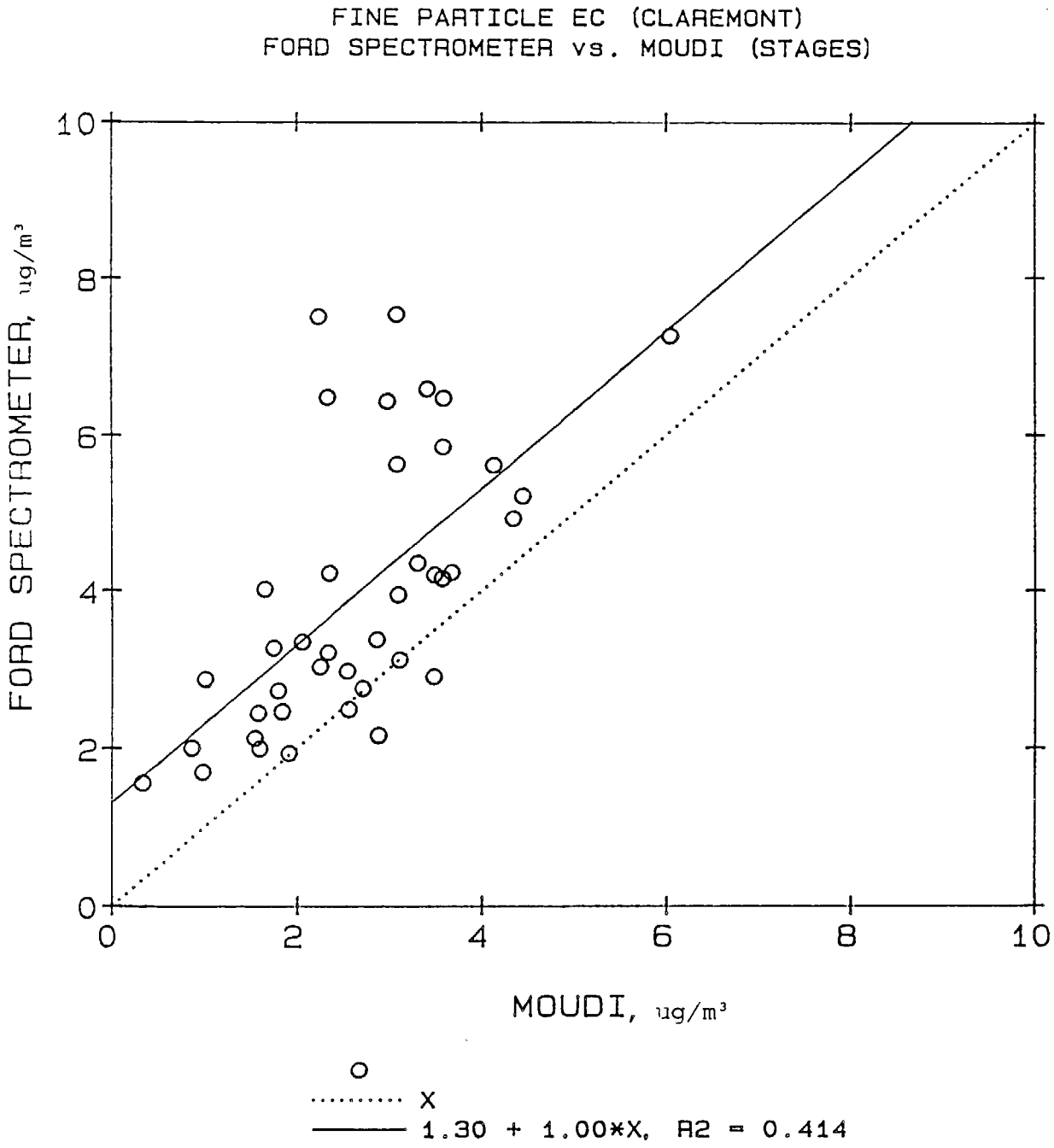


Figure 24. Fine particle EC collected with the Ford spectrometer versus the MOUDI.

## ACKNOWLEDGMENTS

This research was supported primarily by the Coordinating Research Council, 219 Perimeter Center Parkway, Atlanta, GA 30346. The California Air Resources Board contributed support for travel expenses incurred during the Fall study measurements.

## REFERENCES

1. Marple V.A. and Rubow K.L. (1984) Final Report on DOE Contract No. DE–FG22–83PC61255, Dept. Mech. Eng., Univ. of MN, 111 Church St. SE, Minneapolis, MN 55455.

2. Mueller P.K., Fung K.K., Heisler S.L. Grosjean D. and Hidy G.M. (1982) in Particulate Carbon: Atmospheric Life Cycle, G.T. Wolff, T.L. Klimisch, Eds, Plenum Press, NY.

3. McMurry P.H. and Zhang X.Q. (1989) Size distributions of ambient organic and elemental carbon. Aerosol Sci. Technol., 10:430–437.

4. John W. and Reischl G. (1980) J. Air Pollut. Control Assoc. 30:872.

5. McMurry, P.H. and X.Q. Zhang (1988) The Carbonaceous Species Methods Comparison Study: University of Minnesota Results, Report to the Coordinating Research Council Inc, 219 Perimeter Center Parkway, Atlanta, GA 30346.

6. A.C. Szkarlat and S.M. Japar (1981) Light absorption by airborne aerosols: comparison of integrating plate and spectrophone techniques, Applied Optics 20:1151–1154.

7. Hansen, A.D.A., H. Rosen, and T. Novakov (1984) The Aethalometer–an instrument for the real–time measurement of optical absorption by aerosol particles, Sci. Total Environ. 36:191–194.

APPENDIX I

# SUMMARY OF MOUDI SAMPLES ACQUIRED DURING SCAQS

# CLAREMONT SAMPLES

| Date | Julian Date | Sample ID | Start Time | Stop Time | Elapsed Time(min) | Volume ($m^3$) |
|---|---|---|---|---|---|---|
| 19–JUN–87 | 170 | CL–MN–MI–170 | 06:18 | 09:32 | 188 | 5.55 |
| 19–JUN–87 | 170 | CL–MN–MI–170 | 10:01 | 13:33 | 212 | 6.25 |
| 19–JUN–87 | 170 | CL–MN–MI–170 | 14:13 | 17:32 | 199 | 5.87 |
| 19–JUN–87 | 170 | CL–MN–MI–170 | 18:14 | 01:00 | 406 | 12.0 |
| 24–JUN–87 | 175 | CL–MN–MI–175 | 06:00 | 09:40 | 220 | 6.60 |
| 24–JUN–87 | 175 | CL–MN–MI–175 | 10:01 | 13:34 | 213 | 6.39 |
| 24–JUN–87 | 175 | CL–MN–MI–175 | 14:00 | 17:33 | 213 | 6.39 |
| 24–JUN–87 | 175 | CL–MN–MI–175 | 18:00 | 05:33 | 693 | 20.7 |
| 25–JUN–87 | 176 | CL–MN–MI–176 | 06:00 | 09:30 | 210 | 6.30 |
| 25–JUN–87 | 176 | CL–MN–MI–176 | 10:05 | 13:36 | 211 | 6.33 |
| 25–JUN–87 | 176 | CL–MN–MI–176 | 14:00 | 17:33 | 213 | 6.39 |
| 25–JUN–87 | 176 | CL–MN–MI–176 | 18:00 | 01:00 | 420 | 12.6 |
| 13–JUL–87 | 194 | CL–MN–MI–194 | 06:00 | 09:39 | 219 | 6.62 |
| 13–JUL–87 | 194 | CL–MN–MI–194 | 10:07 | 13:33 | 206 | 6.63 |
| 13–JUL–87 | 194 | CL–MN–MI–194 | 14:05 | 17:44 | 219 | 6.62 |
| 13–JUL–87 | 194 | CL–MN–MI–194 | 18:20 | 05:29 | 669 | 20.2 |
| 14–JUL–87 | 195 | CL–MN–MI–195 | 06:00 | 09:39 | 219 | 6.57 |
| 14–JUL–87 | 195 | CL–MN–MI–195 | 10:00 | 13:30 | 210 | 6.30 |
| 14–JUL–87 | 195 | CL–MN–MI–195 | 14:00 | 17:30 | 210 | 6.30 |
| 14–JUL–87 | 195 | CL–MN–MI–195 | 18:00 | 05:30 | 690 | 20.7 |
| 15–JUL–87 | 196 | CL–MN–MI–196 | 06:00 | 09:37 | 217 | 6.36 |
| 15–JUL–87 | 196 | CL–MN–MI–196 | 10:22 | 13:38 | 196 | 6.02 |
| 15–JUL–87 | 196 | CL–MN–MI–196 | 14:00 | 17:30 | 210 | 6.30 |
| 15–JUL–87 | 196 | CL–MN–MI–196 | 18:00 | 01:00 | 420 | 12.7 |
| 27–AUG–87 | 239 | CL–MN–MI–239 | 06:07 | 09:49 | 222 | 6.68 |
| 27–AUG–87 | 239 | CL–MN–MI–239 | 10:01 | 13:46 | 225 | 6.77 |
| 27–AUG–87 | 239 | CL–MN–MI–239 | 13:54 | 17:48 | 234 | 7.04 |
| 27–AUG–87 | 239 | CL–MN–MI–239 | 17:56 | 05:50 | 714 | 21.5 |
| 28–AUG–87 | 240 | CL–MN–MI–240 | 06:02 | 09:44 | 222 | 6.68 |
| 28–AUG–87 | 240 | CL–MN–MI–240 | 09:52 | 13:39 | 227 | 6.83 |
| 28–AUG–87 | 240 | CL–MN–MI–240 | 13:47 | 17:51 | 244 | 7.34 |
| 28–AUG–87 | 240 | CL–MN–MI–240 | 18:00 | 05:50 | 710 | 21.5 |
| 29–AUG–87 | 241 | CL–MN–MI–241 | 05:58 | 09:56 | 238 | 7.16 |
| 29–AUG–87 | 241 | CL–MN–MI–241 | 10:04 | 13:43 | 219 | 6.59 |
| 29–AUG–87 | 241 | CL–MN–MI–241 | 13:50 | 17:50 | 240 | 7.22 |
| 29–AUG–87 | 241 | CL–MN–MI–241 | 17:56 | 00:53 | 417 | 12.6 |
| 02–SEP–87 | 245 | CL–MN–MI–245 | 06:00 | 09:50 | 230 | 6.92 |
| 02–SEP–87 | 245 | CL–MN–MI–245 | 09:56 | 13:48 | 232 | 6.98 |
| 02–SEP–87 | 245 | CL–MN–MI–245 | 13:53 | 17:59 | 246 | 7.38 |
| 02–SEP–87 | 245 | CL–MN–MI–245 | 18:09 | 05:54 | 705 | 21.2 |
| 03–SEP–87 | 246 | CL–MN–MI–246 | 06:01 | 09:54 | 233 | 7.01 |
| 03–SEP–87 | 246 | CL–MN–MI–246 | 10:00 | 13:49 | 229 | 6.89 |
| 03–SEP–87 | 246 | CL–MN–MI–246 | 13:57 | 17:46 | 229 | 6.89 |
| 03–SEP–87 | 246 | CL–MN–MI–246 | 17:54 | 00:30 | 396 | 11.9 |

# RUBIDOUX SAMPLES

| Date | Julian Date | Sample ID | Start Time | Stop Time | Elapsed Time(min) | Volume ($m^3$) |
|---|---|---|---|---|---|---|
| 19–JUN–87 | 170 | RB–MN–MI–170 | 06:05 | 09:32 | 207 | 6.25 |
| 19–JUN–87 | 170 | RB–MN–MI–170 | 10:05 | 13:45 | 200 | 6.04 |
| 19–JUN–87 | 170 | RB–MN–MI–170 | 14:00 | 17:30 | 210 | 6.43 |
| 19–JUN–87 | 170 | RB–MN–MI–170 | 18:25 | 01:00 | 395 | 11.1 |
| 24–JUN–87 | 175 | RB–MN–MI–175 | 06:16 | 09:30 | 194 | 5.72 |
| 24–JUN–87 | 175 | RB–MN–MI–175 | 10:00 | 13:37 | 217 | 6.73 |
| 24–JUN–87 | 175 | RB–MN–MI–175 | 14:00 | 17:37 | 217 | 6.73 |
| 24–JUN–87 | 175 | RB–MN–MI–175 | 18:00 | 05:42 | 702 | 21.8 |
| 25–JUN–87 | 176 | RB–MN–MI–176 | 06:00 | 09:30 | 210 | 6.43 |
| 25–JUN–87 | 176 | RB–MN–MI–176 | 10:00 | 13:30 | 210 | 6.51 |
| 25–JUN–87 | 176 | RB–MN–MI–176 | 14:00 | 17:30 | 210 | 6.52 |
| 25–JUN–87 | 176 | RB–MN–MI–176 | 18:00 | 01:00 | 420 | 13.0 |
| 13–JUL–87 | 194 | RB–MN–MI–194 | 05:58 | 09:40 | 222 | 6.88 |
| 13–JUL–87 | 194 | RB–MN–MI–194 | 09:58 | 13:28 | 210 | 6.51 |
| 13–JUL–87 | 194 | RB–MN–MI–194 | 13:50 | 17:25 | 215 | 6.67 |
| 13–JUL–87 | 194 | RB–MN–MI–194 | 17:50 | 05:32 | 702 | 21.0 |
| 14–JUL–87 | 195 | RB–MN–MI–195 | 06:00 | 09:28 | 208 | 6.45 |
| 14–JUL–87 | 195 | RB–MN–MI–195 | 10:00 | 13:34 | 214 | 6.63 |
| 14–JUL–87 | 195 | RB–MN–MI–195 | 14:00 | 17:35 | 215 | 6.67 |
| 14–JUL–87 | 195 | RB–MN–MI–195 | 18:00 | 05:40 | 700 | 21.7 |
| 15–JUL–87 | 196 | RB–MN–MI–196 | 05:58 | 09:32 | 214 | 6.63 |
| 15–JUL–87 | 196 | RB–MN–MI–196 | 09:58 | 13:40 | 222 | 6.88 |
| 15–JUL–87 | 196 | RB–MN–MI–196 | 14:00 | 17:30 | 210 | 6.51 |
| 15–JUL–87 | 196 | RB–MN–MI–196 | 18:00 | 01:00 | 420 | 13.0 |
| 27–AUG–87 | 239 | RB–MN–MI–239 | 05:55 | 09:30 | 215 | 6.69 |
| 27–AUG–87 | 239 | RB–MN–MI–239 | 10:00 | 13:33 | 213 | 6.65 |
| 27–AUG–87 | 239 | RB–MN–MI–239 | 14:00 | 17:30 | 210 | 6.55 |
| 27–AUG–87 | 239 | RB–MN–MI–239 | 18:00 | 05:40 | 700 | 21.5 |
| 28–AUG–87 | 240 | RB–MN–MI–240 | 06:00 | 09:40 | 220 | 6.75 |
| 28–AUG–87 | 240 | RB–MN–MI–240 | 10:00 | 13:40 | 220 | 6.75 |
| 28–AUG–87 | 240 | RB–MN–MI–240 | 14:00 | 17:35 | 215 | 6.60 |
| 28–AUG–87 | 240 | RB–MN–MI–240 | 18:00 | 05:40 | 700 | 21.5 |
| 29–AUG–87 | 241 | RB–MN–MI–241 | 06:00 | 09:35 | 215 | 6.60 |
| 29–AUG–87 | 241 | RB–MN–MI–241 | 10:00 | 13:40 | 220 | 6.75 |
| 29–AUG–87 | 241 | RB–MN–MI–241 | 14:00 | 17:40 | 220 | 6.84 |
| 29–AUG–87 | 241 | RB–MN–MI–241 | 18:00 | 01:00 | 420 | 12.9 |
| 02–SEP–87 | 245 | RB–MN–MI–245 | 06:00 | 09:35 | 215 | 6.69 |
| 02–SEP–87 | 245 | RB–MN–MI–245 | 10:00 | 13:40 | 220 | 6.75 |
| 02–SEP–87 | 245 | RB–MN–MI–245 | 14:00 | 17:40 | 220 | 6.75 |
| 02–SEP–87 | 245 | RB–MN–MI–245 | 18:00 | 05:40 | 700 | 21.0 |
| 03–SEP–87 | 246 | RB–MN–MI–246 | 06:00 | 09:40 | 220 | 6.84 |
| 03–SEP–87 | 246 | RB–MN–MI–246 | 10:00 | 13:40 | 220 | 6.84 |
| 03–SEP–87 | 246 | RB–MN–MI–246 | 14:00 | 17:40 | 220 | 6.60 |
| 03–SEP–87 | 246 | RB–MN–MI–246 | 18:00 | 01:05 | 425 | 13.0 |

# Los Angeles Samples

| Date | Julian Date | Sample ID | Start Time | Stop Time | Elapsed Time(min) | Volume ($m^3$) |
|---|---|---|---|---|---|---|
| 11–NOV–87 | 315 | LA–MN–MI–307 | 06:27 | 09:30 | 183 | 5.49 |
| 11–NOV–87 | 315 | LA–MN–MI–307 | 10:00 | 13:30 | 210 | 6.30 |
| 11–NOV–87 | 315 | LA–MN–MI–307 | 14:00 | 17:30 | 210 | 6.30 |
| 11–NOV–87 | 315 | LA–MN–MI–307 | 18:00 | 05:30 | 690 | 20.7 |
| 12–NOV–87 | 316 | LA–MN–MI–308 | 06:00 | 09:30 | 210 | 6.30 |
| 12–NOV–87 | 316 | LA–MN–MI–308 | 10:00 | 13:30 | 210 | 6.30 |
| 12–NOV–87 | 316 | LA–MN–MI–308 | 14:00 | 17:30 | 210 | 6.30 |
| 12–NOV–87 | 316 | LA–MN–MI–308 | 18:00 | 05:30 | 690 | 20.7 |
| 13–NOV–87 | 317 | LA–MN–MI–309 | 06:00 | 09:30 | 210 | 6.30 |
| 13–NOV–87 | 317 | LA–MN–MI–309 | 10:00 | 13:30 | 210 | 6.30 |
| 13–NOV–87 | 317 | LA–MN–MI–309 | 14:00 | 17:30 | 210 | 6.30 |
| 13–NOV–87 | 317 | LA–MN–MI–309 | 18:00 | 00:00 | 360 | 10.8 |
| 03–DEC–87 | 337 | LA–MN–MI–329 | 06:00 | 09:30 | 210 | 6.30 |
| 03–DEC–87 | 337 | LA–MN–MI–329 | 10:00 | 13:30 | 210 | 6.30 |
| 03–DEC–87 | 337 | LA–MN–MI–329 | 14:00 | 17:30 | 210 | 6.30 |
| 03–DEC–87 | 337 | LA–MN–MI–329 | 18:00 | 00:00 | 360 | 10.8 |
| 10–DEC–87 | 344 | LA–MN–MI–336 | 06:00 | 09:30 | 210 | 6.30 |
| 10–DEC–87 | 344 | LA–MN–MI–336 | 10:00 | 13:30 | 210 | 6.30 |
| 10–DEC–87 | 344 | LA–MN–MI–336 | 14:00 | 17:30 | 210 | 6.30 |
| 10–DEC–87 | 344 | LA–MN–MI–336 | 18:00 | 05:30 | 690 | 20.7 |
| 11–DEC–87 | 345 | LA–MN–MI–337 | 06:00 | 09:30 | 210 | 6.30 |
| 11–DEC–87 | 345 | LA–MN–MI–337 | 10:00 | 13:30 | 210 | 6.30 |
| 11–DEC–87 | 345 | LA–MN–MI–337 | 14:00 | 17:30 | 210 | 6.30 |
| 11–DEC–87 | 345 | LA–MN–MI–337 | 18:00 | 00:00 | 240 | 7.20 |

# LONG BEACH SAMPLES

| Date | Julian Date | Sample ID | Start Time | Stop Time | Elapsed Time(min) | Volume ($m^3$) |
|---|---|---|---|---|---|---|
| 11–NOV–87 | 315 | LB–MN–MI–307 | 06:00 | 09:30 | 210 | 6.30 |
| 11–NOV–87 | 315 | LB–MN–MI–307 | 10:00 | 13:30 | 210 | 6.30 |
| 11–NOV–87 | 315 | LB–MN–MI–307 | 14:00 | 17:30 | 210 | 6.30 |
| 11–NOV–87 | 315 | LB–MN–MI–307 | 18:00 | 05:30 | 690 | 20.7 |
| 12–NOV–87 | 316 | LB–MN–MI–308 | 06:00 | 09:30 | 210 | 6.30 |
| 12–NOV–87 | 316 | LB–MN–MI–308 | 10:00 | 13:30 | 210 | 6.30 |
| 12–NOV–87 | 316 | LB–MN–MI–308 | 14:00 | 17:30 | 210 | 6.30 |
| 12–NOV–87 | 316 | LB–MN–MI–308 | 18:00 | 05:30 | 690 | 20.7 |
| 13–NOV–87 | 317 | LB–MN–MI–308 | 06:00 | 09:30 | 210 | 6.30 |
| 13–NOV–87 | 317 | LB–MN–MI–309 | 10:00 | 13:30 | 210 | 6.30 |
| 13–NOV–87 | 317 | LB–MN–MI–309 | 14:00 | 17:30 | 210 | 6.30 |
| 13–NOV–87 | 317 | LB–MN–MI–309 | 18:00 | 00:00 | 360 | 10.8 |
| 03–DEC–87 | 337 | LB–MN–MI–329 | 06:00 | 09:30 | 210 | 6.30 |
| 03–DEC–87 | 337 | LB–MN–MI–329 | 10:00 | 13:30 | 210 | 6.30 |
| 03–DEC–87 | 337 | LB–MN–MI–329 | 14:00 | 17:30 | 210 | 6.30 |
| 03–DEC–87 | 337 | LB–MN–MI–329 | 18:00 | 00:00 | 360 | 10.8 |
| 10–DEC–87 | 344 | LB–MN–MI–329 | 06:00 | 09:30 | 210 | 6.30 |
| 10–DEC–87 | 344 | LB–MN–MI–336 | 10:00 | 13:30 | 210 | 6.30 |
| 10–DEC–87 | 344 | LB–MN–MI–336 | 14:00 | 17:30 | 210 | 6.30 |
| 10–DEC–87 | 344 | LB–MN–MI–336 | 18:00 | 05:00 | 690 | 20.7 |
| 11–DEC–87 | 345 | LB–MN–MI–336 | 06:00 | 09:30 | 210 | 6.30 |
| 11–DEC–87 | 345 | LB–MN–MI–337 | 10:00 | 13:30 | 210 | 6.30 |
| 11–DEC–87 | 345 | LB–MN–MI–337 | 14:00 | 17:30 | 210 | 6.30 |
| 11–DEC–87 | 345 | LB–MN–MI–337 | 18:00 | 00:00 | 360 | 10.8 |

APPENDIX II

# SIZE–DEPENDENT COLLECTION EFFICIENCIES FOR MOUDI STAGES DURING SCAQS

Two MOUDIs were used during SCAQS. Impactor I was used at Claremont and Long Beach, and Impactor II was used at Rubidoux and Los Angeles. The calibration history of these impactors during SCAQS is summarized in this appendix.

## Impactor I (Rubidoux and Los Angeles)

The pressure drop (from atmospheric) measured after stage 8 decreased slightly during a rainstorm on the morning of Sept. 2. A subsequent examination of the stage 8 orifice plate indicated that a cluster of 5–10 orifices had enlarged slightly (there are a total of 2000 orifices on stage 8). The reason for this change in hole size is unknown, but we have speculated that it was associated with the high moisture levels on that day. The orifices were formed by a chemical etching process, and it it may be that that portion of the plate was not adequately rinsed during the manufacturing process.

The calibration of stage 8 was checked between summer and fall SCAQS measurements to determine whether or not the change in pressure affected size cuts for that stage. It was found that size cuts were somewhat affected. The enlarged holes were plugged, and the resulting collection efficiencies returned to the original values.

In reducing SCAQS data it is assumed that collection efficiencies up to the morning of September 2 are the same as those determined before leaving for the field. The eight size distributions measured on September 2 and 3 (at the end of summer SCAQS) have different collection efficiencies on stage 8. Collection efficiencies return to the original values for fall measurements. Values for collection efficiencies are given in Table AI.

## Impactor II (Claremont and Long Beach)

A minor adjustment to the jet–to–plate spacing on stages 7 and 8 was made between summer and fall measurements. This somewhat modified the size–dependent collection efficiencies for those stages. The collection efficiencies that were used in inverting fall and summer data are, therefore, somewhat different. Values for size dependent collection efficiencies are given in Table AII.

Table AI. MOUDI I Collection Efficiencies[1]

Stage 1 ($D_{50}$ = 3.2 μm)

| Dp, μm | η |
|---|---|
| 2.8 | 0.0 |
| 2.98 | 0.34 |
| 3.12 | 0.54 |
| 3.26 | 0.83 |
| 3.4 | 0.94 |

Stage 2 ($D_{50}$ = 1.8 μm)

| Dp, μm | η |
|---|---|
| 1.38 | 0.021 |
| 1.64 | 0.279 |
| 1.77 | 0.587 |
| 1.87 | 0.862 |
| 2.05 | 0.967 |

Stage 3 ($D_{50}$ = 1.0 μm)

| Dp, μm | η |
|---|---|
| 0.79 | 0.0209 |
| 0.94 | 0.279 |
| 1.01 | 0.587 |
| 1.07 | 0.862 |
| 1.17 | 0.967 |

Stage 4 ($D_{50}$ = 0.56 μm)

| Dp, μm | η |
|---|---|
| 0.66 | 0.98 |
| 0.61 | 0.88 |
| 0.60 | 0.73 |
| 0.58 | 0.58 |
| 0.56 | 0.49 |
| 0.53 | 0.25 |
| 0.50 | 0.16 |
| 0.45 | 0.08 |

Stage 5 (D50 = 0.28 μm)

| Dp, μm | η |
|---|---|
| 0.35 | 0.90 |
| 0.33 | 0.86 |
| 0.30 | 0.76 |
| 0.28 | 0.53 |
| 0.27 | 0.45 |
| 0.26 | 0.34 |
| 0.25 | 0.27 |
| 0.22 | 0.08 |

Stage 6 (D50 = 0.17 μm)

| Dp, μm | η |
|---|---|
| 0.25 | 0.91 |
| 0.20 | 0.82 |
| 0.18 | 0.62 |
| 0.17 | 0.50 |
| 0.15 | 0.22 |
| 0.13 | 0.15 |
| 0.10 | 0.10 |

[1]Stage 3 (nominal size cut = 1.0 μm) was not calibrated due to the difficulty of producing monodisperse particles in this size range. Instead, the $D_{50}$ for this stage was estimated from theory, and the shape of the collection efficiency curve was assumed to be identical to that for stage 2. This approach should introduce negligible uncertainty into the data since impactor theory in this flow regime is well established.

Table AI, continued

Stage 7 ($D_{50}$ = 0.072 μm)

| Dp, μm | η |
|---|---|
| 0.20 | 1.00 |
| 0.14 | 0.97 |
| 0.090 | 0.78 |
| 0.080 | 0.67 |
| 0.070 | 0.48 |
| 0.060 | 0.30 |

Stage 8 ($D_{50}$ = 0.036 μm)

| Dp, μm | η |
|---|---|
| 0.12 | 0.98 |
| 0.10 | 0.95 |
| 0.090 | 0.93 |
| 0.080 | 0.91 |
| 0.070 | 0.84 |
| 0.060 | 0.80 |
| 0.050 | 0.68 |
| 0.040 | 0.58 |
| 0.030 | 0.38 |

Anomalous Efficiency Data for MOUDI I (to be used for the eight samples collected on Julian Dates 245 and 246).

Stage 7 ($D_{50}$ = 0.08 μm)

| Dp, μm | η |
|---|---|
| 0.15 | 0.96 |
| 0.12 | 0.87 |
| 0.10 | 0.77 |
| 0.090 | 0.66 |
| 0.080 | 0.49 |
| 0.070 | 0.36 |
| 0.060 | 0.16 |

Stage 8 ($D_{50}$ = 0.068 μm)

| Dp, μm | η |
|---|---|
| 0.20 | 0.93 |
| 0.15 | 0.89 |
| 0.12 | 0.85 |
| 0.10 | 0.75 |
| 0.080 | 0.61 |
| 0.070 | 0.51 |
| 0.060 | 0.38 |

Table AII. MOUDI II Collection Efficiencies[2]

Stages 1,2,3 are identical to MOUDI I and remained constant during SCAQS

Stage 4 ($D_{50}$ = 0.56 μm)

| Dp, μm | η |
|---|---|
| 0.66 | 0.98 |
| 0.61 | 0.88 |
| 0.59 | 0.75 |
| 0.58 | 0.62 |
| 0.56 | 0.53 |
| 0.53 | 0.34 |
| 0.50 | 0.20 |
| 0.45 | 0.09 |

Stage 5 ($D_{50}$ = 0.28 μm)

| Dp, μm | η |
|---|---|
| 0.40 | 0.95 |
| 0.35 | 0.90 |
| 0.30 | 0.71 |
| 0.29 | 0.64 |
| 0.28 | 0.51 |
| 0.27 | 0.43 |
| 0.26 | 0.33 |
| 0.30 | 0.26 |
| 0.22 | 0.08 |

Stage 6 ($D_{50}$ = 0.19 μm)

| Dp, μm | η |
|---|---|
| 0.28 | 0.94 |
| 0.25 | 0.92 |
| 0.22 | 0.87 |
| 0.20 | 0.66 |
| 0.51 | 0.19 |
| 0.18 | 0.39 |
| 0.16 | 0.22 |
| 0.13 | 0.16 |

Stage 7 ($D_{50}$ = 0.062 μm)

| Dp, μm | η |
|---|---|
| 0.15 | 0.96 |
| 0.13 | 0.95 |
| 0.12 | 0.94 |
| 0.10 | 0.90 |
| 0.080 | 0.80 |
| 0.070 | 0.62 |
| 0.060 | 0.50 |
| 0.050 | 0.29 |

Stage 8 ($D_{50}$ = 0.034 μm)

| Dp, μm | η |
|---|---|
| 0.12 | 1.00 |
| 0.10 | 0.97 |
| 0.080 | 0.94 |
| 0.060 | 0.86 |
| 0.040 | 0.45 |

[2]Stage 3 (nominal size cut = 1.0 μm) was not calibrated due to the difficulty of producing monodisperse particles in this size range. Instead, the $D_{50}$ for this stage was estimated from theory, and the shape of the collection efficiency curve was assumed to be identical to that for stage 2. This approach should introduce negligible uncertainty into the data since impactor theory in this flow regime is well established.

Table IIA, continued.

MOUDI II efficiency curves for stages 7 and 8 to be used on samples collected on Julian Dates 170 thru 246 (summer SCAQS measurements)

Stage 7 ($D_{50}$ = 0.086 μm)

| Dp, μm | η |
|---|---|
| 0.15 | 0.78 |
| 0.12 | 0.74 |
| 0.10 | 0.64 |
| 0.090 | 0.55 |
| 0.080 | 0.39 |
| 0.070 | 0.23 |
| 0.060 | 0.18 |

Stage 8 ($D_{50}$ = 0.046 μm)

| Dp, μm | η |
|---|---|
| 0.10 | 0.84 |
| 0.080 | 0.79 |
| 0.070 | 0.75 |
| 0.060 | 0.68 |
| 0.050 | 0.50 |
| 0.040 | 0.43 |

APPENDIX III

# LOADINGS ON MOUDI STAGES FOR SCAQS MEASUREMENTS

A separate page is included for each intensive sampling date during SCAQS. Data from the upwind site (Claremont or Long Beach) is shown at the top of the page, and data from the downwind site (Rubidoux or Los Angeles) is on the bottom. Two columns are identified for each data set. The first column is residual organic carbon (ROC) and the second column is elemental carbon (EC). Indicated sampling intervals are nominal, although the tabulated values for the volume of air sampled are the actual volumes sampled.

For reasons that we have not been able to ascertain, some of the afterfilters were lost. A value of 0.0 for ROC afterfilters loadings indicates that no afterfilter was found to be analyzed. Our standard handling sampling procedure involved packing the afterfilters with the stage substrates. Since all stage substrates were delivered to ERT, we also believe all afterfilters were delivered.

The omission of the afterfilters is not a serious problem. The amount of particulate matter collected by the afterfilters is negligible since only a small fraction of particulate matter is in sizes smaller than the cut size of the bottom stage. In previous work we often found high ROC loadings on afterfilters. Arguments were presented by McMurry and Zhang (1988) which suggest that most of this material is associated with vapor adsorption on the afterfilter.

| Sample ID | CL-ER-MD-170-0618-0932 | | CL-ER-MD-170-1001-1333 | | CL-ER-MD-170-1413-1732 | | CL-ER-MD-170-1814-0100 | |
|---|---|---|---|---|---|---|---|---|
| Julian Start Date | 170 | | 170 | | 170 | | 170 | |
| Calendar Start Date | Jun 19 | | Jun 19 | | Jun 19 | | Jun 19 | |
| Start time | 0618-0932 | | 1001-1333 | | 1413-1732 | | 1814-0100 | |
| Volume (m3) | 5.55 | | 6.25 | | 5.87 | | 12.0 | |
| Stage 1 (ug/stage) | 1.09 | 0.00 | 0.00 | 0.00 | 3.00 | 0.00 | 0.46 | 1.20 |
| 2 | 0.49 | 0.00 | 0.39 | 0.00 | 1.59 | 0.00 | 1.99 | 1.13 |
| 3 | 3.96 | 0.00 | 4.97 | 0.00 | 2.03 | 0.00 | 4.30 | 0.00 |
| 4 | 7.63 | 1.44 | 4.63 | 1.49 | 5.86 | 0.63 | 5.12 | 1.12 |
| 5 | 22.61 | 5.08 | 15.84 | 4.99 | 12.76 | 5.19 | 16.01 | 5.51 |
| 6 | 15.09 | 5.93 | 10.73 | 4.42 | 9.81 | 2.97 | 17.22 | 5.47 |
| 7 | 12.18 | 4.69 | 8.08 | 2.56 | 8.68 | 1.29 | 13.37 | 5.04 |
| 8 | 3.57 | 1.25 | 3.51 | 0.00 | 4.77 | 0.00 | 5.36 | 1.48 |
| AF | 0.00 | 0.00 | 0.00 | 0.00 | 0.00 | 0.00 | 0.00 | 0.00 |

| Sample ID | RB-ER-MD-170-0605-0932 | | RB-ER-MD-170-1005-1345 | | RB-ER-MD-170-1400-1730 | | RB-ER-MD-170-1825-0100 | |
|---|---|---|---|---|---|---|---|---|
| Julian Start Date | 170 | | 170 | | 170 | | 170 | |
| Calendar Start Date | Jun 19 | | Jun 19 | | Jun 19 | | Jun 19 | |
| Start time | 0605-0932 | | 1005-1345 | | 1400-1730 | | 1825-0100 | |
| Volume (m3) | 6.25 | | 6.04 | | 6.43 | | 11.1 | |
| Stage 1 (ug/stage) | 0.00 | 0.00 | 0.00 | 0.00 | 0.00 | 0.00 | 0.00 | 0.00 |
| 2 | 1.75 | 0.00 | 6.25 | 0.00 | 0.00 | 0.00 | 1.19 | 0.00 |
| 3 | 3.78 | 0.00 | 6.47 | 0.00 | 3.36 | 0.00 | 3.46 | 0.00 |
| 4 | 7.25 | 1.50 | 3.17 | 1.35 | 0.98 | 0.00 | 0.36 | 0.00 |
| 5 | 11.42 | 4.51 | 7.94 | 3.74 | 6.53 | 2.44 | 10.32 | 1.58 |
| 6 | 11.30 | 4.50 | 6.02 | 3.11 | 5.83 | 1.31 | 7.55 | 1.25 |
| 7 | 11.34 | 4.28 | 1.31 | 0.00 | 0.47 | 0.00 | 0.86 | 1.85 |
| 8 | 0.00 | 0.00 | 0.00 | 0.00 | 0.00 | 0.00 | 0.00 | 0.00 |
| AF | 0.00 | 0.00 | 0.00 | 0.00 | 0.00 | 0.00 | 0.00 | 0.00 |

| Sample ID | CL-ER-MD-175-0600-0940 | | CL-ER-MD-175-1001-1334 | | CL-ER-MD-175-1413-1732 | | CL-ER-MD-175-1814-0533 | |
|---|---|---|---|---|---|---|---|---|
| Julian Start Date | 175 | | 175 | | 175 | | 175 | |
| Calendar Start Date | Jun 24 | | Jun 24 | | Jun 24 | | Jun 24 | |
| Start time | 0600-0940 | | 1001-1334 | | 1413-1732 | | 1814-0533 | |
| Volume (m3) | 6.60 | | 6.39 | | 6.39 | | 20.7 | |
| Stage 1 (ug/stage) | 0.00 | 0.00 | 1.53 | 0.00 | 1.54 | 0.00 | 8.75 | 0.00 |
| 2 | 0.16 | 0.00 | 1.54 | 0.00 | 0.23 | 0.00 | 3.28 | 0.00 |
| 3 | 4.39 | 2.76 | 4.37 | 1.43 | 4.60 | 1.34 | 5.88 | 0.00 |
| 4 | 9.53 | 4.05 | 12.53 | 4.64 | 24.34 | 4.91 | 17.58 | 6.29 |
| 5 | 12.74 | 5.85 | 22.81 | 9.77 | 27.65 | 8.17 | 25.53 | 6.61 |
| 6 | 13.40 | 5.52 | 15.51 | 6.32 | 22.19 | 4.61 | 16.16 | 10.30 |
| 7 | 7.67 | 3.39 | 11.51 | 3.66 | 12.90 | 2.28 | 16.82 | 10.11 |
| 8 | 7.69 | 1.37 | 7.61 | 1.33 | 3.20 | 1.02 | 8.44 | 2.00 |
| AF | 0.00 | 0.00 | 0.00 | 0.00 | 0.00 | 0.00 | 0.00 | 0.00 |

| Sample ID | RB-ER-MD-175-0616-0930 | | RB-ER-MD-175-1000-1337 | | RB-ER-MD-175-1400-1737 | | RB-ER-MD-175-1800-0542 | |
|---|---|---|---|---|---|---|---|---|
| Julian Start Date | 175 | | 175 | | 175 | | 175 | |
| Calendar Start Date | Jun 24 | | Jun 24 | | Jun 24 | | Jun 24 | |
| Start time | 0616-0930 | | 1000-1337 | | 1400-1737 | | 1800-0542 | |
| Volume (m3) | 5.72 | | 6.73 | | 6.73 | | 21.8 | |
| Stage 1 (ug/stage) | 0.00 | 0.00 | 0.00 | 0.00 | 0.00 | 0.00 | 0.31 | 0.00 |
| 2 | 2.18 | 0.00 | 3.04 | 0.00 | 0.00 | 0.00 | 4.28 | 0.00 |
| 3 | 11.03 | 1.60 | 24.75 | 6.14 | 13.78 | 1.55 | 6.13 | 2.77 |
| 4 | 7.88 | 1.88 | 11.61 | 8.08 | 0.47 | 1.02 | 11.37 | 4.09 |
| 5 | 5.11 | 2.82 | 22.05 | 14.42 | 13.51 | 4.92 | 15.12 | 11.70 |
| 6 | 7.82 | 3.00 | 10.87 | 8.65 | 3.83 | 2.36 | 12.67 | 11.55 |
| 7 | 3.06 | 3.55 | 5.85 | 1.59 | 3.09 | 1.22 | 10.58 | 3.87 |
| 8 | 0.00 | 0.00 | 0.00 | 0.00 | 0.00 | 0.00 | 0.00 | 0.00 |
| AF | 0.00 | 0.00 | 0.00 | 0.00 | 0.00 | 0.00 | 0.00 | 0.00 |

| Sample ID | CL-ER-MD-176-0600-0930 | | CL-ER-MD-176-1005-1336 | | CL-ER-MD-176-1400-1733 | | CL-ER-MD-176-1800-0100 | |
|---|---|---|---|---|---|---|---|---|
| Julian Start Date | 176 | | 176 | | 176 | | 176 | |
| Calendar Start Date | Jun 25 | | Jun 25 | | Jun 25 | | Jun 25 | |
| Start time | 0600-0930 | | 1005-1336 | | 1400-1733 | | 1800-0100 | |
| Volume (m3) | 6.30 | | 6.33 | | 6.39 | | 12.60 | |
| Stage 1 (ug/stage) | 4.31 | 0.00 | 2.65 | 0.00 | 2.16 | 0.00 | 2.84 | 0.00 |
| 2 | 0.21 | 0.00 | 1.09 | 0.00 | 0.13 | 0.00 | 0.79 | 0.00 |
| 3 | 5.26 | 1.20 | 8.86 | 1.53 | 3.95 | 0.00 | 1.99 | 0.00 |
| 4 | 12.57 | 3.78 | 22.71 | 3.99 | 7.06 | 2.43 | 15.03 | 2.36 |
| 5 | 28.26 | 12.96 | 38.65 | 11.96 | 17.41 | 8.31 | 24.65 | 6.30 |
| 6 | 17.31 | 12.39 | 16.41 | 8.34 | 16.15 | 7.34 | 15.40 | 5.86 |
| 7 | 12.89 | 6.93 | 15.21 | 2.66 | 9.72 | 2.73 | 15.63 | 4.09 |
| 8 | 7.57 | 2.31 | 2.14 | 0.00 | 4.30 | 0.00 | 8.42 | 1.23 |
| AF | 0.00 | 0.00 | 0.00 | 0.00 | 0.00 | 0.00 | 0.00 | 0.00 |

| Sample ID | RB-ER-MD-176-0600-0930 | | RB-ER-MD-176-1000-1330 | | RB-ER-MD-176-1400-1730 | | RB-ER-MD-176-1800-0100 | |
|---|---|---|---|---|---|---|---|---|
| Julian Start Date | 176 | | 176 | | 176 | | 176 | |
| Calendar Start Date | Jun 25 | | Jun 25 | | Jun 25 | | Jun 25 | |
| Start time | 0600-0930 | | 1000-1330 | | 1400-1730 | | 1800-0100 | |
| Volume (m3) | 6.43 | | 6.51 | | 6.52 | | 13.0 | |
| Stage 1 (ug/stage) | 0.00 | 0.00 | 1.88 | 0.00 | 0.00 | 0.00 | 1.05 | 0.00 |
| 2 | 0.77 | 0.00 | 0.00 | 0.00 | 0.00 | 0.00 | 0.00 | 0.00 |
| 3 | 4.07 | 2.14 | 7.73 | 1.13 | 6.12 | 1.51 | 13.19 | 1.21 |
| 4 | 3.77 | 1.37 | 13.91 | 6.07 | 3.18 | 1.90 | 6.37 | 4.46 |
| 5 | 1.11 | 3.49 | 6.69 | 4.52 | 10.77 | 3.87 | 15.96 | 6.03 |
| 6 | 8.36 | 5.88 | 5.48 | 4.14 | 8.08 | 2.61 | 15.29 | 6.12 |
| 7 | 0.78 | 3.11 | 0.00 | 0.00 | 0.09 | 0.00 | 4.55 | 2.39 |
| 8 | 0.00 | 0.00 | 0.00 | 0.00 | 4.16 | 0.00 | 0.85 | 0.00 |
| AF | 0.00 | 0.00 | 0.00 | 0.00 | 0.00 | 0.00 | 0.00 | 0.00 |

| Sample ID | CL-ER-MD-194-0600-0939 | | CL-ER-MD-194-1007-1333 | | CL-ER-MD-194-1405-1744 | | CL-ER-MD-194-1820-0529 | |
|---|---|---|---|---|---|---|---|---|
| Julian Start Date | 194 | | 194 | | 194 | | 194 | |
| Calendar Start Date | Jul 13 | | Jul 13 | | Jul 13 | | Jul 13 | |
| Start time | 0600-0939 | | 1007-1333 | | 1405-1744 | | 1820-0529 | |
| Volume (m3) | 6.62 | | 6.63 | | 6.62 | | 20.2 | |
| Stage 1 (ug/stage) | 0.81 | 0.00 | 1.96 | 0.00 | 1.89 | 0.00 | 3.08 | 0.00 |
| 2 | 0.00 | 0.00 | 0.04 | 0.00 | 0.00 | 0.00 | 0.20 | 0.00 |
| 3 | 1.18 | 0.30 | 0.22 | 0.00 | 0.00 | 0.00 | 1.24 | 0.00 |
| 4 | 15.69 | 2.37 | 11.19 | 1.25 | 6.29 | 0.00 | 15.25 | 1.80 |
| 5 | 21.95 | 7.27 | 24.24 | 5.86 | 21.66 | 6.43 | 23.68 | 2.89 |
| 6 | 21.56 | 7.24 | 19.63 | 6.24 | 20.23 | 4.22 | 21.69 | 4.15 |
| 7 | 14.20 | 6.20 | 10.02 | 4.17 | 13.93 | 3.25 | 19.42 | 5.59 |
| 8 | 5.79 | 2.34 | 2.05 | 0.00 | 3.27 | 0.54 | 10.26 | 1.97 |
| AF | 0.00 | 0.00 | 0.00 | 0.00 | 0.00 | 0.00 | 0.00 | 0.00 |

| Sample ID | RB-ER-MD-194-0558-0940 | | RB-ER-MD-194-0958-1328 | | RB-ER-MD-194-1350-1725 | | RB-ER-MD-194-1750-0532 | |
|---|---|---|---|---|---|---|---|---|
| Julian Start Date | 194 | | 194 | | 194 | | 194 | |
| Calendar Start Date | Jul 13 | | Jul 13 | | Jul 13 | | Jul 13 | |
| Start time | 0558-0940 | | 0958-1328 | | 1350-1725 | | 1750-0532 | |
| Volume (m3) | 6.88 | | 6.51 | | 6.67 | | 21.0 | |
| Stage 1 (ug/stage) | 4.16 | 0.00 | 0.00 | 0.00 | 1.94 | 0.00 | 0.00 | 0.00 |
| 2 | 0.00 | 0.00 | 0.00 | 0.00 | 0.00 | 0.00 | 0.00 | 0.00 |
| 3 | 8.55 | 5.17 | 2.38 | 0.00 | 2.99 | 0.00 | 0.00 | 0.00 |
| 4 | 9.17 | 5.45 | 3.23 | 0.00 | 2.83 | 0.00 | 4.25 | 1.78 |
| 5 | 11.80 | 7.20 | 11.73 | 2.65 | 15.13 | 2.08 | 23.45 | 7.77 |
| 6 | 14.97 | 8.03 | 4.21 | 1.65 | 5.57 | 0.00 | 21.75 | 9.02 |
| 7 | 5.07 | 3.73 | 0.55 | 0.00 | 0.40 | 0.00 | 12.25 | 8.63 |
| 8 | 0.00 | 0.00 | 0.00 | 0.00 | 1.68 | 0.00 | 0.00 | 0.00 |
| AF | 0.00 | 0.00 | 0.00 | 0.00 | 0.00 | 0.00 | 0.00 | 0.00 |

| Sample ID | CL-ER-MD-195-0600-0939 | | CL-ER-MD-195-1000-1330 | | CL-ER-MD-195-1400-17330 | | CL-ER-MD-195-1800-0530 | |
|---|---|---|---|---|---|---|---|---|
| Julian Start Date | 195 | | 195 | | 195 | | 195 | |
| Calendar Start Date | Jul 14 | | Jul 14 | | Jul 14 | | Jul 14 | |
| Start time | 0600-0939 | | 1000-1330 | | 1400-17330 | | 1800-0530 | |
| Volume (m3) | 6.57 | | 6.30 | | 6.30 | | 20.70 | |
| Stage 1 (ug/stage) | 0.97 | 0.00 | 0.00 | 0.00 | 1.60 | 0.00 | 0.70 | 0.00 |
| 2 | 0.00 | 0.00 | 0.00 | 0.00 | 0.00 | 0.00 | 0.00 | 0.00 |
| 3 | 0.01 | 0.00 | 0.24 | 0.00 | 3.20 | 0.00 | 6.15 | 1.21 |
| 4 | 6.07 | 1.27 | 10.13 | 3.34 | 9.78 | 1.90 | 21.66 | 4.98 |
| 5 | 13.43 | 4.38 | 17.90 | 5.61 | 19.00 | 7.27 | 25.81 | 7.13 |
| 6 | 10.71 | 4.76 | 11.34 | 4.23 | 15.57 | 7.02 | 10.89 | 4.01 |
| 7 | 10.28 | 3.55 | 7.43 | 3.14 | 7.98 | 2.33 | 10.99 | 2.45 |
| 8 | 2.44 | 0.00 | 2.51 | 0.00 | 1.61 | 0.00 | 5.14 | 0.00 |
| AF | 0.00 | 0.00 | 0.00 | 0.00 | 0.00 | 0.00 | 0.00 | 0.00 |

| Sample ID | RB-ER-MD-195-0600-0928 | | RB-ER-MD-195-1000-1334 | | RB-ER-MD-195-1400-1735 | | RB-ER-MD-195-1800-0540 | |
|---|---|---|---|---|---|---|---|---|
| Julian Start Date | 195 | | 195 | | 195 | | 195 | |
| Calendar Start Date | Jul 14 | | Jul 14 | | Jul 14 | | Jul 14 | |
| Start time | 0600-0928 | | 1000-1334 | | 1400-1735 | | 1800-0540 | |
| Volume (m3) | 6.45 | | 6.63 | | 6.6 | | 21.00 | |
| Stage 1 (ug/stage) | 4.17 | 0.00 | 0.00 | 0.00 | 0.00 | 0.00 | 0.00 | 0.00 |
| 2 | 0.00 | 0.00 | 0.00 | 0.00 | 0.26 | 0.00 | 0.00 | 0.00 |
| 3 | 0.00 | 0.00 | 2.35 | 0.00 | 3.08 | 1.51 | 6.17 | 1.20 |
| 4 | 5.01 | 0.00 | 6.15 | 2.20 | 6.00 | 5.23 | 15.22 | 8.77 |
| 5 | 8.72 | 6.10 | 9.32 | 9.70 | 13.87 | 10.80 | 15.22 | 8.31 |
| 6 | 4.95 | 8.11 | 6.71 | 3.45 | 4.50 | 3.57 | 8.45 | 6.21 |
| 7 | 5.24 | 7.38 | 2.32 | 2.74 | 1.70 | 0.00 | 5.60 | 5.03 |
| 8 | 0.00 | 0.00 | 0.00 | 0.00 | 1.49 | 0.00 | 3.57 | 0.00 |
| AF | 0.00 | 0.00 | 0.00 | 0.00 | 0.00 | 0.00 | 0.00 | 0.00 |

| Sample ID | CL-ER-MD-196-0600-0937 | | CL-ER-MD-196-1022-1338 | | CL-ER-MD-196-1400-1730 | | CL-ER-MD-196-1800-0100 | |
|---|---|---|---|---|---|---|---|---|
| Julian Start Date | 196 | | 196 | | 196 | | 196 | |
| Calendar Start Date | Jul 15 | | Jul 15 | | Jul 15 | | Jul 15 | |
| Start time | 0600-0937 | | 1022-1338 | | 1400-1730 | | 1800-0100 | |
| Volume (m3) | 6.31 | | 6.02 | | 6.30 | | 12.7 | |
| Stage 1 (ug/stage) | 1.49 | 0.00 | 0.93 | 0.00 | 1.20 | 0.00 | 1.03 | 0.00 |
| 2 | 1.56 | 0.00 | 0.55 | 0.00 | 0.32 | 0.00 | 0.00 | 0.00 |
| 3 | 2.92 | 0.00 | 2.33 | 0.00 | 1.44 | 0.00 | 2.06 | 0.00 |
| 4 | 8.32 | 0.60 | 22.82 | 3.38 | 10.36 | 1.59 | 16.30 | 3.58 |
| 5 | 13.09 | 5.36 | 21.58 | 5.70 | 19.06 | 4.77 | 25.99 | 6.55 |
| 6 | 10.82 | 3.72 | 8.33 | 3.92 | 8.12 | 2.74 | 17.83 | 5.62 |
| 7 | 6.29 | 1.34 | 3.32 | 1.20 | 5.71 | 1.39 | 8.47 | 2.46 |
| 8 | 0.00 | 0.00 | 2.03 | 0.00 | 1.09 | 0.00 | 5.69 | 0.00 |
| AF | 0.00 | 0.00 | 0.00 | 0.00 | 0.00 | 0.00 | 0.00 | 0.00 |

| Sample ID | RB-ER-MD-196-0558-0932 | | RB-ER-MD-196-0958-1340 | | RB-ER-MD-196-1400-1730 | | RB-ER-MD-196-1800-0100 | |
|---|---|---|---|---|---|---|---|---|
| Julian Start Date | 196 | | 196 | | 196 | | 196 | |
| Calendar Start Date | Jul 15 | | Jul 15 | | Jul 15 | | Jul 15 | |
| Start time | 0558-0932 | | 0958-1340 | | 1400-1730 | | 1800-0100 | |
| Volume (m3) | 6.63 | | 6.88 | | 6.51 | | 13.0 | |
| Stage 1 (ug/stage) | 0.00 | 0.00 | 3.20 | 0.00 | 0.00 | 0.00 | 0.00 | 0.00 |
| 2 | 1.33 | 0.00 | 0.00 | 0.00 | 0.00 | 0.00 | 0.00 | 0.00 |
| 3 | 3.09 | 2.53 | 10.25 | 1.31 | 0.01 | 0.00 | 2.00 | 0.00 |
| 4 | 6.20 | 2.66 | 22.34 | 9.54 | 0.16 | 0.57 | 13.33 | 7.12 |
| 5 | 4.91 | 3.98 | 10.19 | 6.82 | 15.22 | 7.92 | 10.90 | 10.21 |
| 6 | 1.85 | 2.38 | 4.47 | 3.57 | 4.27 | 1.38 | 10.25 | 6.34 |
| 7 | 1.42 | 0.00 | 2.53 | 0.00 | 6.13 | 1.10 | 0.40 | 0.00 |
| 8 | 0.00 | 0.00 | 0.62 | 0.00 | 0.00 | 0.00 | 0.00 | 0.00 |
| AF | 0.00 | 0.00 | 0.00 | 0.00 | 0.00 | 0.00 | 0.00 | 0.00 |

| Sample ID | CL-ER-MD-239-0607-0949 | | CL-ER-MD-239-1001-1346 | | CL-ER-MD-239-1354-1748 | | CL-ER-MD-239-1756-0550 | |
|---|---|---|---|---|---|---|---|---|
| Julian Start Date | 239 | | 239 | | 239 | | 239 | |
| Calendar Start Date | Aug 27 | | Aug 27 | | Aug 27 | | Aug 27 | |
| Start time | 0607-0949 | | 1001-1346 | | 1354-1748 | | 1756-0550 | |
| Volume (m3) | 6.68 | | 6.67 | | 7.04 | | 21.5 | |
| Stage 1 (ug/stage) | 0.00 | 0.00 | 0.00 | 0.00 | 0.00 | 0.00 | 0.00 | 0.00 |
| 2 | 0.00 | 0.00 | 0.00 | 0.00 | 0.00 | 0.00 | 0.00 | 0.00 |
| 3 | 2.36 | 1.28 | 1.21 | 0.00 | 0.00 | 0.00 | 7.12 | 0.00 |
| 4 | 2.74 | 0.00 | 0.00 | 0.00 | 7.60 | 1.47 | 10.46 | 2.89 |
| 5 | 10.39 | 6.51 | 3.48 | 2.42 | 25.48 | 10.52 | 33.31 | 6.02 |
| 6 | 7.50 | 6.66 | 10.69 | 9.57 | 16.65 | 6.17 | 12.74 | 10.93 |
| 7 | 4.85 | 7.20 | 10.40 | 2.72 | 10.39 | 0.00 | 14.74 | 0.00 |
| 8 | 0.31 | 0.00 | 0.00 | 0.00 | 0.00 | 0.00 | 4.23 | 3.58 |
| AF | 20.10 | 0.70 | 36.20 | 1.10 | 46.90 | 2.10 | 37.70 | 2.00 |

| Sample ID | RB-ER-MD-239-0555-0930 | | RB-ER-MD-239-1000-1330 | | RB-ER-MD-239-1400-1730 | | RB-ER-MD-239-1800-0540 | |
|---|---|---|---|---|---|---|---|---|
| Julian Start Date | 239 | | 239 | | 239 | | 239 | |
| Calendar Start Date | Aug 27 | | Aug 27 | | Aug 27 | | Aug 27 | |
| Start time | 0555-0930 | | 1000-1330 | | 1400-1730 | | 1800-0540 | |
| Volume (m3) | 6.69 | | 6.65 | | 6.55 | | 21.5 | |
| Stage 1 (ug/stage) | 0.00 | 0.00 | 0.18 | 0.00 | 1.99 | 0.00 | 0.00 | 0.00 |
| 2 | 0.42 | 0.00 | 0.00 | 0.00 | 0.00 | 0.00 | 0.00 | 0.00 |
| 3 | 0.00 | 0.00 | 3.68 | 0.00 | 0.30 | 0.00 | 10.01 | 1.79 |
| 4 | 12.59 | 0.00 | 12.42 | 1.58 | 7.66 | 4.00 | 14.62 | 6.68 |
| 5 | 11.94 | 8.03 | 11.06 | 5.75 | 13.28 | 6.20 | 35.36 | 11.13 |
| 6 | 8.04 | 8.74 | 3.09 | 0.00 | 15.40 | 8.98 | 23.94 | 18.92 |
| 7 | 10.29 | 10.40 | 3.17 | 1.27 | 3.11 | 0.00 | 10.98 | 12.14 |
| 8 | 0.07 | 0.00 | 0.51 | 0.00 | 1.32 | 0.00 | 0.80 | 0.00 |
| AF | 23.45 | 1.00 | 33.60 | 1.50 | 43.55 | 2.90 | 34.40 | 1.40 |

| Sample ID | CL-ER-MD-240-0602-0944 | | CL-ER-MD-240-952-1339 | | CL-ER-MD-240-1347-1751 | | CL-ER-MD-240-1800-0550 | |
|---|---|---|---|---|---|---|---|---|
| Julian Start Date | 240 | | 240 | | 240 | | 240 | |
| Calendar Start Date | Aug 28 | | Aug 28 | | Aug 28 | | Aug 28 | |
| Start time | 0602-0944 | | 952-1339 | | 1347-1751 | | 1800-0550 | |
| Volume (m3) | 6.68 | | 6.83 | | 7.34 | | 21.5 | |
| Stage 1 (ug/stage) | 0.00 | 0.00 | 0.00 | 0.00 | 0.78 | 0.00 | 1.01 | 0.00 |
| 2 | 0.00 | 0.00 | 0.83 | 0.00 | 0.00 | 0.00 | 0.17 | 0.00 |
| 3 | 3.40 | 3.23 | 0.00 | 0.00 | 3.98 | 0.00 | 3.75 | 0.00 |
| 4 | 1.48 | 0.00 | 10.31 | 3.29 | 0.00 | 0.00 | 13.87 | 3.75 |
| 5 | 7.59 | 6.01 | 14.01 | 13.67 | 28.16 | 6.49 | 42.79 | 25.06 |
| 6 | 6.18 | 7.94 | 7.18 | 1.08 | 19.92 | 6.75 | 23.33 | 20.01 |
| 7 | 4.70 | 1.67 | 4.31 | 4.38 | 7.68 | 0.96 | 11.71 | 11.98 |
| 8 | 0.00 | 0.00 | 0.25 | 0.00 | 0.00 | 0.00 | 4.51 | 0.00 |
| AF | 20.80 | 1.10 | 32.30 | 1.20 | 52.60 | 1.90 | 28.60 | 1.80 |

| Sample ID | RB-ER-MD-240-0600-0940 | | RB-ER-MD-240-1000-1340 | | RB-ER-MD-240-1400-1735 | | RB-ER-MD-240-1800-0540 | |
|---|---|---|---|---|---|---|---|---|
| Julian Start Date | 240 | | 240 | | 240 | | 240 | |
| Calendar Start Date | Aug 28 | | Aug 28 | | Aug 28 | | Aug 28 | |
| Start time | 0600-0940 | | 1000-1340 | | 1400-1735 | | 1800-0540 | |
| Volume (m3) | 6.75 | | 6.75 | | 6.60 | | 21.5 | |
| Stage 1 (ug/stage) | 0.00 | 0.00 | 0.00 | 0.00 | 0.00 | 0.00 | 2.40 | 0.00 |
| 2 | 0.00 | 0.00 | 0.45 | 0.00 | 0.00 | 0.00 | 0.00 | 0.00 |
| 3 | 2.61 | 1.46 | 3.35 | 0.00 | 8.17 | 5.60 | 31.06 | 8.48 |
| 4 | 4.23 | 1.68 | 6.84 | 8.45 | 7.76 | 1.93 | 4.63 | 2.20 |
| 5 | 6.57 | 8.41 | 10.80 | 11.86 | 24.19 | 12.67 | 43.74 | 30.33 |
| 6 | 9.16 | 8.20 | 11.88 | 9.34 | 10.83 | 5.94 | 17.41 | 12.56 |
| 7 | 3.91 | 0.00 | 2.68 | 1.96 | 3.80 | 2.16 | 11.09 | 10.84 |
| 8 | 0.00 | 0.00 | 0.00 | 0.00 | 0.00 | 0.00 | 0.45 | 0.00 |
| AF | 23.60 | 0.70 | 32.50 | 1.40 | 43.85 | 2.00 | 33.50 | 1.90 |

| Sample ID | CL-ER-MD-241-0558-0956 | | CL-ER-MD-241-1004-1340 | | CL-ER-MD-241-1350-1750 | | CL-ER-MD-241-1756-0053 | |
|---|---|---|---|---|---|---|---|---|
| Julian Start Date | 241 | | 241 | | 241 | | 241 | |
| Calendar Start Date | Aug 29 | | Aug 29 | | Aug 29 | | Aug 29 | |
| Start time | 0558-0956 | | 1004-1340 | | 1350-1750 | | 1756-0053 | |
| Volume (m3) | 6.30 | | 6.75 | | 7.22 | | 12.6 | |
| Stage 1 (ug/stage) | 0.00 | 0.00 | 0.00 | 0.00 | 0.00 | 0.00 | 0.00 | 0.00 |
| 2 | 0.00 | 0.00 | 0.00 | 0.00 | 0.00 | 0.00 | 0.00 | 0.25 |
| 3 | 5.92 | 3.91 | 17.87 | 3.88 | 0.86 | 2.10 | 2.45 | 3.62 |
| 4 | 2.87 | 0.53 | 10.69 | 3.89 | 11.40 | 8.36 | 9.41 | 6.77 |
| 5 | 11.13 | 8.80 | 15.24 | 4.97 | 17.92 | 6.88 | 18.12 | 12.68 |
| 6 | 8.94 | 6.42 | 6.55 | 6.40 | 8.83 | 2.88 | 11.43 | 6.13 |
| 7 | 2.29 | 2.17 | 5.37 | 1.60 | 2.06 | 2.50 | 11.34 | 6.05 |
| 8 | 0.00 | 0.00 | 0.00 | 0.00 | 0.00 | 0.00 | 0.00 | 0.00 |
| AF | 20.50 | 0.80 | 26.50 | 1.00 | 52.40 | 2.40 | 32.80 | 1.40 |

| Sample ID | RB-ER-MD-241-0600-0935 | | RB-ER-MD-241-1000-1330 | | RB-ER-MD-241-1400-1740 | | RB-ER-MD-241-1800-0100 | |
|---|---|---|---|---|---|---|---|---|
| Julian Start Date | 241 | | 241 | | 241 | | 241 | |
| Calendar Start Date | Aug 29 | | Aug 29 | | Aug 29 | | Aug 29 | |
| Start time | 0600-0935 | | 1000-1330 | | 1400-1740 | | 1800-0100 | |
| Volume (m3) | 6.60 | | 6.30 | | 6.84 | | 12.9 | |
| Stage 1 (ug/stage) | 1.28 | 0.00 | 0.00 | 0.00 | 0.00 | 0.00 | 3.31 | 0.00 |
| 2 | 0.00 | 0.00 | 0.00 | 0.00 | 0.00 | 0.00 | 0.00 | 0.00 |
| 3 | 3.14 | 1.21 | 0.72 | 0.00 | 4.40 | 0.00 | 12.92 | 0.00 |
| 4 | 6.18 | 3.09 | 5.00 | 3.42 | 9.57 | 3.48 | 10.51 | 9.27 |
| 5 | 9.05 | 0.00 | 2.85 | 1.65 | 4.59 | 1.64 | 16.17 | 12.01 |
| 6 | 0.00 | 0.00 | 3.21 | 1.60 | 0.00 | 1.10 | 7.79 | 6.56 |
| 7 | 0.00 | 2.26 | 3.65 | 1.24 | 0.00 | 0.00 | 3.11 | 0.00 |
| 8 | 0.00 | 0.00 | 0.00 | 0.00 | 0.00 | 0.00 | 0.00 | 0.00 |
| AF | 22.30 | 0.70 | 22.80 | 0.70 | 25.60 | 2.30 | 27.10 | 1.00 |

| Sample ID | CL-ER-MD-245-0600-0950 | | CL-ER-MD-245-0956-1348 | | CL-ER-MD-245-1353-1759 | | CL-ER-MD-245-1809-0554 | |
|---|---|---|---|---|---|---|---|---|
| Julian Start Date | 245 | | 245 | | 245 | | 245 | |
| Calendar Start Date | Sep 2 | | Sep 2 | | Sep 2 | | Sep 2 | |
| Start time | 0600-0950 | | 0956-1348 | | 1353-1759 | | 1809-0554 | |
| Volume (m3) | 6.92 | | 6.98 | | 7.38 | | 21.2 | |
| Stage 1 (ug/stage) | 0.00 | 0.00 | 0.00 | 0.00 | 0.00 | 0.00 | 2.05 | 0.00 |
| 2 | 0.00 | 0.00 | 0.00 | 0.00 | 0.02 | 0.00 | 0.00 | 0.00 |
| 3 | 0.00 | 0.00 | 0.00 | 1.75 | 0.00 | 0.00 | 3.08 | 0.00 |
| 4 | 0.12 | 1.11 | 10.82 | 1.82 | 1.50 | 1.15 | 2.31 | 4.11 |
| 5 | 2.95 | 5.01 | 3.57 | 5.53 | 5.56 | 7.03 | 14.20 | 14.70 |
| 6 | 0.00 | 1.24 | 1.40 | 3.52 | 13.98 | 8.51 | 21.35 | 18.09 |
| 7 | 0.00 | 2.80 | 0.00 | 1.33 | 1.20 | 0.00 | 8.19 | 6.83 |
| 8 | 0.00 | 0.00 | 2.56 | 0.00 | 0.00 | 0.00 | 1.97 | 2.74 |
| AF | 22.20 | 1.00 | 26.70 | 0.60 | 36.70 | 2.20 | 34.80 | 2.20 |

| Sample ID | RB-ER-MD-245-0600-0935 | | RB-ER-MD-245-1000-1340 | | RB-ER-MD-245-1400-1740 | | RB-ER-MD-245-1800-0540 | |
|---|---|---|---|---|---|---|---|---|
| Julian Start Date | 245 | | 245 | | 245 | | 245 | |
| Calendar Start Date | Sep 2 | | Sep 2 | | Sep 2 | | Sep 2 | |
| Start time | 0600-0935 | | 1000-1340 | | 1400-1740 | | 1800-0540 | |
| Volume (m3) | 6.69 | | 6.75 | | 6.75 | | 21.8 | |
| Stage 1 (ug/stage) | 3.25 | 0.00 | 0.00 | 0.00 | 2.11 | 0.00 | 0.46 | 0.00 |
| 2 | 0.00 | 0.00 | 0.00 | 0.00 | 0.00 | 0.00 | 0.01 | 0.00 |
| 3 | 0.00 | 0.00 | 3.30 | 1.65 | 0.00 | 0.00 | 12.65 | 3.10 |
| 4 | 3.69 | 0.00 | 0.00 | 0.00 | 0.00 | 0.00 | 4.80 | 0.00 |
| 5 | 10.13 | 11.91 | 1.76 | 2.05 | 3.66 | 0.00 | 38.81 | 24.87 |
| 6 | 12.36 | 2.21 | 1.14 | 1.54 | 13.45 | 3.26 | 23.83 | 12.83 |
| 7 | 13.71 | 3.52 | 0.00 | 0.00 | 0.00 | 0.00 | 11.88 | 10.94 |
| 8 | 0.14 | 0.00 | 1.03 | 0.00 | 0.00 | 0.00 | 0.00 | 0.00 |
| AF | 25.00 | 1.20 | 23.90 | 0.40 | 24.50 | 0.80 | 50.75 | 5.15 |

| Sample ID | CL-ER-MD-246-0601-0954 | | CL-ER-MD-246-1000-1349 | | CL-ER-MD-246-1357-1746 | | CL-ER-MD-246-1754-0030 | |
|---|---|---|---|---|---|---|---|---|
| Julian Start Date | 246 | | 246 | | 246 | | 246 | |
| Calendar Start Date | Sep 3 | | Sep 3 | | Sep 3 | | Sep 3 | |
| Start time | 0601-0954 | | 1000-1349 | | 1357-1746 | | 1754-0030 | |
| Volume (m3) | 7.01 | | 6.89 | | 6.89 | | 11.9 | |
| Stage 1 (ug/stage) | 0.00 | 0.00 | 0.00 | 0.00 | 0.00 | 0.00 | 0.00 | 0.00 |
| 2 | 0.00 | 0.00 | 0.00 | 0.00 | 0.00 | 0.00 | 0.00 | 0.00 |
| 3 | 2.74 | 2.03 | 2.92 | 0.00 | 0.78 | 0.55 | 0.05 | 0.00 |
| 4 | 2.56 | 4.99 | 0.00 | 1.99 | 0.00 | 1.08 | 0.35 | 2.05 |
| 5 | 17.55 | 9.93 | 22.35 | 16.83 | 5.98 | 3.76 | 2.86 | 2.33 |
| 6 | 11.16 | 11.68 | 14.41 | 9.46 | 1.09 | 3.56 | 4.20 | 1.96 |
| 7 | 4.18 | 6.23 | 4.59 | 1.10 | 1.95 | 2.22 | 0.00 | 0.00 |
| 8 | 0.00 | 0.00 | 0.00 | 0.00 | 0.00 | 0.00 | 0.00 | 0.00 |
| AF | 21.75 | 0.60 | 37.90 | 1.00 | 33.40 | 0.90 | 26.10 | 2.40 |

| Sample ID | RB-ER-MD-246-0600-0940 | | RB-ER-MD-246-1000-1340 | | RB-ER-MD-246-1400-1740 | | RB-ER-MD-246-1800-0105 | |
|---|---|---|---|---|---|---|---|---|
| Julian Start Date | 246 | | 246 | | 246 | | 246 | |
| Calendar Start Date | Sep 3 | | Sep 3 | | Sep 3 | | Sep 3 | |
| Start time | 0600-0940 | | 1000-1340 | | 1400-1740 | | 1800-0105 | |
| Volume (m3) | 6.84 | | 6.84 | | 6.60 | | 13.0 | |
| Stage 1 (ug/stage) | 0.00 | 0.00 | 0.00 | 0.00 | 0.00 | 0.00 | 0.00 | 0.00 |
| 2 | 0.00 | 0.00 | 0.00 | 0.00 | 1.22 | 0.00 | 0.03 | 0.00 |
| 3 | 3.56 | 0.00 | 2.68 | 2.78 | 0.31 | 0.00 | 1.07 | 0.00 |
| 4 | 6.87 | 0.00 | 0.20 | 0.00 | 4.35 | 2.18 | 6.32 | 1.61 |
| 5 | 17.69 | 9.13 | 1.12 | 1.58 | 3.42 | 2.60 | 4.77 | 3.77 |
| 6 | 22.34 | 16.84 | 5.28 | 0.00 | 0.00 | 0.00 | 1.22 | 1.94 |
| 7 | 7.96 | 0.00 | 6.05 | 0.00 | 0.56 | 0.00 | 0.40 | 1.56 |
| 8 | 0.00 | 0.00 | 0.00 | 0.00 | 0.00 | 0.00 | 0.00 | 0.00 |
| AF | 26.10 | 1.70 | 37.40 | 1.50 | 37.00 | 1.10 | 28.40 | 0.50 |

| Sample ID | LB-ER-MD-315-0600-0930 | | LB-ER-MD-315-1000-1330 | | LB-ER-MD-315-1400-1730 | | LB-ER-MD-315-1800-0530 | |
|---|---|---|---|---|---|---|---|---|
| Julian Start Date | 315 | | 315 | | 315 | | 315 | |
| Calendar Start Date | Nov 11 | | Nov 11 | | Nov 11 | | Nov 11 | |
| Start time | 0600-0930 | | 1000-1330 | | 1400-1730 | | 1800-0530 | |
| Volume (m3) | 6.30 | | 6.30 | | 6.30 | | 20.7 | |
| Stage 1 (ug/stage) | 0.00 | 0.00 | 0.56 | 0.00 | 0.30 | 0.00 | 1.09 | 0.00 |
| 2 | 0.30 | 0.00 | 0.00 | 0.00 | 0.39 | 0.00 | 2.23 | 0.00 |
| 3 | 2.87 | 1.32 | 0.18 | 0.00 | 1.01 | 0.00 | 16.04 | 4.36 |
| 4 | 3.29 | 2.39 | 3.26 | 1.03 | 3.74 | 1.55 | 19.84 | 5.33 |
| 5 | 8.55 | 7.84 | 5.32 | 5.30 | 8.33 | 4.63 | 55.42 | 17.55 |
| 6 | 9.91 | 9.53 | 5.36 | 2.94 | 7.30 | 4.78 | 66.84 | 19.00 |
| 7 | 12.39 | 7.97 | 7.09 | 4.06 | 6.00 | 5.03 | 43.32 | 28.68 |
| 8 | 4.74 | 0.00 | 0.00 | 0.00 | 1.22 | 0.00 | 9.35 | 1.83 |
| AF | 0.00 | 0.00 | 0.00 | 0.00 | 0.00 | 0.00 | 0.00 | 0.00 |

| Sample ID | LA-ER-MD-315-0600-0930 | | LA-ER-MD-315-1000-1330 | | LA-ER-MD-315-1400-1730 | | LA-ER-MD-315-1800-0530 | |
|---|---|---|---|---|---|---|---|---|
| Julian Start Date | 315 | | 315 | | 315 | | 315 | |
| Calendar Start Date | Nov 11 | | Nov 11 | | Nov 11 | | Nov 11 | |
| Start time | 0600-0930 | | 1000-1330 | | 1400-1730 | | 1800-0600 | |
| Volume (m3) | 6.30 | | 6.30 | | 6.30 | | 20.7 | |
| Stage 1 (ug/stage) | 0.00 | 0.00 | 0.20 | 0.00 | 0.00 | 0.00 | 0.06 | 0.00 |
| 2 | 1.74 | 0.00 | 0.00 | 0.00 | 0.26 | 0.00 | 2.58 | 1.32 |
| 3 | 0.13 | 1.31 | 0.00 | 0.00 | 0.43 | 0.00 | 16.49 | 6.55 |
| 4 | 1.18 | 2.52 | 0.00 | 1.08 | 1.50 | 1.31 | 21.97 | 16.40 |
| 5 | 5.48 | 6.95 | 2.00 | 4.27 | 7.03 | 6.28 | 41.40 | 34.39 |
| 6 | 6.82 | 8.72 | 5.84 | 6.56 | 6.95 | 7.70 | 47.06 | 46.42 |
| 7 | 11.53 | 12.61 | 3.03 | 3.26 | 4.92 | 5.33 | 35.65 | 27.38 |
| 8 | 5.49 | 3.25 | 0.11 | 0.00 | 1.59 | 1.01 | 11.06 | 4.64 |
| AF | 0.00 | 0.00 | 0.00 | 0.00 | 0.00 | 0.00 | 0.00 | 0.00 |

| Sample ID | LB-ER-MD-316-0600-0930 | | LB-ER-MD-316-1000-1330 | | LB-ER-MD-316-1400-1730 | | LB-ER-MD-316-1800-0530 | |
|---|---|---|---|---|---|---|---|---|
| Julian Start Date | 316 | | 316 | | 316 | | 316 | |
| Calendar Start Date | Nov 12 | | Nov 12 | | Nov 12 | | Nov 12 | |
| Start time | 0600-0930 | | 1000-1330 | | 1400-1730 | | 1800-0530 | |
| Volume (m3) | 6.30 | | 6.30 | | 6.30 | | 20.7 | |
| Stage 1 (ug/stage) | 0.41 | 0.00 | 0.22 | 0.00 | 0.10 | 0.00 | 8.18 | 3.13 |
| 2 | 0.16 | 0.00 | 0.00 | 0.00 | 0.00 | 0.00 | 0.29 | 0.00 |
| 3 | 4.37 | 2.32 | 2.36 | 0.00 | 2.98 | 0.00 | 3.08 | 1.19 |
| 4 | 9.04 | 3.32 | 14.66 | 2.09 | 10.46 | 1.66 | 21.46 | 11.85 |
| 5 | 27.25 | 19.69 | 28.37 | 9.62 | 13.75 | 10.92 | 53.17 | 19.38 |
| 6 | 28.86 | 17.28 | 12.64 | 9.57 | 12.93 | 7.29 | 29.83 | 16.62 |
| 7 | 20.49 | 7.01 | 3.21 | 3.55 | 4.52 | 4.47 | 32.07 | 8.34 |
| 8 | 3.41 | 2.25 | 0.00 | 0.00 | 0.00 | 0.00 | 36.13 | 7.47 |
| AF | 0.00 | 0.00 | 0.00 | 0.00 | 0.00 | 0.00 | 0.00 | 0.00 |

| Sample ID | LA-ER-MD-316-0600-0930 | | LA-ER-MD-316-1000-1330 | | LA-ER-MD-316-1400-1730 | | LA-ER-MD-316-1800-0530 | |
|---|---|---|---|---|---|---|---|---|
| Julian Start Date | 316 | | 316 | | 316 | | 316 | |
| Calendar Start Date | Nov 12 | | Nov 12 | | Nov 12 | | Nov 12 | |
| Start time | 0600-0930 | | 1000-1330 | | 1400-1730 | | 1800-0530 | |
| Volume (m3) | 6.30 | | 6.30 | | 6.30 | | 20.7 | |
| Stage 1 (ug/stage) | 0.12 | 0.00 | 0.00 | 0.00 | 0.00 | 0.00 | 0.00 | 0.00 |
| 2 | 0.00 | 0.00 | 0.68 | 0.00 | 0.57 | 0.00 | 2.80 | 1.48 |
| 3 | 2.72 | 2.32 | 2.23 | 1.28 | 2.13 | 0.00 | 29.05 | 10.61 |
| 4 | 2.78 | 3.92 | 10.35 | 3.36 | 15.13 | 2.38 | 32.40 | 11.18 |
| 5 | 14.65 | 14.98 | 18.08 | 9.21 | 27.38 | 13.37 | 62.76 | 32.69 |
| 6 | 13.80 | 16.83 | 10.76 | 7.19 | 18.59 | 8.93 | 59.61 | 51.71 |
| 7 | 19.47 | 16.04 | 8.07 | 5.36 | 4.93 | 2.77 | 39.29 | 27.41 |
| 8 | 6.03 | 3.08 | 0.48 | 0.00 | 0.00 | 0.00 | 4.05 | 1.71 |
| AF | 0.00 | 0.00 | 0.00 | 0.00 | 0.00 | 0.00 | 0.00 | 0.00 |

| Sample ID | LB-ER-MD-317-0600-0930 | | LB-ER-MD-317-1000-1330 | | LB-ER-MD-317-1400-1730 | | LB-ER-MD-317-1800-0000 | |
|---|---|---|---|---|---|---|---|---|
| Julian Start Date | 317 | | 317 | | 317 | | 317 | |
| Calendar Start Date | Nov 13 | | Nov 13 | | Nov 13 | | Nov 13 | |
| Start time | 0600-0930 | | 1000-1330 | | 1400-1730 | | 1800-0000 | |
| Volume (m3) | 6.30 | | 6.30 | | 6.30 | | 10.8 | |
| Stage 1 (ug/stage) | 0.00 | 0.00 | 0.35 | 0.00 | 0.84 | 0.00 | 0.00 | 0.00 |
| 2 | 0.00 | 0.00 | 0.01 | 0.00 | 0.00 | 0.00 | 0.00 | 0.00 |
| 3 | 7.17 | 2.47 | 0.00 | 0.00 | 0.12 | 0.73 | 1.30 | 0.00 |
| 4 | 9.77 | 5.08 | 6.91 | 2.74 | 2.79 | 1.93 | 4.70 | 1.29 |
| 5 | 11.44 | 6.10 | 11.91 | 4.65 | 3.27 | 3.69 | 6.37 | 6.33 |
| 6 | 3.77 | 4.02 | 1.88 | 1.86 | 0.57 | 1.90 | 1.66 | 1.85 |
| 7 | 2.86 | 4.73 | 1.42 | 2.52 | 2.03 | 2.75 | 1.66 | 2.07 |
| 8 | 0.15 | 0.00 | 0.00 | 0.00 | 0.00 | 0.00 | 0.00 | 0.00 |
| AF | 0.00 | 0.00 | 0.00 | 0.00 | 0.00 | 0.00 | 0.00 | 0.00 |

| Sample ID | LA-ER-MD-317-0600-0930 | | LA-ER-MD-317-1000-1330 | | LA-ER-MD-317-1400-1730 | | LA-ER-MD-317-1800-0000 | |
|---|---|---|---|---|---|---|---|---|
| Julian Start Date | 317 | | 317 | | 317 | | 317 | |
| Calendar Start Date | Nov 13 | | Nov 13 | | Nov 13 | | Nov 13 | |
| Start time | 0600-0930 | | 1000-1330 | | 1400-1730 | | 1800-0000 | |
| Volume (m3) | 6.30 | | 6.30 | | 6.30 | | 10.8 | |
| Stage 1 (ug/stage) | 0.00 | 0.00 | 0.00 | 0.00 | 0.00 | 0.00 | 0.00 | 0.00 |
| 2 | 0.37 | 0.00 | 0.40 | 0.00 | 0.00 | 0.00 | 0.00 | 0.00 |
| 3 | 10.68 | 6.21 | 17.33 | 4.04 | 6.68 | 2.26 | 5.92 | 3.16 |
| 4 | 20.15 | 7.66 | 26.31 | 11.72 | 13.15 | 6.93 | 7.06 | 5.47 |
| 5 | 16.95 | 11.19 | 26.73 | 15.81 | 10.37 | 6.67 | 11.74 | 7.53 |
| 6 | 14.03 | 12.86 | 18.58 | 15.41 | 5.63 | 6.23 | 10.58 | 7.67 |
| 7 | 6.68 | 5.30 | 6.33 | 5.05 | 3.36 | 4.01 | 7.80 | 4.68 |
| 8 | 1.92 | 0.00 | 0.45 | 0.00 | 0.00 | 0.00 | 2.24 | 0.00 |
| AF | 0.00 | 0.00 | 0.00 | 0.00 | 0.00 | 0.00 | 0.00 | 0.00 |

| Sample ID | LB-ER-MD-337-0600-0930 | | LB-ER-MD-337-1000-1330 | | LB-ER-MD-337-1400-1730 | | LB-ER-MD-337-1800-0000 | |
|---|---|---|---|---|---|---|---|---|
| Julian Start Date | 337 | | 337 | | 337 | | 337 | |
| Calendar Start Date | Dec 3 | | Dec 3 | | Dec 3 | | Dec 3 | |
| Start time | 0600-0930 | | 1000-1330 | | 1400-1730 | | 1800-0000 | |
| Volume (m3) | 6.30 | | 6.30 | | 6.30 | | 10.8 | |
| Stage 1 (ug/stage) | 0.00 | 0.00 | 0.09 | 0.00 | 0.00 | 0.00 | 0.00 | 0.00 |
| 2 | 1.77 | 1.36 | 0.58 | 0.00 | 0.70 | 0.00 | 2.62 | 0.00 |
| 3 | 72.50 | 31.74 | 23.36 | 5.27 | 12.64 | 0.00 | 38.14 | 16.31 |
| 4 | 44.35 | 27.49 | 59.57 | 26.50 | 37.09 | 20.27 | 19.57 | 11.21 |
| 5 | 56.69 | 32.22 | 37.78 | 27.50 | 30.49 | 22.91 | 48.29 | 22.98 |
| 6 | 41.32 | 32.15 | 17.06 | 14.87 | 19.10 | 12.68 | 41.24 | 18.05 |
| 7 | 19.90 | 12.38 | 5.20 | 6.47 | 4.36 | 5.35 | 31.89 | 12.03 |
| 8 | 3.50 | 4.23 | 0.00 | 1.06 | 0.00 | 0.00 | 7.43 | 2.29 |
| AF | 0.00 | 0.00 | 0.00 | 0.00 | 0.00 | 0.00 | 0.00 | 0.00 |

| Sample ID | LA-ER-MD-337-0600-0930 | | LA-ER-MD-337-1000-1330 | | LA-ER-MD-337-1400-1730 | | LA-ER-MD-337-1800-0000 | |
|---|---|---|---|---|---|---|---|---|
| Julian Start Date | 337 | | 337 | | 337 | | 337 | |
| Calendar Start Date | Dec 3 | | Dec 3 | | Dec 3 | | Dec 3 | |
| Start time | 0600-0930 | | 1000-1330 | | 1400-1730 | | 1800-0000 | |
| Volume (m3) | 6.30 | | 6.30 | | 6.30 | | 10.8 | |
| Stage 1 (ug/stage) | 0.00 | 0.00 | 0.36 | 0.00 | 1.16 | 0.00 | 0.00 | 0.00 |
| 2 | 0.00 | 0.00 | 0.00 | 0.00 | 0.00 | 0.00 | 1.40 | 0.00 |
| 3 | 8.18 | 3.72 | 3.56 | 1.88 | 9.11 | 2.32 | 29.69 | 12.81 |
| 4 | 28.59 | 15.93 | 11.29 | 7.61 | 30.79 | 16.02 | 47.50 | 22.51 |
| 5 | 31.61 | 24.27 | 14.65 | 11.97 | 28.17 | 17.82 | 55.42 | 34.24 |
| 6 | 25.43 | 27.74 | 9.22 | 8.68 | 15.88 | 13.39 | 35.70 | 33.23 |
| 7 | 13.56 | 10.07 | 6.66 | 4.69 | 5.37 | 5.00 | 36.53 | 27.22 |
| 8 | 5.93 | 2.07 | 1.06 | 0.00 | 0.72 | 0.00 | 4.79 | 1.34 |
| AF | 0.00 | 0.00 | 0.00 | 0.00 | 0.00 | 0.00 | 0.00 | 0.00 |

| Sample ID | LB-ER-MD-344-0600-0930 | | LB-ER-MD-344-1000-1330 | | LB-ER-MD-344-1400-1730 | | LB-ER-MD-344-1800-0530 | |
|---|---|---|---|---|---|---|---|---|
| Julian Start Date | 344 | | 344 | | 344 | | 344 | |
| Calendar Start Date | Dec 10 | | Dec 10 | | Dec 10 | | Dec 10 | |
| Start time | 0600-0930 | | 1000-1330 | | 1400-1730 | | 1800-0530 | |
| Volume (m3) | 6.30 | | 6.30 | | 6.30 | | 20.7 | |
| Stage 1 (ug/stage) | 0.00 | 0.00 | 0.00 | 0.00 | 0.00 | 0.00 | 0.00 | 0.00 |
| 2 | 1.03 | 0.00 | 0.00 | 0.00 | 0.00 | 0.00 | 2.72 | 0.00 |
| 3 | 11.43 | 3.94 | 4.71 | 2.38 | 2.60 | 0.00 | 29.39 | 7.34 |
| 4 | 25.67 | 10.14 | 11.98 | 7.51 | 4.88 | 1.02 | 37.97 | 9.33 |
| 5 | 56.52 | 29.19 | 28.58 | 22.63 | 13.04 | 6.49 | 76.71 | 50.15 |
| 6 | 29.33 | 19.06 | 17.15 | 13.29 | 11.49 | 7.13 | 95.49 | 22.46 |
| 7 | 16.83 | 13.01 | 11.64 | 4.08 | 11.68 | 4.76 | 62.04 | 13.91 |
| 8 | 3.55 | 1.86 | 0.00 | 0.00 | 0.12 | 0.00 | 18.07 | 4.43 |
| AF | 0.00 | 0.00 | 0.00 | 0.00 | 0.00 | 0.00 | 0.00 | 0.00 |

| Sample ID | LA-ER-MD-344-0600-0930 | | LA-ER-MD-344-1000-1330 | | LA-ER-MD-344-1400-1730 | | LA-ER-MD-344-1800-0530 | |
|---|---|---|---|---|---|---|---|---|
| Julian Start Date | 344 | | 344 | | 344 | | 344 | |
| Calendar Start Date | Dec 10 | | Dec 10 | | Dec 10 | | Dec 10 | |
| Start time | 0600-0930 | | 1000-1330 | | 1400-1730 | | 1800-0530 | |
| Volume (m3) | 6.30 | | 6.30 | | 6.30 | | 20.7 | |
| Stage 1 (ug/stage) | 0.00 | 0.00 | 0.00 | 0.00 | 0.00 | 0.00 | 0.00 | 0.00 |
| 2 | 0.00 | 0.00 | 0.00 | 0.00 | 0.00 | 0.00 | 4.18 | 0.00 |
| 3 | 6.17 | 1.61 | 2.03 | 0.77 | 2.09 | 0.62 | 36.88 | 11.50 |
| 4 | 6.25 | 4.70 | 3.88 | 1.87 | 5.77 | 1.32 | 49.85 | 18.13 |
| 5 | 17.83 | 15.36 | 13.82 | 7.05 | 12.06 | 4.35 | 83.81 | 72.29 |
| 6 | 20.62 | 22.83 | 12.77 | 8.74 | 12.67 | 7.94 | 120.32 | 90.17 |
| 7 | 22.21 | 17.05 | 8.79 | 4.56 | 6.22 | 5.81 | 52.34 | 32.07 |
| 8 | 10.04 | 3.89 | 0.99 | 0.00 | 1.66 | 0.64 | 14.07 | 3.59 |
| AF | 0.00 | 0.00 | 0.00 | 0.00 | 0.00 | 0.00 | 0.00 | 0.00 |

| Sample ID | LB-ER-MD-345-0600-0930 | | LB-ER-MD-345-1000-1330 | | LB-ER-MD-345-1400-1730 | | LB-ER-MD-345-1800-0000 | |
|---|---|---|---|---|---|---|---|---|
| Julian Start Date | 345 | | 345 | | 345 | | 345 | |
| Calendar Start Date | Dec 11 | | Dec 11 | | Dec 11 | | Dec 11 | |
| Start time | 0600-0930 | | 1000-1330 | | 1400-1730 | | 1800-0000 | |
| Volume (m3) | 6.30 | | 6.30 | | 6.30 | | 10.8 | |
| Stage 1 (ug/stage) | 0.00 | 0.00 | 0.00 | 0.00 | 0.00 | 0.00 | 1.87 | 1.44 |
| 2 | 0.04 | 0.00 | 0.00 | 0.00 | 0.00 | 0.00 | 4.73 | 2.27 |
| 3 | 11.35 | 5.06 | 1.96 | 2.38 | 6.63 | 4.01 | 28.27 | 18.26 |
| 4 | 13.96 | 7.62 | 9.29 | 11.27 | 8.99 | 9.67 | 26.33 | 15.37 |
| 5 | 22.54 | 17.57 | 12.60 | 15.84 | 14.83 | 13.54 | 13.50 | 30.68 |
| 6 | 22.84 | 16.52 | 7.74 | 11.18 | 15.53 | 14.94 | 49.20 | 33.91 |
| 7 | 13.44 | 13.79 | 4.89 | 7.34 | 10.88 | 11.46 | 47.07 | 31.65 |
| 8 | 1.16 | 2.10 | 1.44 | 1.40 | 3.27 | 2.48 | 15.96 | 2.19 |
| AF | 0.00 | 0.00 | 0.00 | 0.00 | 0.00 | 0.00 | 0.00 | 0.00 |

| Sample ID | LA-ER-MD-345-0600-0930 | | LA-ER-MD-345-1000-1330 | | LA-ER-MD-345-1400-1730 | | LA-ER-MD-345-1800-0000 | |
|---|---|---|---|---|---|---|---|---|
| Julian Start Date | 345 | | 345 | | 345 | | 345 | |
| Calendar Start Date | Dec 11 | | Dec 11 | | Dec 11 | | Dec 11 | |
| Start time | 0600-0930 | | 1000-1330 | | 1400-1730 | | 1800-0000 | |
| Volume (m3) | 6.30 | | 6.30 | | 6.30 | | 10.8 | |
| Stage 1 (ug/stage) | 0.00 | 0.00 | 3.52 | 0.00 | 0.49 | 0.00 | 0.61 | 0.00 |
| 2 | 1.25 | 0.00 | 0.47 | 0.00 | 0.25 | 0.00 | 4.19 | 3.41 |
| 3 | 9.68 | 6.82 | 5.50 | 3.83 | 5.89 | 4.40 | 32.84 | 21.30 |
| 4 | 15.34 | 14.46 | 20.42 | 21.12 | 19.60 | 15.05 | 46.27 | 40.40 |
| 5 | 42.77 | 42.16 | 24.91 | 31.86 | 29.38 | 23.88 | 84.56 | 77.36 |
| 6 | 43.27 | 46.83 | 19.21 | 17.64 | 17.19 | 18.20 | 64.98 | 66.14 |
| 7 | 37.03 | 28.65 | 7.35 | 5.52 | 12.90 | 8.65 | 31.10 | 23.71 |
| 8 | 12.60 | 5.76 | 0.48 | 0.00 | 2.87 | 1.78 | 8.02 | 3.87 |
| AF | 0.00 | 0.00 | 0.00 | 0.00 | 0.00 | 0.00 | 0.00 | 0.00 |

APPENDIX IV

# LOGNORMAL FITS TO SCAQS MOUDI DATA

All MOUDI data acquired during SCAQS were fitted with bimodal lognormal distributions. Results of the lognormal fits are provided in the following tables. Two tables (EC and ROC) are given for each of the four sites. A mass of zero in mode two indicates that data could be adequately fit with one lognormal mode.

CLAREMONT ORGANIC CARBON DATA

| Julian Date | Nominal Start Time | Total Mass ($\mu g/m^3$) | Fitted Lognormal Parameters | | | | | |
|---|---|---|---|---|---|---|---|---|
| | | | $M_1$ | $D_1$ | $\sigma_1$ | $M_2$ | $D_2$ | $\sigma_2$ |
| 170 | 0600 | 12.135 | 10.74 | 0.275 | 1.757 | 1.014 | 1.128 | 1.355 |
| 170 | 1000 | 7.570 | 6.05 | 0.278 | 1.652 | 1.045 | 1.205 | 1.285 |
| 170 | 1400 | 8.123 | 5.083 | 0.244 | 1.603 | 1.46 | 0.713 | 1.506 |
| 170 | 1800 | 5.240 | 2.019 | 0.233 | 1.317 | 3.571 | 0.251 | 3.779 |
| 175 | 0600 | 8.419 | 3.867 | 0.238 | 1.286 | 3.105 | 0.714 | 1.609 |
| 175 | 1000 | 12.115 | 6.542 | 0.252 | 1.487 | 3.651 | 0.671 | 1.544 |
| 175 | 1400 | 16.190 | 8.807 | 0.238 | 1.391 | 6.564 | 0.669 | 1.384 |
| 175 | 1800 | 4.494 | 1.859 | 0.249 | 1.415 | 1.719 | 0.649 | 1.554 |
| 176 | 0600 | 14.029 | 8.951 | 0.276 | 1.577 | 3.074 | 0.769 | 1.593 |
| 176 | 1000 | 17.018 | 13.34 | 0.441 | 1.736 | 2.647 | 0.161 | 1.236 |
| 176 | 1400 | 9.526 | 3.2 | 0.241 | 1.27 | 6.061 | 0.378 | 2.554 |
| 176 | 1800 | 6.725 | 5.236 | 0.272 | 1.913 | 0.77 | 0.689 | 1.275 |
| 194 | 0600 | 12.355 | 7.763 | 0.234 | 1.397 | 3.539 | 0.655 | 1.326 |
| 194 | 1000 | 11.221 | 7.273 | 0.243 | 1.367 | 3.481 | 0.582 | 1.408 |
| 194 | 1400 | 10.239 | 7.853 | 0.231 | 1.445 | 1.854 | 0.559 | 1.394 |
| 194 | 1800 | 4.725 | 3.132 | 0.229 | 1.558 | 0.962 | 0.674 | 1.298 |
| 195 | 0600 | 6.684 | 4.788 | 0.211 | 1.554 | 1.791 | 0.566 | 1.441 |
| 195 | 1000 | 7.763 | 5.452 | 0.262 | 1.528 | 2.175 | 0.647 | 1.34 |
| 195 | 1400 | 9.324 | 2.893 | 0.234 | 1.264 | 6.354 | 0.416 | 2.064 |
| 195 | 1800 | 3.929 | 1.367 | 0.625 | 1.548 | 2.621 | 0.283 | 2.307 |
| 196 | 0600 | 6.385 | 3.117 | 0.219 | 1.334 | 3.394 | 0.564 | 1.713 |
| 196 | 1000 | 10.525 | 5.352 | 0.67 | 1.311 | 4.459 | 0.3 | 1.405 |
| 196 | 1400 | 7.508 | 7.708 | 0.383 | 1.938 | 0 | 0 | 0 |
| 196 | 1800 | 6.141 | 3.177 | 0.258 | 1.329 | 2.275 | 0.618 | 1.395 |
| 239 | 0600 | 4.468 | 0.764 | 0.19 | 1.244 | 3.411 | 0.313 | 1.634 |
| 239 | 1000 | 4.091 | 2.779 | 0.18 | 1.243 | 1.276 | 0.238 | 1.361 |
| 239 | 1400 | 9.542 | 2.06 | 0.192 | 1.264 | 7.807 | 0.341 | 1.626 |
| 239 | 1800 | 3.989 | 2.452 | 0.393 | 1.442 | 1.109 | 0.146 | 1.406 |
| 240 | 0600 | 3.706 | 3.233 | 0.248 | 1.598 | 0.679 | 1.245 | 1.249 |
| 240 | 1000 | 5.857 | 3.214 | 0.577 | 1.415 | 2.758 | 0.233 | 1.426 |
| 240 | 1400 | 9.607 | 9.329 | 0.28 | 1.435 | 0.802 | 1.244 | 1.25 |
| 240 | 1800 | 4.886 | 1.675 | 0.279 | 1.379 | 2.962 | 0.388 | 1.833 |
| 241 | 0600 | 4.945 | 3.603 | 0.274 | 1.342 | 1.416 | 1.188 | 1.333 |
| 241 | 1000 | 8.845 | 3.123 | 1.225 | 1.249 | 6.218 | 0.369 | 2.006 |
| 241 | 1400 | 6.520 | 3.291 | 0.274 | 1.293 | 3.319 | 0.599 | 1.395 |
| 241 | 1800 | 4.187 | 1.53 | 0.26 | 1.239 | 2.004 | 0.535 | 1.656 |
| 245 | 0600 | 0.486 | 0.554 | 0.395 | 1.246 | 0 | 0 | 0 |
| 245 | 1000 | 2.912 | 2.183 | 0.714 | 1.261 | 1.244 | 0.029 | 1.319 |
| 245 | 1400 | 3.532 | 0.989 | 0.276 | 1.178 | 2.242 | 0.24 | 1.133 |
| 245 | 1800 | 2.568 | 1.671 | 0.238 | 1.236 | 0.822 | 0.411 | 2.766 |
| 246 | 0600 | 6.061 | 5.595 | 0.29 | 1.457 | 0.607 | 1.208 | 1.292 |
| 246 | 1000 | 7.026 | 6.915 | 0.29 | 1.414 | 0.601 | 1.242 | 1.261 |
| 246 | 1400 | 1.555 | 1.085 | 0.402 | 1.227 | 0.433 | 0.155 | 1.202 |
| 246 | 1800 | 0.629 | 0.450 | 0.249 | 1.161 | 0.170 | 0.301 | 1.237 |

CLAREMONT ELEMENTAL CARBON DATA

| Julian Date | Nominal Start Time | Total Mass ($\mu g/m^3$) | Fitted Lognormal Parameters | | | | | |
|---|---|---|---|---|---|---|---|---|
| | | | $M_1$ | $D_1$ | $\sigma_1$ | $M_2$ | $D_2$ | $\sigma_2$ |
| 170 | 0600 | 3.349 | 2.789 | 0.219 | 1.455 | 0.439 | 0.591 | 1.347 |
| 170 | 1000 | 2.117 | 1.05 | 0.216 | 1.316 | 1.137 | 0.378 | 1.644 |
| 170 | 1400 | 1.688 | 1.72 | 0.298 | 1.495 | 0 | 0 | 0 |
| 170 | 1800 | 1.721 | 1.372 | 0.22 | 1.583 | 0.116 | 0.565 | 1.327 |
| 175 | 0600 | 3.475 | 1.773 | 0.233 | 1.363 | 1.585 | 0.786 | 1.768 |
| 175 | 1000 | 4.249 | 0.819 | 0.247 | 1.263 | 3.369 | 0.38 | 2 |
| 175 | 1400 | 3.740 | 1.676 | 0.257 | 1.368 | 1.847 | 0.592 | 1.574 |
| 175 | 1800 | 1.706 | 1.107 | 0.215 | 1.362 | 0.411 | 0.688 | 1.288 |
| 176 | 0600 | 6.281 | 2.172 | 0.239 | 1.253 | 3.959 | 0.31 | 1.978 |
| 176 | 1000 | 4.500 | 1.998 | 0.254 | 1.273 | 2.526 | 0.433 | 1.752 |
| 176 | 1400 | 3.256 | 1.537 | 0.239 | 1.247 | 1.817 | 0.375 | 1.688 |
| 176 | 1800 | 1.575 | 1.209 | 0.234 | 1.457 | 0.303 | 0.607 | 1.359 |
| 194 | 0600 | 3.916 | 3.154 | 0.226 | 1.539 | 0.487 | 0.635 | 1.345 |
| 194 | 1000 | 2.834 | 1.482 | 0.202 | 1.305 | 1.441 | 0.332 | 1.581 |
| 194 | 1400 | 2.198 | 2.357 | 0.267 | 1.638 | 0 | 0 | 0 |
| 194 | 1800 | 0.818 | 0.682 | 0.179 | 1.572 | 0.125 | 0.663 | 1.311 |
| 195 | 0600 | 2.125 | 1.107 | 0.195 | 1.293 | 1.102 | 0.35 | 1.642 |
| 195 | 1000 | 2.589 | 1.259 | 0.198 | 1.323 | 1.471 | 0.494 | 1.559 |
| 195 | 1400 | 2.940 | 1.532 | 0.241 | 1.234 | 1.486 | 0.372 | 1.673 |
| 195 | 1800 | 0.956 | 0.326 | .0211 | 1.355 | 0.653 | 0.528 | 1.65 |
| 196 | 0600 | 1.691 | 1.03 | 0.245 | 1.301 | 0.661 | 0.387 | 1.352 |
| 196 | 1000 | 2.414 | 1.418 | 0.256 | 1.293 | 1.074 | 0.596 | 1.406 |
| 196 | 1400 | 1.664 | 1.712 | 0.309 | 1.664 | 0 | 0 | 0 |
| 196 | 1800 | 1.445 | 0.937 | 0.24 | 1.315 | 0.553 | 0.585 | 1.423 |
| 239 | 0600 | 3.436 | 1.926 | 0.172 | 1.236 | 1.494 | 0.333 | 1.368 |
| 239 | 1000 | 2.335 | 2.308 | 0.225 | 1.181 | 0 | 0 | 0 |
| 239 | 1400 | 2.883 | 2.016 | 0.281 | 1.205 | 0.984 | 0.419 | 1.422 |
| 239 | 1800 | 1.132 | 0.827 | 0.256 | 1.162 | 0.525 | 0.027 | 1.328 |
| 240 | 0600 | 2.991 | 2.444 | 0.255 | 1.233 | 0.64 | 1.258 | 1.243 |
| 240 | 1000 | 3.557 | 2.685 | 0.442 | 1.236 | 0.858 | 0.147 | 1.18 |
| 240 | 1400 | 2.253 | 1.674 | 0.258 | 1.185 | 0.614 | .338 | 1.307 |
| 240 | 1800 | 2.938 | 3.012 | 0.26 | 1.548 | 0 | 0 | 0 |
| 241 | 0600 | 3.465 | 2.871 | 0.279 | 1.399 | 0.736 | 1.287 | 1.222 |
| 241 | 1000 | 3.292 | 1.901 | 0.248 | 1.234 | 1.484 | 0.958 | 1.514 |
| 241 | 1400 | 3.606 | 2.795 | 0.614 | 1.537 | 0.888 | 0.187 | 1.308 |
| 241 | 1800 | 2.817 | 2.542 | 0.347 | 1.908 | 0.250 | 1.169 | 1.293 |
| 245 | 0600 | 1.613 | 0.996 | 0.428 | 1.264 | 0.616 | 0.155 | 1.198 |
| 245 | 1000 | 2.215 | 1.716 | 0.286 | 1.459 | 0.587 | 1.017 | 1.523 |
| 245 | 1400 | 2.650 | 0.666 | 0.319 | 1.254 | 1.933 | 0.258 | 0.862 |
| 245 | 1800 | 2.245 | 1.217 | 0.241 | 1.215 | 0.935 | 0.359 | 1.844 |
| 246 | 0600 | 5.532 | 2.989 | 0.223 | 1.272 | 2.79 | 0.496 | 2.067 |
| 246 | 1000 | 4.664 | 2.93 | 0.28 | 1.211 | 1.74 | 0.395 | 1.383 |
| 246 | 1400 | 1.773 | 0.896 | 0.213 | 1.331 | 0.872 | 0.373 | 1.711 |
| 246 | 1800 | 0.534 | 0.332 | 0.268 | 1.210 | 0.235 | 0.700 | 1.283 |

RUBIDOUX ORGANIC CARBON DATA

| Julian Date | Nominal Start Time | Total Mass ($\mu g/m^3$) | Fitted Lognormal Parameters | | | | | |
|---|---|---|---|---|---|---|---|---|
| | | | $M_1$ | $D_1$ | $\sigma_1$ | $M_2$ | $D_2$ | $\sigma_2$ |
| 170 | 0600 | 7.543 | 4.372 | 0.182 | 1.576 | 3.239 | 0.645 | 1.854 |
| 170 | 1000 | 4.720 | 2.295 | 0.277 | 1.369 | 2.579 | 1.565 | 1.655 |
| 170 | 1400 | 2.726 | 2 | 0.273 | 1.229 | 0.716 | 1.225 | 1.274 |
| 170 | 1800 | 2.002 | 1.56 | 0.281 | 1.262 | 0.471 | 1.343 | 1.39 |
| 175 | 0600 | 6.373 | 3.925 | 1.077 | 1.509 | 2.384 | 0.226 | 1.29 |
| 175 | 1000 | 12.007 | 4.841 | 1.246 | 1.269 | 7.028 | 0.336 | 1.687 |
| 175 | 1400 | 5.327 | 2.416 | 1.307 | 1.206 | 2.712 | 0.363 | 1.316 |
| 175 | 1800 | 2.871 | 1.309 | 0.197 | 1.535 | 1.448 | 0.676 | 1.838 |
| 176 | 0600 | 2.993 | 1.508 | 0.225 | 1.145 | 1.362 | 1.023 | 1.381 |
| 176 | 1000 | 5.665 | 3.853 | 0.859 | 1.395 | 1.668 | 0.265 | 1.204 |
| 176 | 1400 | 5.143 | 3.021 | 0.281 | 1.233 | 1.858 | 0.026 | 1.334 |
| 176 | 1800 | 4.544 | 2.833 | 0.263 | 1.393 | 1.604 | 1.177 | 1.343 |
| 194 | 0600 | 8.067 | 4.047 | 0.235 | 1.289 | 3.501 | 0.887 | 1.609 |
| 194 | 1000 | 3.508 | 2.508 | 0.324 | 1.351 | 1.113 | 0.847 | 1.656 |
| 194 | 1400 | 4.735 | 3.216 | 0.319 | 1.3 | 1.113 | 0.935 | 1.609 |
| 194 | 1800 | 2.930 | 2.493 | 0.241 | 1.473 | 0.412 | 0.53 | 1.381 |
| 195 | 0600 | 4.501 | 3.684 | 0.361 | 1.98 | 0.657 | 4.447 | 1.309 |
| 195 | 1000 | 4.182 | 1.883 | 0.245 | 1.317 | 2.299 | 0.63 | 1.643 |
| 195 | 1400 | 3.198 | 1.241 | 0.300 | 1.251 | 2.128 | 0.575 | 1.657 |
| 195 | 1800 | 2.583 | 1.415 | 0.717 | 1.527 | 0.941 | 0.248 | 1.46 |
| 196 | 0600 | 2.928 | 2.198 | 0.716 | 1.662 | 0.621 | 0.206 | 1.613 |
| 196 | 1000 | 8.047 | 6.058 | 0.783 | 1.46 | 1.411 | 0.238 | 1.389 |
| 196 | 1400 | 4.095 | 2.961 | 0.387 | 1.293 | 1.43 | 0.13 | 1.374 |
| 196 | 1800 | 2.927 | 1.544 | 0.264 | 1.206 | 1.409 | 0.728 | 1.282 |
| 239 | 0600 | 6.880 | 3.11 | 0.648 | 0.648 | 1.356 | 4.198 | 1.741 |
| 239 | 1000 | 5.414 | 3.695 | 0.65 | 1.529 | 1.79 | 0.233 | 2.169 |
| 239 | 1400 | 6.836 | 4.516 | 0.25 | 1.242 | 1.886 | 0.664 | 1.343 |
| 239 | 1800 | 4.430 | 3.02 | 0.27 | 1.503 | 1.433 | 0.828 | 1.651 |
| 240 | 0600 | 4.203 | 2.551 | 0.226 | 1.3 | 1.668 | 0.756 | 1.711 |
| 240 | 1000 | 5.714 | 3.292 | 0.245 | 1.242 | 2.432 | 0.723 | 1.628 |
| 240 | 1400 | 8.691 | 6.94 | 0.336 | 1.534 | 1.846 | 1.181 | 1.304 |
| 240 | 1800 | 5.128 | 3.12 | 0.336 | 1.412 | 1.647 | 1.297 | 1.21 |
| 241 | 0600 | 3.119 | 1.817 | 0.427 | 1.356 | 1.322 | 0.907 | 1.465 |
| 241 | 1000 | 2.449 | 1.094 | 0.705 | 1.299 | 1.404 | 0.179 | 1.574 |
| 241 | 1400 | 2.945 | 2.935 | 0.758 | 1.508 | .145 | 0.307 | 1.202 |
| 241 | 1800 | 4.270 | 1.404 | 1.176 | 1.304 | 2.727 | 0.354 | 1.707 |
| 245 | 0600 | 6.870 | 4.422 | 0.163 | 1.484 | 2.314 | 0.418 | 1.669 |
| 245 | 1000 | 1.147 | 0.587 | 0.033 | 1.262 | 0.62 | 1.288 | 1.221 |
| 245 | 1400 | 2.913 | 0.699 | 0.265 | 1.18 | 1.986 | 0.231 | 0.879 |
| 245 | 1800 | 4.279 | 3.567 | 0.294 | 1.528 | 0.686 | 1.276 | 1.223 |
| 246 | 0600 | 9.272 | 4.868 | 0.235 | 1.245 | 4.815 | 0.457 | 2.342 |
| 246 | 1000 | 2.433 | 2.027 | 0.167 | 1.392 | 0.498 | 1.294 | 1.217 |
| 246 | 1400 | 1.565 | 1.0 | 1.113 | 1.179 | 1.296 | 0.589 | 1.334 |
| 246 | 1800 | 1.095 | 1.36 | 0.243 | 1.164 | 0.601 | 0.776 | 1.223 |

RUBIDOUX ELEMENTAL CARBON DATA

| Julian Date | Nominal Start Time | Total Mass ($\mu g/m^3$) | Fitted Lognormal Parameters | | | | | |
|---|---|---|---|---|---|---|---|---|
| | | | $M_1$ | $D_1$ | $\sigma_1$ | $M_2$ | $D_2$ | $\sigma_2$ |
| 170 | 0600 | 2.382 | 2.069 | 0.204 | 1.663 | 0.416 | 0.573 | 1.429 |
| 170 | 1000 | 1.242 | 0.939 | 0.269 | 1.21 | 0.382 | 0.613 | 1.426 |
| 170 | 1400 | 0.595 | 0.278 | 0.381 | 1.351 | 0.37 | 0.276 | 1.208 |
| 170 | 1800 | 0.394 | 0.243 | 0.138 | 1.417 | 0.18 | 0.353 | 1.376 |
| 175 | 0600 | 2.207 | 01.506 | 0.179 | 1.653 | 0.843 | 0.828 | 1.71 |
| 175 | 1000 | 5.971 | 02.743 | 0.27 | 1.281 | 3.448 | 0.753 | 1.761 |
| 175 | 1400 | 1.700 | 01.379 | 0.323 | 1.536 | 0.292 | 1.243 | 1.247 |
| 175 | 1800 | 1.614 | 0.803 | 0.243 | 1.278 | 0.867 | 0.496 | 2.204 |
| 176 | 0600 | 2.538 | 01.851 | 0.222 | 1.362 | 0.685 | 1.046 | 1.539 |
| 176 | 1000 | 2.516 | 01.252 | 0.264 | 1.207 | 1.307 | 0.739 | 1.292 |
| 176 | 1400 | 1.570 | 0.927 | 0.277 | 1.23 | 0.735 | 0.849 | 1.612 |
| 176 | 1800 | 1.605 | 0.916 | 0.236 | 1.316 | 0.666 | 0.665 | 1.467 |
| 194 | 0600 | 4.441 | 02.426 | 0.232 | 1.364 | 2.094 | 0.896 | 1.616 |
| 194 | 1000 | 0.683 | 0.477 | 0.274 | 1.207 | 0.272 | 0.385 | 1.381 |
| 194 | 1400 | 0.332 | 0.383 | 0.395 | 1.266 | 0 | 0 | 0 |
| 194 | 1800 | 1.292 | 01.182 | 0.199 | 1.628 | 0.158 | 0.541 | 1.428 |
| 195 | 0600 | 3.461 | 03.631 | 0.207 | 1.634 | 0 | 0 | 0 |
| 195 | 1000 | 2.818 | 02.204 | 0.386 | 1.422 | 0.631 | 0.145 | 1.424 |
| 195 | 1400 | 3.199 | 1.195 | 0.297 | 1.244 | 2.096 | 0.556 | 1.608 |
| 195 | 1800 | 1.407 | 0.576 | 0.686 | 1.32 | 0.843 | 0.224 | 1.646 |
| 196 | 0600 | 1.799 | 0.906 | 0.283 | 1.247 | 0.999 | 0.932 | 1.532 |
| 196 | 1000 | 3.189 | 2.014 | 0.702 | 1.303 | 01.228 | 0.278 | 1.235 |
| 196 | 1400 | 1.742 | 1.496 | 0.393 | 1.276 | 0.282 | 0.142 | 1.455 |
| 196 | 1800 | 1.878 | 1.129 | 0.277 | 1.228 | 0.871 | 0.661 | 1.332 |
| 239 | 0600 | 4.313 | 4.783 | 0.196 | 1.822 | 0 | 0 | 0 |
| 239 | 1000 | 1.366 | 1.202 | 0.439 | 1.304 | 0.255 | 0.116 | 1.257 |
| 239 | 1400 | 3.044 | 2.393 | 0.255 | 1.189 | 0.808 | 0.722 | 1.258 |
| 239 | 1800 | 2.345 | 1.757 | 0.21 | 1.374 | 0.536 | 0.685 | 1.417 |
| 240 | 0600 | 3.136 | 0.659 | 0.374 | 1.374 | 2.192 | 0.262 | 1.19 |
| 240 | 1000 | 5.018 | 2.947 | 0.257 | 1.266 | 2.228 | 0.64 | 1.36 |
| 240 | 1400 | 4.492 | 3.432 | 0.32 | 1.454 | 1.075 | 1.268 | 1.234 |
| 240 | 1800 | 2.982 | 2.237 | 0.337 | 1.452 | 0.449 | 1.286 | 1.214 |
| 241 | 0600 | 1.041 | 0.731 | 0.814 | 1.326 | 0.414 | 0.108 | 1.207 |
| 241 | 1000 | 1.256 | 0.707 | 0.705 | 1.268 | 0.6 | 0.207 | 1.492 |
| 241 | 1400 | 0.988 | 0.704 | 0.714 | 1.257 | 0.35 | 0.267 | 1.217 |
| 241 | 1800 | 2.210 | 1.222 | 0.28 | 1.235 | 1.131 | 0.661 | 1.329 |
| 245 | 0600 | 2.800 | 2.23 | 0.4 | 1.261 | 0.798 | 0.13 | 1.275 |
| 245 | 1000 | 0.831 | 0.584 | 0.281 | 1.239 | 0.313 | 1.283 | 1.225 |
| 245 | 1400 | 0.494 | 0.427 | 0.218 | 1.126 | 0.119 | 0.247 | 1.164 |
| 245 | 1800 | 2.395 | 1.284 | 0.374 | 1.316 | 1.132 | 0.171 | 1.52 |
| 246 | 0600 | 4.122 | 1.266 | 0.287 | 1.21 | 3.025 | 0.243 | 1.152 |
| 246 | 1000 | 0.692 | 0.508 | 1.305 | 1.209 | 0.291 | 0.391 | 1.246 |
| 246 | 1400 | 0.759 | 0.864 | 0.531 | 1.516 | 0 | 0 | 0 |
| 246 | 1800 | 0.704 | 0.608 | 0.392 | 1.717 | 0.141 | 0.143 | 1.416 |

LONG BEACH ORGANIC CARBON DATA

| Julian Date | Nominal Start Time | Total Mass ($\mu g/m^3$) | Fitted Lognormal Parameters | | | | | |
|---|---|---|---|---|---|---|---|---|
| | | | $M_1$ | $D_1$ | $\sigma_1$ | $M_2$ | $D_2$ | $\sigma_2$ |
| 315 | 0600 | 5.197 | 3.508 | 0.23 | 1.482 | 1.547 | 0.059 | 1.563 |
| 315 | 1000 | 2.385 | 2.096 | 0.199 | 1.676 | 0.356 | 0.647 | 1.334 |
| 315 | 1400 | 3.075 | 2.407 | 0.243 | 1.449 | 0.592 | 0.593 | 1.367 |
| 315 | 1800 | 9.376 | 4.554 | 0.237 | 1.258 | 5.291 | 0.435 | 3.343 |
| 316 | 0600 | 8.233 | 5.319 | 0.235 | 1.261 | 8.016 | 0.301 | 2.123 |
| 316 | 1000 | 3.941 | 4.146 | 0.285 | 1.249 | 4.52 | 0.556 | 1.44 |
| 316 | 1400 | 3.863 | 3.452 | 0.253 | 1.235 | 2.42 | 0.652 | 1.41 |
| 316 | 1800 | 3.147 | 4.636 | 0.041 | 1.439 | 4.897 | 0.322 | 1.557 |
| 317 | 0600 | 4.367 | 3.154 | 0.462 | 1.593 | 1.191 | 1.148 | 1.331 |
| 317 | 1000 | 2.572 | 1.398 | 0.391 | 1.278 | 1.379 | 0.596 | 1.396 |
| 317 | 1400 | 0.570 | 0.531 | 0.51 | 1.437 | 0.095 | 0.116 | 1.303 |
| 317 | 1800 | 1.453 | 1.341 | 0.493 | 1.698 | 0.127 | 0.124 | 1.396 |
| 337 | 0600 | 36.434 | 18.038 | 1.153 | 1.355 | 19.313 | 0.286 | 1.515 |
| 337 | 1000 | 21.503 | 16.35 | 0.739 | 1.463 | 5.236 | 0.268 | 1.256 |
| 337 | 1400 | 15.266 | 6.101 | 0.272 | 1.233 | 9.233 | 0.739 | 1.407 |
| 337 | 1800 | 17.52 | 11.132 | 0.263 | 1.517 | 5.101 | 1.201 | 1.309 |
| 344 | 0600 | 21.321 | 7.788 | 0.279 | 1.387 | 13.136 | 0.485 | 1.915 |
| 344 | 1000 | 10.565 | 2.542 | 0.263 | 1.33 | 8.017 | 0.376 | 1.909 |
| 344 | 1400 | 5.746 | 4.87 | 0.235 | 1.598 | 0.771 | 0.691 | 1.557 |
| 344 | 1800 | 14.438 | 8.237 | 0.234 | 1.287 | 4.743 | 0.745 | 1.81 |
| 345 | 0600 | 12.163 | 6.898 | 0.239 | 1.318 | 5.211 | 0.792 | 1.729 |
| 345 | 1000 | 4.600 | 2.67 | 0.269 | 1.408 | 1.892 | 0.639 | 1.345 |
| 345 | 1400 | 8.116 | 2.999 | 0.236 | 1.249 | 5.814 | 0.552 | 3.083 |
| 345 | 1800 | 17.31 | 8.267 | 0.210 | 1.246 | 5.305 | 0.979 | 1.462 |

LONG BEACH ELEMENTAL CARBON DATA

| Julian Date | Nominal Start Time | Total Mass ($\mu g/m^3$) | Fitted Lognormal Parameters | | | | | |
|---|---|---|---|---|---|---|---|---|
| | | | $M_1$ | $D_1$ | $\sigma_1$ | $M_2$ | $D_2$ | $\sigma_2$ |
| 315 | 0600 | 4.611 | 2.07 | 0.228 | 1.284 | 2.926 | 0.263 | 2.727 |
| 315 | 1000 | 2.114 | 0.93 | 0.383 | 1.395 | 1.236 | 0.171 | 1.679 |
| 315 | 1400 | 2.538 | 2.156 | 0.222 | 1.53 | 0.34 | 0.627 | 1.332 |
| 315 | 1800 | 3.554 | 3.218 | 0.198 | 1.743 | 0.4 | 1.038 | 1.493 |
| 316 | 0600 | 8.233 | 3.441 | 0.251 | 1.223 | 3.891 | 0.336 | 1.597 |
| 316 | 1000 | 3.941 | 1.937 | 0.246 | 1.218 | 2.007 | 0.342 | 1.667 |
| 316 | 1400 | 3.863 | 3.316 | 0.272 | 1.455 | 0.439 | 0.501 | 1.401 |
| 316 | 1800 | 3.147 | 1.878 | 0.27 | 1.355 | 0.869 | 0.043 | 1.305 |
| 317 | 0600 | 3.555 | 2.066 | 0.223 | 1.679 | 1.548 | 0.759 | 1.597 |
| 317 | 1000 | 1.867 | 1.454 | 0.456 | 1.639 | 0.532 | 0.143 | 1.552 |
| 317 | 1400 | 1.747 | 1.41 | 0.381 | 1.893 | 0.353 | 0.127 | 1.487 |
| 317 | 1800 | 1.06 | 0.780 | 0.391 | 1.350 | 0.289 | 0.151 | 1.535 |
| 337 | 0600 | 22.470 | 10.324 | 0.252 | 1.268 | 11.533 | 0.98 | 1.548 |
| 337 | 1000 | 12.963 | 7.037 | 0.662 | 1.402 | 5.496 | 0.264 | 1.326 |
| 337 | 1400 | 9.716 | 4.996 | 0.268 | 1.348 | 4.921 | 0.649 | 1.338 |
| 337 | 1800 | 7.395 | 4.946 | 0.271 | 1.509 | 2.510 | 1.138 | 1.378 |
| 344 | 0600 | 12.253 | 3.708 | 0.26 | 1.329 | 8.215 | 0.369 | 2.004 |
| 344 | 1000 | 7.920 | 3.164 | 0.267 | 1.26 | 4.675 | 0.434 | 1.693 |
| 344 | 1400 | 3.080 | 2.576 | 0.238 | 1.364 | 0.367 | 0.516 | 1.314 |
| 344 | 1800 | 4.983 | 4.091 | 0.325 | 1.465 | 0.461 | 1.2 | 1.276 |
| 345 | 0600 | 9.946 | 3.508 | 0.237 | 1.297 | 7.211 | 0.394 | 3.122 |
| 345 | 1000 | 7.843 | 4.142 | 0.249 | 1.369 | 3.153 | 0.646 | 1.429 |
| 345 | 1400 | 8.905 | 4.948 | 0.23 | 1.332 | 3.082 | 0.709 | 1.55 |
| 345 | 1800 | 12.571 | 8.464 | 0.228 | 1.493 | 3.577 | 1.027 | 1.525 |

LOS ANGELES ORGANIC CARBON DATA

| Julian Date | Nominal Start Time | Total Mass ($\mu g/m^3$) | Fitted Lognormal Parameters | | | | | |
|---|---|---|---|---|---|---|---|---|
| | | | $M_1$ | $D_1$ | $\sigma_1$ | $M_2$ | $D_2$ | $\sigma_2$ |
| 315 | 0600 | 3.739 | 4.007 | 0.131 | 2.15 | 0 | 0 | 0 |
| 315 | 1000 | 1.010 | 0.987 | 0.205 | 1.188 | 0 | 0 | 0 |
| 315 | 1400 | 2.300 | 2.363 | 0.246 | 1.568 | 0 | 0 | 0 |
| 315 | 1800 | 7.672 | 4.928 | 0.221 | 1.493 | 2.179 | 0.828 | 1.629 |
| 316 | 0600 | 8.008 | 6.201 | 0.147 | 1.789 | 1.685 | 0.364 | 1.343 |
| 316 | 1000 | 6.666 | 7.816 | 0.365 | 2.216 | 0 | 0 | 0 |
| 316 | 1400 | 9.628 | 5.521 | 0.262 | 1.268 | 4.269 | 0.591 | 1.414 |
| 316 | 1800 | 10.161 | 6.985 | 0.236 | 1.552 | 3.232 | 0.924 | 1.583 |
| 317 | 0600 | 9.747 | 5.951 | 0.762 | 1.537 | 3.775 | 0.235 | 1.328 |
| 317 | 1000 | 13.934 | 4.982 | 0.25 | 1.296 | 9.379 | 0.779 | 1.661 |
| 317 | 1400 | 5.030 | 3.658 | 0.739 | 1.53 | 1.406 | 0.248 | 1.397 |
| 317 | 1800 | 4.198 | 2.572 | 0.239 | 1.564 | 1.421 | 0.915 | 1.566 |
| 337 | 0600 | 16.553 | 7.994 | 0.241 | 1.372 | 7.397 | 0.68 | 1.416 |
| 337 | 1000 | 6.012 | 2.118 | 0.69 | 1.389 | 3.908 | 0.265 | 1.683 |
| 337 | 1400 | 12.987 | 8.05 | 0.687 | 1.422 | 4.857 | 0.261 | 1.316 |
| 337 | 1800 | 19.54 | 11.768 | 0.745 | 1.837 | 8.794 | 0.188 | 1.732 |
| 344 | 0600 | 11.765 | 8.392 | 0.223 | 1.656 | 2.779 | 0.058 | 1.585 |
| 344 | 1000 | 5.364 | 0.721 | 0.226 | 1.268 | 4.69 | 0.264 | 1.757 |
| 344 | 1400 | 4.994 | 3.425 | 0.235 | 1.335 | 1.452 | 0.575 | 1.448 |
| 344 | 1800 | 16.248 | 9.527 | 0.228 | 1.29 | 5.996 | 0.785 | 1.76 |
| 345 | 0600 | 24.078 | 18.114 | 0.228 | 1.626 | 4.322 | 0.866 | 1.719 |
| 345 | 1000 | 11.416 | 5.649 | 0.249 | 1.322 | 5.343 | 0.658 | 1.422 |
| 345 | 1400 | 12.511 | 14.923 | 0.4 | 2.477 | 0 | 0 | 0 |
| 345 | 1800 | 25.18 | 7.524 | 0.243 | 1.305 | 18.504 | 0.556 | 2.428 |

LOS ANGELES ELEMENTAL CARBON DATA

| Julian Date | Nominal Start Time | Total Mass ($\mu g/m^3$) | Fitted Lognormal Parameters | | | | | |
|---|---|---|---|---|---|---|---|---|
| | | | $M_1$ | $D_1$ | $\sigma_1$ | $M_2$ | $D_2$ | $\sigma_2$ |
| 315 | 0600 | 5.613 | 5.053 | 0.164 | 1.905 | .67 | 0.792 | 1.661 |
| 315 | 1000 | 2.406 | 1.971 | 0.223 | 1.335 | .387 | 0.55 | 1.405 |
| 315 | 1400 | 3.433 | 2.86 | 0.224 | 1.478 | .349 | 0.583 | 1.332 |
| 315 | 1800 | 6.347 | 4.242 | 0.22 | 1.372 | 1.662 | 0.661 | 1.573 |
| 316 | 0600 | 9.075 | 4.099 | 0.218 | 1.494 | 5.932 | 0.201 | 3.409 |
| 316 | 1000 | 4.190 | 3.034 | 0.232 | 1.653 | 1.24 | 0.584 | 1.798 |
| 316 | 1400 | 4.357 | 1.029 | 0.249 | 1.236 | 3.33 | 0.33 | 1.561 |
| 316 | 1800 | 6.333 | 4.497 | 0.22 | 1.345 | 1.669 | 0.769 | 1.877 |
| 317 | 0600 | 6.860 | 3.808 | 0.232 | 1.323 | 3.133 | 0.822 | 1.679 |
| 317 | 1000 | 8.259 | 4.398 | 0.239 | 1.289 | 3.804 | 0.673 | 1.536 |
| 317 | 1400 | 4.144 | 2.191 | 0.22 | 1.443 | 1.916 | 0.715 | 1.439 |
| 317 | 1800 | 2.690 | 1.482 | 0.220 | 1.421 | 1.188 | 0.750 | 1.663 |
| 337 | 0600 | 13.300 | 7.963 | 0.236 | 1.29 | 4.751 | 0.651 | 1.458 |
| 337 | 1000 | 5.529 | 3.244 | 0.243 | 1.458 | 2.227 | 0.65 | 1.459 |
| 337 | 1400 | 8.659 | 4.529 | 0.249 | 1.355 | 4.044 | 0.664 | 1.355 |
| 337 | 1800 | 12.08 | 7.501 | 0.207 | 1.550 | 4.88 | 0.743 | 1.687 |
| 344 | 0600 | 10.387 | 7.99 | 0.213 | 1.446 | 1.428 | 0.655 | 1.464 |
| 344 | 1000 | 3.648 | 1.671 | 0.226 | 1.286 | 2.074 | 0.303 | 2.127 |
| 344 | 1400 | 3.282 | 2.685 | 0.205 | 1.419 | .446 | 0.686 | 1.54 |
| 344 | 1800 | 10.544 | 5.86 | 0.236 | 1.261 | 4.622 | 0.388 | 2.112 |
| 345 | 0600 | 22.965 | 8.452 | 0.228 | 1.298 | 14.724 | 0.318 | 2.401 |
| 345 | 1000 | 12.693 | 6.302 | 0.264 | 1.351 | 6.291 | 0.625 | 1.43 |
| 345 | 1400 | 11.421 | 5.991 | 0.242 | 1.379 | 4.938 | 0.638 | 1.519 |
| 345 | 1800 | 21.87 | 7.918 | 0.241 | 1.265 | 14.149 | 0.521 | 2.13 |